Domain wall injection in antiferromagnets

by

Raphael Kromin

1. supervisor: Prof. Dr. Karin Everschor-Sitte
2. supervisor: Prof. Dr. Olena Gomonay

Contents

1. Introduction

The demand for smaller and faster computer technologies is rising fast. Electrical currents are used for data storage devices as RAM and HDD in most computers today [41]. However, those setups are at the brink of their minimal size. Interactions between information cells and overheating of the devices complicate further progress [4]. In contrast, magnetic devices, which use the spin degree of freedom, do not heat up and can be manufactured in nanometre sizes. Magnetoresistive RAM or MRAM is one possible application [35].

Another promising spintronic device is the magnetic racetrack memory system [34] [35]. Spin-polarised currents can create and move magnetic domain wall structures between two oppositely magnetised domains in ferromagnetic nanowires [38]. The magnetisation of a domain encodes a bit of information. It has been validated experimentally that the domain walls can be moved with velocities up to $750ms^{-1}$ [35]. The combination of a nanowire sized system with a high density of domains and the possibility to move the information that fast leads to a highly enhanced computer speed. This enables data analysis faster than ever. Immense information like genetic code could be saved and studied to tackle diseases based on simulations instead of trials.

It is essential to know the static and dynamic domain wall properties to build such a device. This thesis is focused on the mathematical description of those characteristics for the ferromagnetic and the synthetic antiferromagnetic case. At first, the micromagnetic ferromagnetic LLG equations are formulated and domain walls are classified [38]. Also, racetrack memory system traits are discussed [34] [35].

The third chapter is based on the recalculation of all ferromagnetic qualities. The domain wall profile and width describe the static case [46]. A collective coordinate approach can describe the domain wall movement along the nanowire by spin currents [36] [37] [45]. The domain wall creation is discussed at a pinned magnetisation point for currents above a critical value [38] [39]. This current is compared to a larger ferromagnetic instability current [32]. It can be seen that the domain wall creation and movement are possible for the ferromagnet and that racetrack systems can be developed.

The new calculations of the thesis are shown in chapter 4. In contrast to a ferromagnet, a synthetic antiferromagnet is not constraint in size because it has no net magnetisation. The smallest and fastest racetrack devices could be possible [35]. It is important to know if domain walls can be created and moved in such a system. Antiferromagnetic LLG equations are defined and used to calculate a shedding current as in the ferromagnetic case [19] [23] [28] [38]. Then, it is compared to the instability current of the system.

1. Introduction

At last, simulations of synthetic antiferromagnetic domain walls are presented in chapter 5 [17] [50]. They are used to confirm the theory of the shedding current and validate a set of material parameters. Finally, the simulation checks the instability current plausibility.

2. Domain wall and micromagnetism basics

This chapter is an outline of the main equations of micromagnetism. At first, the concept of magnetic domain walls is described. Then, one-dimensional nanowire systems are justified as realistic systems. After that, the Landau-Lifshitz-Gilbert (LLG) equation for ferromagnetic systems is developed. This is followed by an explication of all effective field terms arising in this thesis for the equation. In the end, the spin-transfer torque is introduced and explained for one-dimensional systems.

2.1. Domain walls

Ferromagnetic systems are spin systems with a majority of spins or magnetic moments pointing along the same direction. The latter can be measured as a macroscopic magnetisation m. A quasi-one-dimensional ferromagnetic system has two ground states, which are the two antiparallel magnetisation directions. A region with a constant magnetisation value is called a domain. Magnetic systems with the geometry of a wire in the nanometre length scale in size are called nanowires. The two ground state domains are energetically equal, as the ground state of the system is the energetic minimum. However, a merging of both domains is not a ground state any more, since two magnetic moments with an opposite direction would be adjoining neighbours. This status would be energetically unfavourable. That is why a structure called domain wall will form in between those two domains separating both and reaching a stable state.

A domain wall is characterised by a constant rotation of the magnetisation from one state to another. Usually, this can occur in the two different ways shown in figure 2.1. The axis of this system is given by the red, blue and green vectors shown in the top left. The magnetisation changes colour according to the direction it is pointing. In both cases displayed in the figure, the possible ground states are either pointing along the red axis or antiparallel. The domain wall in the left nanowire rotates orthogonally to the plane given by the red and green axes changing in the blue direction. A domain wall with such a rotation perpendicular to the domain wall propagation direction is called the Bloch wall. The second case is given by the nanowire on the right. The magnetisation rotates in the plane given by the red and green axes along the domain wall propagation direction. This case is called the Néel domain wall.

Another way to characterise a domain wall depends on the ground state configuration
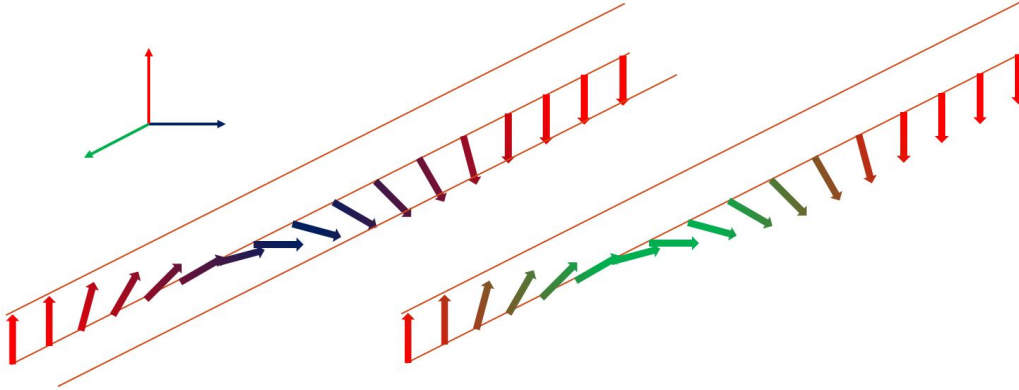
Figure 2.1.: The plot displays a one-dimensional nanowire characterised by magneti-
sation vectors. The two ground states of the magnetisation are pointing
along the red axis or antiparallel to it. Then, two different types of do-
main walls are possible. A Bloch domain wall is shown on the left. It
is characterised by a magnetisation rotation perpendicular to the domain
wall propagation direction. The domain wall shown on the right is a
Néel domain wall, a domain wall with a magnetisation rotation along the
domain wall propagation direction. Source: Author's illustration.
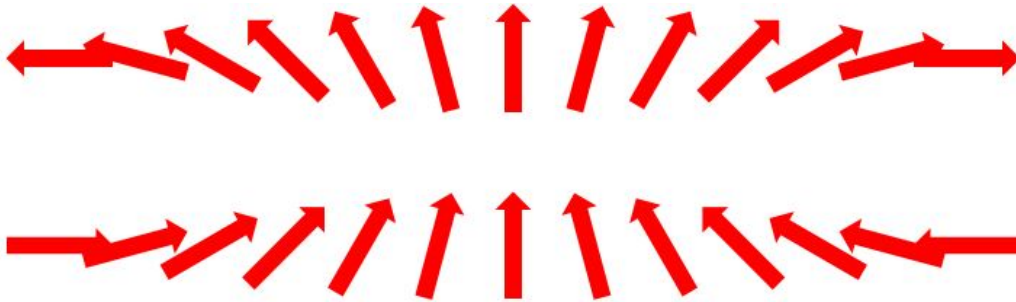
Figure 2.2.: The plot displays a one-dimensional nanowire characterised by magneti-
sation vectors. The two ground states of the magnetisation are pointing
to the left or pointing to the right. The case shown in the top part is a
tail-to-tail domain wall where the ground state magnetisation vectors are
pointing away from each other. The case shown at the bottom is called
head-to-head domain wall, where the ground state magnetisation vectors
are pointing towards each other. Source: Author's illustration.

itself independently of the rotation sense of the domain wall. When the two ground states are antiparallel, they either can point towards each other or away from each other just as for a usual ferromagnet. These two configurations are shown and named in figure 2.2. On the top, both magnetisation vectors are pointing away from each other. This is called a tail-to-tail domain wall, since the heads of the vector arrows are pointing away from each other. The bottom case shows both ground state magnetisation vectors pointing towards each other, pointing head-to-head vector wise that is why such a domain wall is called a head-to-head domain wall.

Both of these configurations can exist as a Bloch or Néel domain wall. Hence, domain walls are characterised by both properties. Even though domain walls exist in higher dimensions than one dimension, the main part of this thesis focuses on domain wall properties in one dimension. This is due a focus on a future application in racetrack memory systems built in nanowires.

2.2. Dimensionality of the nanowire

Up to this point it is ambiguous how a one-dimensional nanowire system can be realised in reality. Of course, this is an approximation for a system in two or three dimensions. A one-dimensional Ising model as a chain of single atoms interacting with each neighbour, but far away from any external source besides an electron current applied, is impossible to build.

However, several methods for a creation of lower dimensional systems exist with a size in the order of $10nm$ [13]. For example, ferromagnetic full-Heusler alloys can be produced with a thickness of $20nm$ by the molecular beam epitaxy method, in which the material is growing layer by layer on a substrate [49]. While these systems are not one dimensional, they are small enough to be treated as being one dimensional. In the ferromagnet, neighbouring spins are parallel independently of the three dimensions. The neighbour to the left is the same as the one below in a spin lattice system. That is why the approximation to magnetisation is valid.

A 180° domain wall rotates from one direction to the other. It can also be treated one-dimensionally even though the system is not because the spins of a plane in the thin film are the same. Each slice of the wire contains parallel aligned magnetic moments. They change along with one of the three dimensions towards the other ground-state magnetisation, making the other two obsolete. This holds for Bloch and Néel walls. Also, the sizes of both domain wall types are typically in the size of hundreds of nanometres [14]. Therefore, only this one dimension is the relevant one in terms of magnetisation change.

2.3. The Landau-Lifshitz-Gilbert equation

The Landau-Lifshitz-Gilbert equation - called the LLG equation - is a fundamental equation to describe the time evolution of the magnetisation in a ferromagnetic sys-

tem. It can be used to determine domain wall properties.

The starting point of this formalism is given by the atomistic description of a ferromagnetic system. The Ising model describes a spin lattice system favouring either parallel or antiparallel aligned spins in an external magnetic field by interactions between nearest neighbours [3] [24]. This model is used to describe ferromagnetic behaviour and the phase transition to the ferromagnetic state.

If the correlation length of spins is greater than the next neighbour interaction, a coarse graining is possible as adjoining neighbours behave similarly. This process can be described by a block spin transformation combining neighbouring spins to a new total value [3]. An iteration of this process leads to a system described by the magnetisation instead of the single spin values. All spins pointing along one direction correspond to a saturated magnetisation that will be normalised to a length of $|\boldsymbol{m}| = 1$ in this thesis.

The rescaling of such spin systems to larger length scales shows that the behaviour of such a magnetic state can be characterised by a single parameter, the order parameter $\boldsymbol{m}$ in the ferromagnetic case. This order parameter describes the structure of the different phases of the system and the phase transition point in between. Hence, in this micromagnetic description, the time evolution of the magnetisation is the relevant physical quantity to help describe how ferromagnetic systems behave.

The LLG equation originates from both Landau and Lifshitz [29], who wanted to describe the time evolution of ferromagnetic systems in an effective magnetic field. This includes external magnetic fields applied to the system as well as all interactions between the magnetic moments and material properties summarised in a total magnetic energy E. The simplest version without damping is given by the following equation [51] from Landau and Lifshitz [29]:

$$\dot{\boldsymbol{m}} = \gamma \boldsymbol{m} \times \boldsymbol{H}_{\text{eff}} \quad \text{with} \quad \boldsymbol{H}_{\text{eff}} = \frac{\delta E}{\delta \boldsymbol{m}}. \tag{2.1}$$

It describes the time evolution of the magnetisation vector $\dot{\boldsymbol{m}}$ at a point $\boldsymbol{r}$ making a precession movement around the effective field $\boldsymbol{H}_{\text{eff}}$ felt at this point. The length of the magnetisation vector is constant and the origin of the vector has a fixed coordinate. This implies that it can only rotate around this origin and will precess around the energetically favourable direction. The possible change of the magnetisation vector with a constant magnitude is perpendicular to the magnetisation itself. Hence, it can be displayed by a vector moving along the surface of the possible movement of $\boldsymbol{m}$ given by a sphere, just as shown in figure 2.3. The constant in front of the effective field term γ is called gyromagnetic ratio [51] depending on the Landé-factor and the Bohr magneton.

Another term added by Gilbert [18] phenomenologically explains damping of the precession movement of $\boldsymbol{m}$ until it is pointing strictly along the effective field direction. This is also called relaxation of the magnetisation towards the effective field direction [20]. The equation (2.1) changes to the following form [18]:

$$\dot{\boldsymbol{m}} = \gamma \boldsymbol{m} \times \boldsymbol{H}_{\text{eff}} + \alpha \boldsymbol{m} \times \dot{\boldsymbol{m}} \quad \text{with} \quad \boldsymbol{H}_{\text{eff}} = \frac{\delta E}{\delta \boldsymbol{m}}. \tag{2.2}$$

The damping constant α is called Gilbert damping parameter. Figure 2.3 shows how each of the two LLG equation terms changes the magnetisation movement.
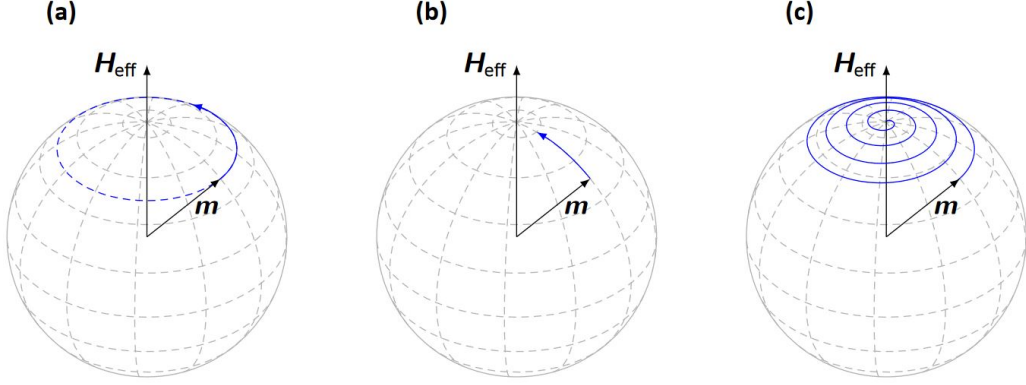
Figure 2.3.: The plot displays the movement of the magnetisation vector moving according to the LLG equation. (a) shows the precession of $\boldsymbol{m}$ around the effective field based on the $\boldsymbol{m} \times \boldsymbol{H}_{\text{eff}}$ term. (b) shows the damping of $\boldsymbol{m}$ according to the $\alpha \boldsymbol{m} \times \dot{\boldsymbol{m}}$ term. (c) shows the final motion of $\boldsymbol{m}$ with both terms combined. Source: Abert 2013: [1].

2.3.1. The effective field

The effective field $\boldsymbol{H}_{\text{eff}}$ builds the main part of the LLG equation as it describes the precession of the magnetisation. Next, all contributing terms of this field are elaborated. $\boldsymbol{H}_{\text{eff}} = \frac{\delta E}{\delta \boldsymbol{m}}$ is the definition of the effective magnetic field, each magnetisation vector is pointing along in the ferromagnet as a functional derivative of the total magnetic energy with respect to the magnetisation. It is the magnetic field felt by each magnetic moment of the system based on the interaction with external magnetic fields and other magnetic moments. Also, material properties can lead to a energetically favourable magnetisation direction or twisting.

The total magnetic energy or free energy E described in this thesis is the sum of the major interactions used to model the ferromagnetic and antiferromagnetic systems.

$$E = \int dV (E_{\text{exch}} + E_{\text{anis}} + E_{\text{DMI}} + E_{\text{ext}}) \tag{2.3}$$

External magnetic fields E_{ext} are added for clarification so that all contributions add up to a total integral, but they will not be used further. The equation shows how all interactions add up and are integrated over the space of the system V to the total free energy E.

The first part is given by the exchange interaction E_{exch}. It originates from the spin coupling term in the Ising model. For a ferromagnetic state, the energy of the Ising model is minimal if neighbouring spins are parallel aligned and reach the maximum

when they are antiparallel, called collinear antiferromagnetic state. Deviations between two neighbouring spins are penalised. They will rotate until they are parallel and in the energetic minimum state. This is why the exchange interaction is also called stiffness interaction since it models stiffness between two spins when one of both is rotated away from the minimum.

The expression resolves to a gradient term after coarse-graining is applied:

$$E_{\text{exch}} = A(\nabla \boldsymbol{m})^2 \tag{2.4}$$

with the exchange interaction constant A determining the strength of the stiffness.

The second part of the free energy is the anisotropy a system can have. Materials with anisotropic behaviour have energetically favourable magnetisation directions. This can occur due to material properties such as different crystal structures, geometries such as thin films or it can be through certain temperatures [25]. The exchange interaction of ferromagnetic systems favouring neighbouring parallel spins in a system with an anisotropic direction causes all spins to point along the same direction - with the anisotropy or against the direction - as the ground state of the system. The symmetry considered in this thesis is an easy axis or uniaxial anisotropy for a one-dimensional nanowire system. This means that the ground state directions are either along the nanowire direction or antiparallel to it. Setting this one-dimensional system along the x-axis leads to the following anisotropy model of the thesis:

$$E_{\text{anis}} = \lambda(1 - \boldsymbol{m}_x^2). \tag{2.5}$$

The term of the form $1 - \boldsymbol{m}_x^2$ is defined this way because the ground state $\boldsymbol{m}_x = \pm 1$ will lead to a vanishing energy contribution instead of a negative one. It could also be defined by just the $\boldsymbol{m}_x^2$ term. The only difference is an energy shift of the ground state energy, which does not change the effective field. The anisotropy constant λ is greater than zero to get a energetically favourable magnetisation direction. A negative λ can be used to discourage the magnetisation direction for the system specifically.

A more general approach to the anisotropy is given by a term of the form $1 - (\boldsymbol{k} \cdot \boldsymbol{m})^2$ for arbitrary anisotropy directions $\boldsymbol{k}$. It could also be the case that there is more than one favourable direction. For example two orthogonal states are energetically the same. In such cases, a 90° domain wall is built between the states instead of a 180° one. However, the typical domain walls are 180° ones in this thesis. Also, higher order anisotropy terms are possible but not considered.

The third term considered is the Dzyaloshinskii-Moriya interaction [12] [33], which is called DMI in this thesis from now on. It is a chiral interaction favouring twisted structures because it originates from spin-orbit interactions. It is also called asymmetric exchange because it changes the chirality based on the order of magnetic moments considered for the interaction. Systems with "broken spatial inversion symmetry" [22] prefer a chiral formation of the magnetisation. This can either be a right-hand or left-hand twisting. It is most generally modelled by $E_{DMI} = D_{ijk} m_i \partial_j m_k$ [22] as a term linear in spatial derivatives. m_i and m_k denote two single coordinates of the magnetisation vector $\boldsymbol{m}$ and D_{ijk} is the interaction strength as a third rank tensor,

which can be facilitated for different crystal symmetries. The DMI is different depending on whether a particle is at the surface or in the bulk.

However, the DMI for the one-dimensional nanowire reduces to the following term:

$$E_{DMI} = D\boldsymbol{m} \cdot (\nabla \times \boldsymbol{m}) = D\boldsymbol{m} \cdot (\hat{\boldsymbol{x}} \times \partial \boldsymbol{m}) \qquad (2.6)$$

in the ferromagnetic case. The interaction strength is not a tensor anymore but modelled as a simple scalar D. The spatial derivative ∇ resolves to a single derivative $\hat{\boldsymbol{x}}\frac{\partial}{\partial x} = \hat{\boldsymbol{x}}\partial$ in the one-dimensional case for a wire along the x direction since the only spatial change is along the wire direction.

Other interactions in ferromagnetic or antiferromagnetic systems are combined in the E_{ext} term which is neglected. It contains external magnetic fields, which are not applied within the thesis, and dipolar field interactions. The latter is negligible in magnitude for antiferromagnets [26]. Also, higher order contributions in magnetisation and interactions between three or more magnetic moments are not considered.

2.3.2. Spin-transfer torque

It is possible to influence and change magnetic systems with spin-polarised currents. The LLG equation can be expanded by another term accounting for this formalism. Spin-polarised currents are electrical currents where a large number of spins are pointing along the same direction. The magnitude of the polarisation P can vary between zero and one. A theoretical usage of such currents for manipulating ferromagnetic systems was first predicted by Slonczewski [40] and Berger [7] in 1996.

The spins in ordinary electron currents are randomly distributed in all directions while surpassing non-magnetic materials. However, if it enters a ferromagnet, an interface scattering of spins blocks those having a different direction than the ferromagnet magnetisation while letting the parallel ones through the material [42]. This effect is used for the giant magnetoresistance effect (GMR effect), where the electrical resistance change of two ferromagnetic layers, separated by a non-magnetic layer, is measured for the case of parallel and antiparallel aligned magnetisation directions. It was discovered by the groups of Grünberg et al. [8] and Fert et al. [5] awarding them a Nobel prize in 2007 due to the impact it has on implementations, such as the magnetoresistive random-access memory called MRAM.

Such a spin-polarised current can be subjected to the physical systems of interest in this thesis, the one-dimensional nanowire. When the current is applied, the polarised spins interact with the magnetic moments in the vicinity. The electrons exchange spin angular momentum with the local magnetic moments so that they follow the magnetisation direction. However, in a domain wall structure, the electron spin follows the magnetisation change of such a domain wall adiabatically. It changes direction as shown in figure 2.4.

A polarised spin current is applied to a nanowire with a velocity $\boldsymbol{\nu}$ from left to right while having a starting spin direction to the left, just as the red magnetisation direction of the wire. A domain wall separates this left pointing region from a right pointing

one by a constant rotation of the magnetisation from left to right. The torque between electron and magnetic moment of the wire causes the spin of the electrons to change along with the magnetic moment direction. However, neighbouring magnetic moments along the domain wall region have slightly different spin directions. That is why the magnetic moments already passed by the spins are pulled along the electron spin direction, and the domain wall starts to move. This does not imply a movement of the magnetic moments in the nanowire. It is just a rotation of the magnetisation if it is not parallel to the electron spin direction. The effect of the spin change is due to angular momentum conservation.

Mathematically, this effect can be described by newly added terms to the LLG equa-
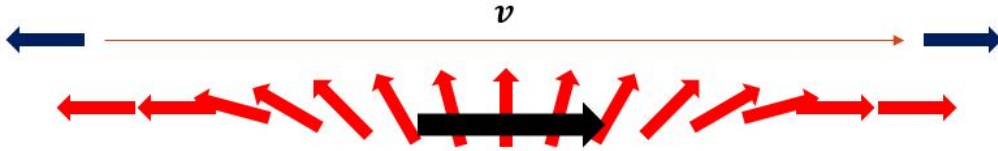
Figure 2.4.: A one-dimensional wire system with two opposite magnetisation directions separated by a domain wall region in red is subjected to a spin-polarised current with a spin direction to the left and a velocity $\boldsymbol{\nu}$ to the right in blue. The domain wall consisting of many magnetic moments is varying gradually in space which causes the electron to change adiabatically along with the magnetisation of the wire. However, the magnetic moments to the left of the electron position also shift to the electron spin direction, causing a domain wall movement. Source: Author's illustration.

tion with damping (2.2). The spin-polarised current does change the magnetisation direction by a torque if they are not parallel. Slonczewski's ansatz from 1996 [40] can be abstracted to a continuous limit of infinitely many and infinitely thin layers into two terms getting the Landau-Lifshitz-Gilbert-Slonczewski equation [44]:

$$\dot{\boldsymbol{m}} = \gamma \boldsymbol{m} \times \boldsymbol{H}_{\text{eff}} + \alpha \boldsymbol{m} \times \dot{\boldsymbol{m}} - (\boldsymbol{\nu} \cdot \nabla)\boldsymbol{m} + \beta \boldsymbol{m} \times (\boldsymbol{\nu} \cdot \nabla)\boldsymbol{m} \quad \text{with} \quad \boldsymbol{H}_{\text{eff}} = \frac{\delta E}{\delta \boldsymbol{m}}. \quad (2.7)$$

The first term $(\boldsymbol{\nu} \cdot \nabla)\boldsymbol{m}$ describes the precession of the magnetisation around the spin current direction as for the effective field. Therefore, the second term is a damping of this precession perpendicular to the first term $\beta \boldsymbol{m} \times (\boldsymbol{\nu} \cdot \nabla)\boldsymbol{m}$. It is proportional to the dimensionless prefactor β, which is of the same order as the other damping parameter α [44], describing the same effect to the magnetisation as the α dependent damping term.

The second parameter occuring in this spin-transfer torque description is the spin current velocity [38]:

$$\boldsymbol{\nu} = \frac{P\mu_B}{2eM_s(1+\beta^2)}\boldsymbol{j}. \quad (2.8)$$

It depends on the current polarisation P, the Bohr magneton μ_B, the electron charge e as well as the saturation magnetisation M_s, which is set equal to one within this thesis. It also depends on the damping factor β and the electrical current density $\boldsymbol{j}$. This means that the spin current velocity interacting with the magnetisation of the ferromagnetic system is pointing along the same direction as the electrons move $\boldsymbol{j}$ with a polarisation dependent strength. The effect is stronger when the current has a higher polarisation.

In one-dimensional nanowire systems, the spatial derivative is modified to ∂ as mentioned for the DMI contribution to the total magnetic energy. This also means that the spin current velocity needs to be applied along the wire direction to be fully utilised. The spatial product $\boldsymbol{\nu} \cdot \hat{\boldsymbol{x}} \partial$ ensures this.

The theory following in the next chapters is based on one-dimensional ferromagnetic nanowires and their static and dynamic domain wall description. Such systems can be realised because each spin at any given point in space can be approximated to a magnetisation vector showing dynamics by the LLG equation.

3. Ferromagnetic domain wall description

This chapter points out the relevant state of research on ferromagnetic systems for this thesis having described the governing equations in the last chapter.

First, the magnetic racetrack memory system is introduced as a potential application for one-dimensional domain wall systems. Then, the magnetic energy of the ferromagnetic system is analysed and the width and profile of a ferromagnetic domain wall in one dimension are determined based on the calculations of Tretiakov and Abanov [46]. Next, the movement of one-dimensional domain walls with an applied current is presented with a collective coordinate approach as in the scientific paper of Rodrigues et al. [37].

The ferromagnetic LLG equation will be used to analyse a one-dimensional semi-infinitely long nanowire system subjected to a spin current based on the calculations of Sitte et al. [39] and Rodrigues et al. [38]. The stability of the system is not given above a critical current threshold at that domain wall shedding starts.

The critical current of shedding calculated is compared to another critical current. The second current calculated is the spin current beyond which the ferromagnetic system will get unstable itself. This computation is based on the work of Masell et al. [32].

This procedures have been discussed with Davi R. Rodrigues.

3.1. Magnetic racetrack memory

Before the mathematical description starts, a chapter is dedicated to the relevant physical system, namely the one-dimensional nanowire containing domain walls. A central part of the calculations in this thesis are critical current determinations. Currents exceeding those values affect domain wall movement and existence. In the paragraph, a future application of domain wall systems is highlighted.

The use of computer technologies is rising fast and the demand for smaller and faster devices is constantly rising. On the one hand, data storing devices have been a success so far, but they have the problem of heating and scaling. On the other hand, magnetic devices could operate more efficiently without temperature rising, and data bits could be smaller than now. Spintronic devices use the spin degree of freedom of the electron to store information as bits. However, components in the nanometre regime have now reached a size that cannot be decreased any more [35].

Parkin et al. [34] [35] proposed a new method to digitally store information besides the used principles of magnetoresistive random-access memory (MRAM) and magnetic hard disc drives (HDD). They proposed a magnetic racetrack memory device. This is a nanowire, as discussed in the theory chapter above, or a grid of nanowires. As

3. Ferromagnetic domain wall description

discussed, magnetic domains within those wires, the ground states of the ferromagnet, are separated by domain walls.

Each domain with a fixed length refers to a bit of information and the domain walls separate two possible bits. This chapter concludes that a domain wall can be created and shedded in a ferromagnet when subjected to a spin-transfer torque. Therefore, the theory predicts that different domains and domain walls can be created in the nanowire and moved by spin-polarised currents. After that, they can be read out at a second point for further computation.

Figure 3.1 displays two different racetrack approaches. The racetrack shown at the top is a ferromagnetic one built onto a substrate with a spin current applied along the nanowire direction. The bottom racetrack shows a synthetic antiferromagnet constructed from two ferromagnetic layers linked through a non-magnetic layer in between. The racetrack system domains are subjected to a spin current along the wire direction as in the approach above.

The ferromagnetic racetrack displayed is the third version of those memory systems
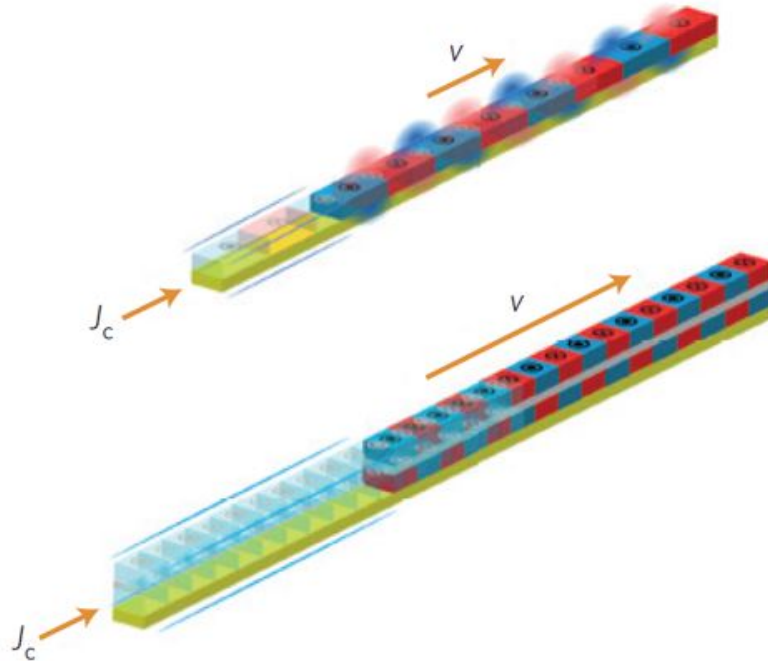
Figure 3.1.: The plot displays two different approaches of the magnetic race track memory system. The top one is a ferromagnetic nanowire on a substrate, and the bottom one is a synthetic antiferromagnet on a substrate. Both are subjected to a spin current along the wire to move the domain walls. Source: Parkin et al. 2015: [35].

called racetrack 3.0. It inherits the property of its predecessor, version 2.0, which has a significant magnetic anisotropy. This leads to narrow and robust domain walls that

can be moved simultaneously in the same direction with the same speed. The material of the 3.0 version is built from inversion symmetry missing structures to enhance the DMI term in the magnetic energy of the system. Because of this missing symmetry, it is possible to reach velocities of $350ms^{-1}$ for the domain wall movements instead of $100ms^{-1}$ without the chiral interaction [35].

The ferromagnetic chapter is centred on the domain wall creation and movement to enable creating a racetrack memory system. However, each ferromagnetic domain has a finite magnetisation value. Hence, they produce demagnetisation fields interacting with each other. This is a limiting factor for the domain wall density that corresponds to the data density stored in the wire.

Therefore, another racetrack method, the racetrack memory 4.0, was proposed as a synthetic antiferromagnet or SAF. It is shown at the bottom of figure 3.1. The racetrack is built from two sub-racetracks with a mirrored magnetisation. An antiferromagnetic coupling is built by an ultra-thin layer in between. The main benefit of the antiferromagnetic structure is that the demagnetisation fields do not exist in an antiferromagnet. The net magnetisation of such a system is nearly zero as neighbouring magnetic moments will rotate to neutralise the magnetisation. Therefore, a higher density of domain walls can be achieved. Also, domain wall velocities of about $750ms^{-1}$ have been measured for such systems. Atomic layer deposition methods fabricate such racetrack systems [35].

In the next chapter, an antiferromagnetic description for critical currents will be presented for that chapter's ferromagnetic case.

3.2. Domain wall profile

Within this section, the domain wall profile of a ferromagentic nanowire system is derived based on the scientific paper by Tretiakov and Abanov [46]. It is important to analyse the domain wall properties before an application is feasible. The starting point for this calculation is the total magnetic energy E of such a system. It is given by the contributing interactions integrated over the nanowire volume $\int dV$:

$$E = \int dV (A(\nabla \boldsymbol{m})^2 + D\boldsymbol{m} \cdot (\nabla \times \boldsymbol{m}) + \lambda(1 - m_x^2)) \tag{3.1}$$

with a given exchange interaction constant A, a DMI strength D and an easy axis anisotropy along the nanowire direction x with a strength λ. For the ferromagnet, A is a positive valued constant. The DMI strength D is assumed to be constant along the wire. In the case of such a one-dimensional system, the spatial variation ∇ is just given by the variation along the wire $\nabla \to \partial/\partial x \equiv \partial$.

$$E = \int dV (A(\partial \boldsymbol{m})^2 + D\boldsymbol{m} \cdot (\hat{\boldsymbol{x}} \times \partial \boldsymbol{m}) + \lambda(1 - m_x^2)) \tag{3.2}$$

The magnetisation $\boldsymbol{m}$ is saturated and normalised $|\boldsymbol{m}| = 1$.
The LLG equation with spin-transfer torque (2.7) is used to describe the magnetisation

dynamics. A constant valued magnetisation inherits the property of $0.5\partial(\boldsymbol{m}^2) = \partial\boldsymbol{m} \cdot \boldsymbol{m} = 0$ meaning that the variation of $\boldsymbol{m}$ is perpendicular to $\boldsymbol{m}$ itself. Consequently, the spatial variation of the magnetisation can be described by a plane of solutions orthogonal to the magnetisation vector itself with two parameters $\Gamma(x,t)$ and $\Lambda(x,t)$ depending on space and time describing the two independent directions. Such an ansatz is shown in the following equation:

$$\partial\boldsymbol{m} = \Gamma(x,t)\hat{\boldsymbol{x}} \times \boldsymbol{m} + \Lambda(x,t)\boldsymbol{m} \times (\hat{\boldsymbol{x}} \times \boldsymbol{m}). \tag{3.3}$$

The Λ dependent term can be improved with the $bac - cab$ rule for triple products (A.1) into $\boldsymbol{m} \times (\hat{\boldsymbol{x}} \times \boldsymbol{m}) = \hat{\boldsymbol{x}} - m_x\boldsymbol{m}$. Therefore, the x component of the derivative is given by $\partial m_x = 1 - m_x^2$. The squared derivative can be edited as well (B.1): $(\partial\boldsymbol{m})^2 = (1 - m_x^2)(\Gamma^2 + \Lambda^2)$.

In the simplest case where no current is applied $\boldsymbol{\nu} = 0$ the time independent configuration minimizes the total magnetic energy E (3.2). The DMI term can be rearranged to $D\boldsymbol{m} \cdot (\hat{\boldsymbol{x}} \times \partial\boldsymbol{m}) = D\partial\boldsymbol{m} \cdot (\boldsymbol{m} \times \hat{\boldsymbol{x}}) = -D\partial\boldsymbol{m} \cdot (\hat{\boldsymbol{x}} \times \boldsymbol{m})$, since it is a spatial product. Afterwards, a completion of the square with the exchange term leads to:

$$E = \int dV (A \left(\partial\boldsymbol{m} - \frac{D}{2A}(\hat{\boldsymbol{x}} \times \boldsymbol{m}) \right)^2 + \left(\lambda - \frac{D^2}{4A} \right)(1 - m_x^2)). \tag{3.4}$$

The minimum of this equation depends on two contributing terms. It depends on the sign in front of $\lambda - \frac{D^2}{4A}$. On the one hand, if $4A\lambda < D^2$, then the second term is negative. Therefore, the total energy is at the minimum if the $1 - m_x^2$ factor is maximal, constraining $m_x = 0$. In this case, if $\partial\boldsymbol{m} = \frac{D}{2A}(\hat{\boldsymbol{x}} \times \boldsymbol{m})$ holds, the first of the two term vanishes. Then, the solution of $\boldsymbol{m}$ is given by a spiral because the spatial variation of the magnetisation is always orthogonal to itself and the nanowire axis x. While the x coordinate of $\boldsymbol{m}$ has to be zero to fulfil this constraint, the other two dimensions can be set to $\sin(\omega x)$ and $\cos(\omega x)$, neglecting a phase factor, depending on the chirality of the rotation. The ω of $\boldsymbol{m} = (0, \sin(\omega x), \cos(\omega x))^T$ is given by the prefactor in front of the rotation $\omega = \frac{D}{2A}$.

On the other hand, if $4A\lambda > D^2$, then the second term is positive and $1 - m_x^2$ needs to be minimal for a total minimum of the magnetic energy. $m_x = \pm 1$ are the two saturated magnetisation values leading to such a minimum. Both are the different ground states of the one-dimensional nanowire system. This implies that both are equally favourable since they are energetically identical. That is why the system should contain both states. Hence, a domain wall is needed to separate the ground state magnetisation values to build a stable state.

The spatial variation of $\boldsymbol{m}$ given by equation (3.3) can be inserted into the equation (3.4) using the properties given at (B.1):

$$E = \int dV (A(1 - m_x^2)(\Gamma^2 + \Lambda^2) + D\boldsymbol{m} \cdot (\hat{\boldsymbol{x}} \times (\Gamma\hat{\boldsymbol{x}} \times \boldsymbol{m} + \Lambda\boldsymbol{m} \times (\hat{\boldsymbol{x}} \times \boldsymbol{m}))) + \lambda(1 - m_x^2))$$

$$= \int dV \left(A \left(\Gamma - \frac{D}{2A} \right)^2 + A\Lambda^2 - \frac{D^2}{4A} + \lambda \right)(1 - m_x^2).$$

$$(3.5)$$

This term is minimised for $\Gamma = \frac{D}{2A}$ which is the same as the spiral prefactor ω. A parametrization of $m_x = \tanh(f(x))$ can be used to rewrite the total magnetic energy into an $f(x)$-only dependent form. $f(x)$ is a function of the spatial coordinate x along the nanowire describing the magnetisation value at this point. It is used for a Lagrangian type description of the magnetic energy.

$m_x = \tanh(f(x))$ inserted into $1 - m_x^2$, which resolves to $1 - \tanh(f(x))^2 = \frac{\cosh(f(x))^2 - \sinh(f(x))^2}{\cosh(f(x))^2} = \frac{1}{\cosh(f(x))^2}$. The hyperbolic functions inherit the property of $\cosh(f(x))^2 - \sinh(f(x))^2 = 1$ for every value $f(x)$. The Λ^2 is $f(x)$ dependent, which is given by $\Lambda = \partial f(x)$ (B.2). Hence, the total energy resolves to:

$$E = A \int dV \frac{\left((\partial f(x))^2 - \frac{D^2}{4A^2} + \frac{\lambda}{A}\right)}{\cosh(f(x))^2} = A \int dV \frac{\left((\partial f(x))^2 + \Xi^{-2}\right)}{\cosh(f(x))^2}. \qquad (3.6)$$

In this notation, $\Xi^{-2} = \frac{\lambda}{A} - \frac{D^2}{4A^2} = \frac{\lambda}{A} - \Gamma^2$ is dependent on the Γ factor of the minimised energy term.

Although, the total magnetic energy is the sum of all interactions integrated over the total space $\int dV$, this integration is a one-dimensional integral dx for the one-dimensional nanowire. Moreover, the function $f(x)$ as parametrization of m_x is only x dependent. Therefore, the total magnetic energy can be treated as Hamiltonian, describing the total energy of the system. The Noether theorem states that "every continuous symmetry of a system entails a conservation law" (Altland and Simons 2010 [3]). For Hamiltonians, such symmetry is given by a missing direct dependency of x to the integration parameter dx. The $f(x)$ dependency occurs only indirectly and therefore does not affect the Noether theorem.

Usually, a Hamiltonian is integrated over time dt, inheriting energy conservation if it is not directly time-dependent. In this case, the conservation is a "time" x that leads to the constant energy of the system. This energy has to be the same at every point meaning that the value at $x \to \infty$ can be used. The energy has to vanish at infinity because if it does not, the total energy of the system would be infinitely large. Combining this fact with the Noether theorem, stating that the total energy is conserved, implies that it has to be zero everywhere. Therefore, the integrand has to vanish: $(\partial f(x))^2 + \Xi^{-2} = 0$. As a result, the function $f(x)$ depends on x and Ξ after integrating over x: $f(x) = \pm \frac{x}{\Xi}$. The constant Λ is given by $\Lambda = \partial f(x) = \frac{1}{\Xi}$, which is x independent itself.

Based on this information, all three components of the magnetisation $\boldsymbol{m}$ can be calculated. The obvious starting coordinate is the m_x direction because it is the one used for the parametrization. $m_x = \tanh(f(x)) = \tanh \frac{x}{\Xi}$ and $|\boldsymbol{m}| = 1 = m_x^2 + m_y^2 + m_z^2$ can be combined:

$$1 = m_x^2 + m_y^2 + m_z^2 \longleftrightarrow m_x^2 + m_y^2 = 1 - m_x^2 = 1 - \tanh\left(\frac{x}{\Xi}\right)^2 = \frac{1}{\cosh\left(\frac{x}{\Xi}\right)^2}. \qquad (3.7)$$

3. Ferromagnetic domain wall description

The y and z component can be parametrised by a $\frac{\sin{(g)}}{\cosh{\left(\frac{x}{\Xi}\right)}}$ and $\frac{\cos{(g)}}{\cosh{\left(\frac{x}{\Xi}\right)}}$ function depending on $g(f)$ because of $\sin{(g)}^2 + \cos{(g)}^2 = 1$. The derivative taken from the ansatz dependent on g and the ansatz of the equation (3.3) can be compared to determine g. The computation of one of the components is sufficient and leads to $g(f(x)) = x\Gamma = \frac{xD}{2A}$ (B.3).

Therefore, the magnetisation of a ferromagnetic domain wall in a one-dimensional nanowire with a Dzyaloshinskii-Moriya interaction is given by a spiral solution of:

$$
\begin{aligned}
m_x &= \tanh{((x - x_0)/\Xi)} \\
m_y &= \frac{\cos{(\Gamma(x - x_0) + \phi)}}{\cosh{((x - x_0)/\Xi)}} \\
m_z &= \frac{\sin{(\Gamma(x - x_0) + \phi)}}{\cosh{((x - x_0)/\Xi)}}.
\end{aligned}
\tag{3.8}
$$

This domain wall has a position x_0 along the nanowire and a tilting angle of ϕ in the $y - z$ plane. The $\tanh{(x - x_0)}/\Xi = m_x$ rotates from one magnetisation value to the other, having $m_x = 0$ at x_0. The rotation is classified by a width of the tangent hyperbolic function that corresponds to the domain wall width:

$$
\Xi = \frac{1}{\sqrt{\frac{\lambda}{A} - \frac{D^2}{4A^2}}} = \frac{2A}{\sqrt{4\lambda A - D^2}}.
\tag{3.9}
$$

In the case of no DMI, the width is given by $\sqrt{A/\lambda}$. Also, $\Gamma = 0$ as in the case of no DMI, which shows that the m_y and m_z component do not rotate as sine and cosine along the domain wall but have a constant tilting angle dependency and a damping factor of the cosine hyperbolic fraction with the width Ξ. This domain wall is a Néel domain wall as shown in figure 2.1. The direction of the twisting from DMI is given by the DMI chirality, whether it favours left-handed or right-handed spirals [46].

To summarise, in a system without DMI, the domain wall will have a width of $\sqrt{A/\lambda}$ depending on the exchange interaction strength A and the anisotropic interaction strength λ. The exchange interaction favours a parallel alignment of the neighbouring magnetic moments. This means that the exchange interaction favours a bigger wall width. A larger wall has more magnetic moments within and the angle between the neighbouring moments can be smaller.

However, the anisotropic interaction favours a magnetisation direction along the anisotropic axis. This indicates that the spins having an angle to this axis are pulled in this direction. A greater domain wall possesses more magnetic moments out of plane of the anisotropic axis, which enhances the energy in the system. Therefore, the anisotropic strength favours a smaller domain wall given by the λ^{-1} factor. An interplay of both interactions leads to the resulting domain wall width.

Including DMI, a factor of D^2 - the DMI strength - arises within the square root dependency of the domain wall width. The DMI favours twisting structures and neighbouring orthogonal spins, leading to smaller domain wall structures. Nevertheless, there is a critical value for the DMI strength $D^2 > 4A\lambda$ at which the square root

of the domain wall width gets imaginary. Above this critical value, the ground state of the system will take on a spiral magnetisation direction where no domain wall can be built. This shows that the DMI can lead to smaller domain wall structures and a higher density of domains, which could be used for racetrack memory. However, this DMI strength has a critical value above which the system can not form domain walls at all.

The domain wall profile of a ferromagnetic nanowire system with exchange interaction, an easy axis anisotropy and DMI with an applied spin current is determined in the chapter on domain wall shedding because the formalism of the functional derivative is needed to use the LLG equation needed to determine the profile.

3.3. Rigid body treatment of a domain wall

In the last section, a domain wall profile of ferromagnetic nanowires was calculated. It will be shown that domain walls can be described as rigid structures with fewer variables, as the domain wall structure will not change drastically at low energies. The formalism can be used to determine the dynamics of domain walls - in the case of ferromagnetic and antiferromagnetic nanowires - to see if and how they can be implemented for applications such as a racetrack memory system. This section is based on calculations of the scientific papers of Rodrigues et al. [37] [38] and the corresponding Ph.D. thesis [36].

In a one-dimensional nanowire system with an easy axis anisotropy, the two ground states - given by a magnetisation direction following the wire axis or antiparallel - occur with the same probability. If both of them are present simultaneously, they are separated by a domain wall structure. This is a stable state, as long as there is no spin-polarised current applied that surpasses a critical value. In such a stable nanowire system, the domain wall can be translated along the wire or rotated around the wire axis without changing the profile of the domain wall.

If the current is greater than the critical value the domain wall will start to move along the current direction. Nevertheless, the underlying profile of the domain wall depends on the interaction strengths from the exchange, anisotropy and DMI, which was shown in the previous chapter in terms of the domain wall width Ξ (3.9). Changing the profile itself drastically would need currents higher than the critical current value so that it is stronger than the interactions of the system and favouring different configurations between the magnetic moments.

There could be a greater power consumption than necessary because the essential thing needed for an application such as a racetrack memory system is a domain wall movement that begins above the critical current. The regime reasonable to start looking at first is the start of the domain wall movement where the domain wall profile has a very similar structure to the time independent system. This approximation is used to describe the domain wall movement along the nanowire by just the centre coordinate and rotation of the domain wall instead of every magnetisation vector for

small currents. The description in terms of such coordinates can be crucial to get an unsophisticated domain wall movement. Without such a description, it would be much harder to determine if an applied spin current can manipulate the movement of a domain wall in such way that it can be used as an application.

A. A. Thiele [45] proposed a simplification to the LLG equation (2.2) in terms of the position of a magnetic domain instead of the magnetisation. The approach can be used in a very versatile way. Different domain wall properties [9] [47] or the dynamics of more complicated structures such as skyrmions [15] [21] and antiferromagnetic systems [48] can be determined. The position X or coordinate of the middle of the domain wall and the angle Φ it has to a set axis at this point are the two collective coordinates or soft modes used as governing degrees of freedom for the domain wall. A starting point in all of the cases is the Poisson bracket behaviour of the magnetisation vector based on its properties of an angular momentum $\{m_i(x), m_j(\tilde{x})\} = \varepsilon_{ijk} m_k(x)\delta(x - \tilde{x})$. This magnetisation can be mapped to magnetic moments depending on the spin direction which is behaving as an angular momentum $\boldsymbol{m} = -\gamma \boldsymbol{L}$, $\{L_i, L_j\} = \varepsilon_{ijk} L_k$.

The LLG equation (2.2) can be adapted into a Hamiltonian equation $\dot{\boldsymbol{m}} = \{\boldsymbol{m}, H\} + \Omega_{\boldsymbol{m}}$ with a Poisson bracket and $\Omega_{\boldsymbol{m}}$ containing all damping terms. These Poisson brackets derivatives depend on the generalised coordinates chosen to represent the phase space of the system $(\boldsymbol{q}, \boldsymbol{p})$. Different coordinates, such as the soft modes of the domain wall, will lead to different Poisson brackets and different Hamiltonian equations. All of those conjugated momenta express their equations of motion in the Hamiltonian formalism.

At first, the degrees of freedom of the magnetisation vector $\boldsymbol{m}$ need to be reduced to the set of new coordinates to determine the Poisson bracket relation between those new conjugated momenta. The magnetisation is represented as $\boldsymbol{m}(\boldsymbol{r}, t) \equiv \boldsymbol{m}(\boldsymbol{r}, \boldsymbol{\eta}(t))$ where the time dependency is pulled into the new set of coordinates $\boldsymbol{\eta}$. The time evolution of the magnetisation can be revised applying the chain rule:

$$\dot{\boldsymbol{m}}(\boldsymbol{r}, t) = \sum_{\boldsymbol{\eta}_i} \dot{\boldsymbol{\eta}}_i \partial_{\boldsymbol{\eta}_i} \boldsymbol{m} \tag{3.10}$$

taking the summation over all new coordinates. In this formalism, the time derivative $\dot{\boldsymbol{m}}(\boldsymbol{r}, t)$ can be inserted into the LLG equation together with a multiplication by $\int dV(\boldsymbol{m} \times \partial_{\boldsymbol{\eta}_i} \boldsymbol{m})$. The left side of the equation takes the following form:

$$
\begin{aligned}
\int dV(\boldsymbol{m} \times \partial_{\boldsymbol{\eta}_i} \boldsymbol{m}) \cdot \dot{\boldsymbol{m}} &= \int dV \boldsymbol{m} \cdot (\partial_{\boldsymbol{\eta}_i} \boldsymbol{m} \times \dot{\boldsymbol{m}}) \\
&= \int dV \boldsymbol{m} \cdot (\partial_{\boldsymbol{\eta}_i} \boldsymbol{m} \times \dot{\boldsymbol{m}}) = \int dV \boldsymbol{m} \cdot (\partial_{\boldsymbol{\eta}_i} \boldsymbol{m} \times \sum_{\boldsymbol{\eta}_j} \dot{\boldsymbol{\eta}}_j \partial_{\boldsymbol{\eta}_j} \boldsymbol{m}) \\
&= \sum_{\boldsymbol{\eta}_j} \int dV \boldsymbol{m} \cdot (\partial_{\boldsymbol{\eta}_i} \boldsymbol{m} \times \partial_{\boldsymbol{\eta}_j} \boldsymbol{m}) \dot{\boldsymbol{\eta}}_j = G_{ij}[\boldsymbol{\eta}] \dot{\boldsymbol{\eta}}_j.
\end{aligned}
\tag{3.11}
$$

At first, the spatial product is changed according to (A.3). Then, the ansatz for the time derivative of the magnetisation is inserted. After that, a new quantity called

gyroscopic tensor $G_{ij}[\boldsymbol{\eta}]$ is defined. The right side can be treated similarly:

$$
\begin{aligned}
&\int dV(\boldsymbol{m} \times \partial_{\boldsymbol{\eta}_i} \boldsymbol{m}) \cdot (\gamma \boldsymbol{m} \times \boldsymbol{H}_{\text{eff}} + \alpha \boldsymbol{m} \times \dot{\boldsymbol{m}}) \\
&= \int dV(\boldsymbol{m} \times \partial_{\boldsymbol{\eta}_i} \boldsymbol{m}) \cdot (\gamma \boldsymbol{m} \times \boldsymbol{H}_{\text{eff}} + \alpha \boldsymbol{m} \times \sum_{\boldsymbol{\eta}_j} \dot{\boldsymbol{\eta}}_j \partial_{\boldsymbol{\eta}_j} \boldsymbol{m})) \\
&= \sum_{\boldsymbol{\eta}_j} \int dV(\gamma(\boldsymbol{m}^2(\partial_{\boldsymbol{\eta}_j}\boldsymbol{m} \cdot \boldsymbol{H}_{\text{eff}}) + (\partial_{\boldsymbol{\eta}_j}\boldsymbol{m} \cdot \boldsymbol{m})(\boldsymbol{m} \cdot \boldsymbol{H}_{\text{eff}})) + \\
&\quad \alpha \boldsymbol{m}^2(\partial_{\boldsymbol{\eta}_i}\boldsymbol{m} \cdot \partial_{\boldsymbol{\eta}_j}\boldsymbol{m})\dot{\boldsymbol{\eta}}_j + \alpha(\partial_{\boldsymbol{\eta}_i}\boldsymbol{m} \cdot \boldsymbol{m})(\partial_{\boldsymbol{\eta}_j}\boldsymbol{m} \cdot \boldsymbol{m})\dot{\boldsymbol{\eta}}_j) \\
&= \sum_{\boldsymbol{\eta}_j} \int dV(\gamma \partial_{\boldsymbol{\eta}_i}\boldsymbol{m} \cdot \frac{\delta E}{\delta \boldsymbol{m}} + \alpha(\partial_{\boldsymbol{\eta}_i}\boldsymbol{m} \cdot \partial_{\boldsymbol{\eta}_j}\boldsymbol{m})\dot{\boldsymbol{\eta}}_j) \\
&= \gamma \frac{\delta E}{\delta \boldsymbol{\eta}_i} + \alpha D_{ij}[\boldsymbol{\eta}]\dot{\boldsymbol{\eta}}_j
\end{aligned}
\tag{3.12}
$$

At first, the Lagrange identity (A.2) is used to rewrite the double cross product terms. Then, $\boldsymbol{m}^2 = 1$ is used to revise the equation because the constant length of the vector shows that all derivatives need to be perpendicular to the vector itself $\partial_{\boldsymbol{\eta}_j}\boldsymbol{m} \cdot \boldsymbol{m} = 0$. In this case, a second quantity, called viscosity tensor $D_{ij}[\boldsymbol{\eta}]$, is defined together with a generalised force containing an effective field depending on the new coordinates $\frac{\delta E}{\delta \boldsymbol{\eta}_i}$. The total LLG equation or Thiele equation is given by:

$$
G_{ij}[\boldsymbol{\eta}]\dot{\boldsymbol{\eta}}_j = \gamma \frac{\delta E}{\delta \boldsymbol{\eta}_i} + \alpha D_{ij}[\boldsymbol{\eta}]\dot{\boldsymbol{\eta}}_j.
\tag{3.13}
$$

The index j denotes the collective coordinate j while there is a summation over all collective coordinates i.

The conjugated momenta can be determined using the spin Berry phase of the action. It is a geometrical phase term appearing because of the precession of the magnetisation [36]. It contributes to the action E of the system as a kinetic energy term $E = E_B - \int H dV$. The spin Berry phase can be defined by the area enclosed by the precession $\boldsymbol{A}$ multiplied by the change of the magnetisation $E_B = \int dt \boldsymbol{A} \cdot \dot{\boldsymbol{m}}$. The dimensionality of the action is the same as the one of the spin Berry phase since it is a part of it: $E_B \sim \int dt \boldsymbol{p} \cdot \dot{\boldsymbol{q}}$. The canonical variables can be determined by comparing both definitions to get $\boldsymbol{\eta}_i = \boldsymbol{q}_i$ and $\int dV \boldsymbol{A} \cdot \partial_{\boldsymbol{\eta}_i}\boldsymbol{m} = \boldsymbol{p}_i$. The generalised coordinates are given by the collective coordinates and the generalised momenta depend on the Berry phase contribution arising from the magnetisation vectors. The general Poisson bracket for the collective coordinates in the phase space of $(\boldsymbol{q}, \boldsymbol{p})$ is defined by:

$$
\{\boldsymbol{\eta}_i, \boldsymbol{\eta}_j\} = \sum_k \left(\frac{\partial \boldsymbol{\eta}_i}{\partial \boldsymbol{q}_k} \frac{\partial \boldsymbol{\eta}_j}{\partial \boldsymbol{p}_k} - \frac{\partial \boldsymbol{\eta}_i}{\partial \boldsymbol{p}_k} \frac{\partial \boldsymbol{\eta}_j}{\partial \boldsymbol{q}_k} \right).
\tag{3.14}
$$

The spatial derivative of $\boldsymbol{p}_i$ is needed to determine this structure. It is given by $\partial_{\boldsymbol{\eta}_j}\boldsymbol{p}_i = G_{ij}[\boldsymbol{\eta}]$ [36]. The derivative of the collective coordinates with respect to the

newly defined momentum can be solved using the gyrotropic tensor $\frac{\partial \boldsymbol{\eta}_i}{\partial \boldsymbol{p}_k} = (\frac{\partial \boldsymbol{p}_k}{\partial \boldsymbol{\eta}_i})^{-1} = G_{ki}^{-1} = -G_{ik}^{-1}$. In this case, the general Poisson bracket of two collective coordinates in the $(\boldsymbol{q}, \boldsymbol{p})$ space is:

$$\begin{aligned}
\{\boldsymbol{\eta}_i, \boldsymbol{\eta}_j\} &= \sum_k \left(\frac{\partial \boldsymbol{\eta}_i}{\partial \boldsymbol{\eta}_k} \frac{\partial \boldsymbol{\eta}_j}{\partial \boldsymbol{p}_k} - \frac{\partial \boldsymbol{\eta}_i}{\partial \boldsymbol{\eta}_k} \frac{\partial \boldsymbol{\eta}_j}{\partial \boldsymbol{q}_k} \right) = \sum_k \left(\delta_{ik} \frac{\partial \boldsymbol{\eta}_j}{\partial \boldsymbol{p}_k} - \delta_{jk} \frac{\partial \boldsymbol{\eta}_i}{\partial \boldsymbol{p}_k} \right) \\
&= \sum_k \left(\delta_{ik} G_{kj}^{-1} - \delta_{jk} G_{ki}^{-1} \right) = G_{ij}^{-1} - G_{ji}^{-1} = 2G_{ij}^{-1}.
\end{aligned} \tag{3.15}$$

The derivative of the collective coordinate j with respect to the coordinate i can only be unequal to zero if the indices are the same.

In the case of the collective coordinates $\boldsymbol{\eta}_i = X$ and $\boldsymbol{\eta}_j = \Phi$, $G_{X\Phi}^{-1}$ needs to be determined:

$$\begin{aligned}
\{X, \Phi\} &= 2G_{X,\Phi}^{-1} = 2(\int dV \boldsymbol{m} \cdot (\partial_X \boldsymbol{m} \times \partial_\Phi \boldsymbol{m}))^{-1} = -2(\int dV \boldsymbol{m} \cdot (\partial \boldsymbol{m} \times (\hat{\boldsymbol{n}} \times \boldsymbol{m})))^{-1} \\
&= -2(\int dV \boldsymbol{m} \cdot (\hat{\boldsymbol{n}}(\partial \boldsymbol{m} \cdot \boldsymbol{m}) - \boldsymbol{m}(\partial \boldsymbol{m} \cdot \hat{\boldsymbol{n}})))^{-1} \\
&= 2(\int dV \boldsymbol{m} \cdot (\boldsymbol{m}(\partial \boldsymbol{m} \cdot \hat{\boldsymbol{n}})))^{-1} = 2(\hat{\boldsymbol{n}} \cdot \int dV \partial \boldsymbol{m})^{-1} = \pm 2/2 = \pm 1
\end{aligned} \tag{3.16}$$

The Poisson bracket $\{X, \Phi\}$ of the two collective coordinates X and Φ is a particular case of the relation (3.15) for one set of coordinates given by just two soft modes. These two modes describe the total domain wall behaviour for small currents. The inverse of the gyrotropic tensor $G_{X,\Phi}^{-1}$ is determined using the ansatz:

$$d\boldsymbol{m}(x) = -dX\partial \boldsymbol{m}(x) \pm d\Phi \hat{\boldsymbol{n}} \times \boldsymbol{m}(x) \tag{3.17}$$

for the change of the magnetisation with respect to the two coordinates. Both soft modes span a plane of solutions orthogonally to $\boldsymbol{m}$ as in the ansatz (3.3) for the domain wall width determination. The $d\boldsymbol{m}$ denotes a spatial change of $\boldsymbol{m}$. The dX and $d\Phi$ denote the change of the two soft modes. The change concerning the angle Φ is perpendicular to the magnetisation itself and $\hat{\boldsymbol{n}}$, a vector pointing along the nanowire. This ensures a rotation of the rigid wall around the wire. The change of the middle of the domain wall dX is antiparallel to the spatial derivative of $\boldsymbol{m}$. In this case, the domain wall moves intuitively because the magnetisation changes towards the end of the domain wall when moving in the front direction.

Using such an ansatz, the derivative with respect to X translates into the $\partial \boldsymbol{m}$ term while the ∂_Φ derivative is leads to the $\hat{\boldsymbol{n}} \times \boldsymbol{m}$ contribution straight from the variation definition itself.

After the insertion of both into the gyrotropic tensor, the bac-cab rule (A.1) can be used to rewrite the double cross product. The first term vanishes because $\partial \boldsymbol{m} \cdot \boldsymbol{m} = 0$

due to the constant length constraint of $\boldsymbol{m}$. In the second term, the $\hat{\boldsymbol{n}}$ points along the nanowire direction independently of the integration and can be pulled out of the integration. Also, a $\boldsymbol{m}^2 = 1$ term appears, meaning that the remaining term to be integrated is given by $\partial \boldsymbol{m}$. However, the integration of a derivative reduces to the boundary values of the expression itself, in this case, the magnetisation $\boldsymbol{m}$.

The magnetisation can have two different values, pointing along the nanowire or antiparallel, whereas the nanowire direction vector is defined according to the wire direction. Both point in the x direction with a normalised magnitude. Depending on the domain wall type, there are two cases for magnetisation. The first one is a tail-to-tail domain wall with a magnetisation of -1 at $-\infty$ and $+1$ at $+\infty$. In this case, the total integral is $1 \cdot (1 - (-1)) = 2$. The second case is a head-to-head domain wall where the magnetisation is pointing towards each other. In this case, the integral is $1 \cdot (-1 - (+1)) = -2$.

Inserting both cases into the Poisson bracket determination, distinguishing the two domain wall types with a $\pm$ sign shows $\{X, \Phi\} = 2(\pm 2)^{-1} = \pm 1$. This change of sign from tail-to-tail domain wall $+$ to head-to-head domain wall $-$ is essential when the Hamiltonian equations for X and Φ in the domain wall system are determined.

The magnetic energy of the system E depends on the Hamiltonian H of the system. H includes all interactions considered to be impactful to the time evolution of the system. These contributions are given by the exchange interaction, the anisotropic interaction and they could include DMI. Since the Hamiltonian is time independent because the interactions do not change with time, the change of the total magnetic energy is given by:

$$
\begin{aligned}
\dot{E} &= \int dV \dot{H} = \int dV \frac{\delta H}{\delta \boldsymbol{m}} \cdot \dot{\boldsymbol{m}} = \int dV \, \boldsymbol{H}_{\text{eff}} \cdot \dot{\boldsymbol{m}} \\
&= \nu \partial_X E - \frac{1}{\gamma} \int dV (\alpha \dot{\boldsymbol{m}} + \beta \nu \partial \boldsymbol{m})(\dot{\boldsymbol{m}} + \nu \partial \boldsymbol{m}).
\end{aligned}
\tag{3.18}
$$

The LLG equation (2.7) can be inserted for the $\dot{\boldsymbol{m}}$. The latter is linked and adapted to the second line in the equation (C.1). The first term is the non-dissipative contribution to the change of the total magnetic energy, whereas the integral term depends linearly on both damping constants α and β. Higher order contributions are negligible since the damping constants are much smaller than one.

In the case of no damping, $\alpha = \beta = 0$, the corresponding Hamiltonian equation of motion is given by:

$$
\dot{E} = \{E, H_m\} = \nu \partial_X E
\tag{3.19}
$$

with an effective Hamiltonian $H_m(X, \Phi)$ describing the time evolution. The energy of the system is increases over time when a current is applied. Also, without a current it should not change and the effective Hamiltonian should be given by the Hamiltonian H containing the relevant interactions of the nanowire system. An effective Hamiltonian of $H_m = E(X, \Phi) \pm \nu \Phi$ fulfills such a requirement, which is shown in equation (C.2). Using this information, the Hamiltonian equations for the collective coordinates are

given by:

$$\dot{X} = \{X, H_m\} + \Omega_X = \pm\partial_\Phi H_m + \Omega_X$$

$$(3.20)$$

$$\dot{\Phi} = \{\Phi, H_m\} + \Omega_\Phi = \pm\partial_X H_m + \Omega_\Phi.$$

Those two equations determine the domain wall movement along the nanowire studied as a rigid object. If damping is included, the Hamiltonian equations have a non-vanishing damping factor Ω_i which can be determined using the second term of the equation (3.18). The Poisson brackets reform to the partial derivatives combined with a $\pm$ sign depending on the type of the domain wall because of $\{X, \Phi\} = \pm 1$ and $H_m(X, \Phi)$. Inserting H_m and neglecting the damping term leads to $\dot{X} \sim \pm\partial_\Phi E + \nu$. The domain wall follows the spin-polarised current independently of the domain wall type.

This formalism can be used to simulate and analyse domain wall behaviour at low energy levels and can be pursued to more complex systems such as skyrmions [15] and antiferromagnetic material [48]. In antiferromagnetic material, the formalism can be described for two sets of ferromagnetic coordinates when the antiferromagnet is treated as a combination of two ferromagnetic sublattices. Each ferromagnetic sublattice occupies one domain wall. One of them is a head-to-head domain wall and the other is a tail-to-tail domain wall to ensure zero net magnetisation.

Here, the collective coordinates can be described by combining the sublattice domain wall position $X = (X_1 + X_2)/2$ as the centre and $\Phi = \Phi_2 - \Phi_1$ denoting the angle between the magnetisation vectors at the centre. The magnetisation of the domain wall can be described by $(X_1 + X_2)/2$. In all three definitions, the indices 1 and 2 denote the sublattice one and two. The formalism extends to an effective Hamiltonian in terms of all four collective coordinates. Likewise, it extends to Hamiltonian equations for the combined coordinates having the same structure as the equation (3.20). The antiferromagnetic formalism represented in this way is shown more accurately in the scientific paper of Rodrigues et al. [37].

In conclusion, the width and profile of one-dimensional nanowire system domain walls were derived in the previous section, acknowledging both cases with and without applied spin current. However, the dynamics of such a system can only be directly described by the LLG equation. The collective coordinate approach was used to reduce the number of degrees of freedom to just two variables. The time evolution of those two soft modes have been derived. The influence of an external spin-polarised current has been analysed concerning the energy of the magnetic system and the movement of the domain wall. It was important to see that such a spin-polarised current can move a domain wall and that an application to a system like a racetrack memory system is possible.

3.4. Domain wall shedding

So far, the structure and dynamics of ferromagnetic domain walls have been analysed. Next, the domain wall creation is needed to make an application in racetrack memory systems possible. In this section, a spin-polarised current will be applied along with a semi-infinitely long one-dimensional nanowire system with a pinning at the origin and an easy axis anisotropy as shown in figure 3.2. A current value beyond which domain walls will start to detach from the pinning point and move along the wire is calculated based on the scientific reports of Sitte et al. [39] and Rodrigues et al. [38]. Also, as is the domain wall profile with current based on the calculations of Rodrigues et al. [38]. This procedure was not applied in the domain wall profile chapter, since there would have been a need to calculate the required steps twice.

The detaching, creation or shedding of domain walls is the third major step of a domain wall description. At first, the width and profile without current were determined. After that, the movement of a domain wall as a rigid object was analysed. A method of controlled creation at some point of the wire is needed to write new data in a racetrack memory system by creating domain walls after a particular time or distance. The procedure of the domain wall creation and the system's setup is shown in figure 3.2. A one-dimensional semi-infinitely long nanowire with an easy axis anisotropy along the x-axis is modified by pinning of the magnetisation along the z-axis where $\boldsymbol{m}(x = 0) = \hat{\boldsymbol{z}}$. Such pinning can be achieved trough an external magnetic field or some inhomogeneity in the material itself. The case of no spin current applied is shown at the top of figure 3.2. The magnetisation rotates from the z direction to the x direction or the negative x direction in the $x - z$ plane as the anisotropy favours both states equally.

When a sufficiently small spin-polarised current is applied, the magnetisation will start to twist out of plane and acquires a y component. This twisting is amplified by the DMI favouring chiral states and is shown in the middle of the plot. At the bottom, a situation with a current greater than the critical current value is displayed. Not only does the magnetisation twist off, but a domain wall starts travelling along the wire direction. This is called shedding of the domain wall or domain wall creation by a spin-polarised current.

In the formalism of this chapter, the LLG equation with spin-transfer torque (2.7) is used to describe the magnetisation dynamics. Since it is a equation depending both on time and spatial derivatives, a symmetry analyses based on the Noether theorem [3] is used to adapt the equation. However, before the LLG equation is fully usable the effective field needs to be calculated. This is done by a functional derivative of the total magnetic energy E with respect to the magnetisation change:

$$\frac{\delta E}{\delta \boldsymbol{m}} = \frac{\delta}{\delta \boldsymbol{m}} \int dV (A(\partial \tilde{\boldsymbol{m}})^2 + D\tilde{\boldsymbol{m}} \cdot (\hat{\boldsymbol{x}} \times \partial \tilde{\boldsymbol{m}}) + \lambda(1 - m_x'^2)). \tag{3.21}$$
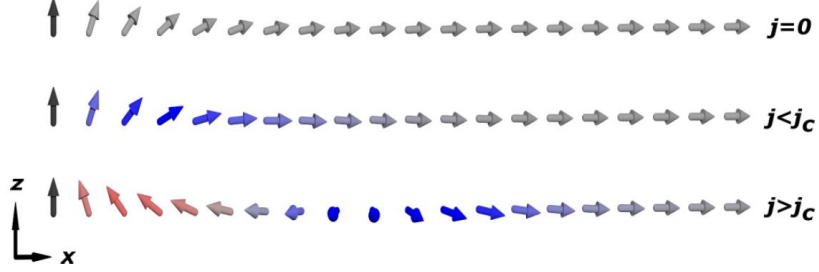
Figure 3.2.: The figure shows the semi-infinitely long nanowire along the x direction with a pinned magnetisation along the z direction at the origin. At the top, no current is applied and the magnetisation is fully in the $x - z$ plane. In the middle, a spin-polarised current below the critical current value is applied along the wire direction, leading to an $\boldsymbol{m}$ twisting out of the $x - z$ plane. Above the critical value, a domain wall starts to travel along the wire, as shown at the bottom. $\boldsymbol{j}$ denotes the spin-polarised current. Source: Sitte et al. 2015: [39]

Each term can be calculated individually because of the integrals linearity, starting with the exchange interaction:

$$\frac{\delta E}{\delta \boldsymbol{m}} \sim \frac{\delta}{\delta \boldsymbol{m}} \int dV A(\partial \tilde{\boldsymbol{m}})^2 = \int dV \frac{\delta}{\delta \boldsymbol{m}} A(\partial \tilde{\boldsymbol{m}})^2 = 2A \int dV \partial \tilde{\boldsymbol{m}} (\frac{\delta}{\delta \boldsymbol{m}} \partial \tilde{\boldsymbol{m}})$$

$$= 2A \int dV \partial \tilde{\boldsymbol{m}} (\partial \frac{\delta \tilde{\boldsymbol{m}}}{\delta \boldsymbol{m}}) = -2A \int dV \partial^2 \tilde{\boldsymbol{m}} \frac{\delta \tilde{\boldsymbol{m}}}{\delta \boldsymbol{m}} \tag{3.22}$$

$$= -2A \int dV \partial^2 \tilde{\boldsymbol{m}} \delta(\boldsymbol{m} - \tilde{\boldsymbol{m}}) = -2A \partial^2 \boldsymbol{m}$$

At the start of the calculation, the functional derivative is moved into the integral. After that, the chain rule of differentiation is applied leading to two similar terms. Then, a partial integration of the $\partial \frac{\delta \tilde{\boldsymbol{m}}}{\delta \boldsymbol{m}}$ term is needed because the spatial derivative of the functional derivative is ambiguous. Since there is no magnetisation change at the ground state of the nanowire the partial derivative of $\boldsymbol{m}$ is zero at the integration boundaries where domain walls are not located. The definition of a functional derivative to the vector itself $\frac{\delta \tilde{\boldsymbol{m}}}{\delta \boldsymbol{m}} = \delta(\boldsymbol{m} - \tilde{\boldsymbol{m}})$ is given by a delta function that vanishes when the functional derivative is evaluated at the same point $\boldsymbol{m}$. Therefore, the integration over the nanowire volume is cancelled with this delta function, leading to the result of $-2A\partial^2 \boldsymbol{m}$.

The second term is the Dzyaloshinskii-Moriya interaction with a constant strength D. The prefactor is no tensor as the system is one-dimensional. The calculation can be done using the epsilon tensor ε_{ijk} to rewrite the cross product. Therefore, a more general ansatz will be calculated using the DMI term with ∇ instead of ∂, substituting

it back afterwards.

$$
\begin{aligned}
\frac{\delta E}{\delta \boldsymbol{m}} &\sim \frac{\delta}{\delta \boldsymbol{m}} \int dV D\tilde{\boldsymbol{m}} \cdot (\nabla \times \tilde{\boldsymbol{m}}) = D \int dV \frac{\delta}{\delta \boldsymbol{m}} (\tilde{\boldsymbol{m}} \cdot (\nabla \times \tilde{\boldsymbol{m}})) \\
&= D \int dV \frac{\delta}{\delta m_i} \varepsilon_{ijk} \tilde{m}_i \partial_j \tilde{m}_k = D \int dV \varepsilon_{ijk} (\frac{\delta \tilde{m}_i}{\delta m_i} (\partial_j \tilde{m}_k) + \tilde{m}_i \frac{\delta}{\delta m_i} (\partial_j \tilde{m}_k)) \\
&= D \int dV \varepsilon_{ijk} (\frac{\delta \tilde{m}_i}{\delta m_i} (\partial_j \tilde{m}_k) - \partial_j \tilde{m}_i \frac{\delta \tilde{m}_k}{\delta m_i}) \\
&= D \int dV \varepsilon_{ijk} \frac{\delta \tilde{m}_i}{\delta m_i} (\partial_j \tilde{m}_k) + \varepsilon_{kji} \frac{\delta \tilde{m}_i}{\delta m_i} (\partial_j \tilde{m}_k) \\
&= 2D \int dV \nabla \times \tilde{\boldsymbol{m}} \delta(\tilde{\boldsymbol{m}} - \boldsymbol{m}) = 2D \nabla \times \boldsymbol{m}
\end{aligned}
\tag{3.23}
$$

At first, the functional derivative is moved into the integral. Then, the term is adjusted using the epsilon tensor. The functional derivates dimension is the same as the dimension of the DMI term, denoted by the subscript i. The product rule of differentiation yields two terms. The second one of these terms is edited by a partial integration in the third line due to the ambiguous derivative of $\partial_j \tilde{m}_k$. In the fourth line, the index of the second epsilon tensor is rotated anti cyclic, which corresponds to adding a minus sign. This shows that both terms show the same derivatives in the same dimension.

Therefore, a factor of two arises in the last line when the terms are adjusted to the vectorial notation. The delta function can be resolved, yielding a $2D\nabla \times \boldsymbol{m}$ term. In the case of a one-dimensional nanowire, this term is reduced to $2D\hat{\boldsymbol{x}} \times \partial \boldsymbol{m}$.

The third contributing interaction is given by the anisotropic interaction favouring spin states in the x-axis. The corresponding functional derivative can be calculated in the following way:

$$
\begin{aligned}
\frac{\delta E}{\delta \boldsymbol{m}} &\sim \frac{\delta}{\delta \boldsymbol{m}} \int dV \lambda(1 - \tilde{m}_x^2) = \lambda \int dV \frac{\delta}{\delta \boldsymbol{m}} (1 - \tilde{m}_x^2) \\
&= \lambda \int dV \frac{\delta}{\delta \boldsymbol{m}} (1 - (\hat{\boldsymbol{x}} \cdot \tilde{\boldsymbol{m}})^2) = -2\lambda \int dV (\hat{\boldsymbol{x}} \cdot \tilde{\boldsymbol{m}}) \frac{\delta \tilde{\boldsymbol{m}}}{\delta \boldsymbol{m}} \hat{\boldsymbol{x}} \\
&= -2\lambda \int dV (\hat{\boldsymbol{x}} \cdot \tilde{\boldsymbol{m}}) \hat{\boldsymbol{x}} \delta(\tilde{\boldsymbol{m}} - \boldsymbol{m}) = -2\lambda(\hat{\boldsymbol{x}} \cdot \boldsymbol{m}) \hat{\boldsymbol{x}} = -2\lambda m_x \hat{\boldsymbol{x}}.
\end{aligned}
\tag{3.24}
$$

The functional derivative is moved into the integral, as in the previous cases. Then, the $\tilde{m}_x$ term is edited into a scalar product of $\tilde{\boldsymbol{m}}$ with the x-axis unity vector. After that, the chain rule is applied. A factor of two arises from the squared term. The derivative of $\hat{\boldsymbol{x}}$ with respect to $\boldsymbol{m}$ is zero. Hence, the functional derivative of $\boldsymbol{m}$ resolves into a delta function, which cancels the integral term. It is important to note that this derivative is unequal to zero only in the x direction, since m_x is the only coordinate contributing. The resulting segment is given by $-2\lambda m_x \hat{\boldsymbol{x}}$.

The three terms added up express the total effective field of the one dimensional nanowire system of a ferromagnet. This is given by:

$$
\frac{\delta E}{\delta \boldsymbol{m}} = -2A\partial^2 \boldsymbol{m} + 2D\hat{\boldsymbol{x}} \times \partial \boldsymbol{m} - 2\lambda m_x \hat{\boldsymbol{x}}.
\tag{3.25}
$$

3. Ferromagnetic domain wall description

The magnetisation will evolve around this direction according to the LLG equation (2.7):

$$\dot{\boldsymbol{m}} = \gamma \boldsymbol{m} \times (-2A\partial^2 \boldsymbol{m} + 2D\hat{\boldsymbol{x}} \times \partial \boldsymbol{m} - 2\lambda m_x \hat{\boldsymbol{x}}) + \alpha \boldsymbol{m} \times \dot{\boldsymbol{m}} - \nu \partial \boldsymbol{m} + \beta \boldsymbol{m} \times \nu \partial \boldsymbol{m}. \quad (3.26)$$

Figure 3.2 displays the three stages expected to happen in the nanowire system with added pinning. When no current is applied, the magnetisation will twist as a 90 degree domain wall with a width whose magnitude depends on the exchange interaction and the anisotropic strength (3.9). The current will twist off the magnetisation at the pinning for small currents since it is perpendicular to the magnetisation at this point. However, this configuration is still a static one. A movement in the system starts when the current is stronger than a certain critical value. That is why the critical current value can be determined by a calculation based on the static state with $\dot{\boldsymbol{m}} = 0$.
The LLG equation reduces to:

$$0 = \gamma \boldsymbol{m} \times (-2A\partial^2 \boldsymbol{m} + 2D\hat{\boldsymbol{x}} \times \partial \boldsymbol{m} - 2\lambda m_x \hat{\boldsymbol{x}}) - \nu \partial \boldsymbol{m} + \beta \boldsymbol{m} \times \nu \partial \boldsymbol{m}. \quad (3.27)$$

The Noether theorem states that "every continuous symmetry of a system entails a conservation law" (Altland and Simons 2010 [3]). The static nanowire system has two of these symmetries that can be used. A translation of the nanowire along the x-axis does not change the magnetic energy of the system. Since the wire is semi-infinitely long the origin of the system is chosen to be at $x = 0$, but it could take any other value as well. This symmetry implies that the linear magnetic momentum is a conserved quantity.
Also, a similar consideration can be taken into account for the conserved quantity of the angular momentum. A rotation of the system around the x-axis may change the angle of a magnetisation structure to one of the other two axes. However, energetically an angle does not change the free energy. The Noether theorem states that a rotation invariance around the x-axis entails the conservation of the total angular momentum around that axis in terms of magnetisation. Both of these conservation laws are valid as long as there is no non-conservative torque present [38]. Mathematically, the two conservation laws can be shown by multiplying the static LLG equation by $\hat{\boldsymbol{x}}$ and $\boldsymbol{m} \times \partial \boldsymbol{m}$.
The first case dealt with is the $\hat{\boldsymbol{x}}$ one.

$$0 = \hat{\boldsymbol{x}} \cdot \left[\gamma \boldsymbol{m} \times (-2A\partial^2 \boldsymbol{m} + 2D\hat{\boldsymbol{x}} \times \partial \boldsymbol{m} - 2\lambda m_x \hat{\boldsymbol{x}}) - \nu \partial \boldsymbol{m} + \beta \boldsymbol{m} \times \nu \partial \boldsymbol{m} \right] \quad (3.28)$$

Since a longer calculation is needed, it is shown in the appendix up to equation (D.2). The resulting equation with dissipation ($\beta \neq 0$) is given by:

$$\partial \left(2A\hat{\boldsymbol{x}} \cdot (\boldsymbol{m} \times \partial \boldsymbol{m}) + D(m_x + \frac{\nu}{2D\gamma})^2 \right) = \frac{\beta \nu}{\gamma} \hat{\boldsymbol{x}} \cdot (\boldsymbol{m} \times \partial \boldsymbol{m}). \quad (3.29)$$

In the second case, the static LLG is multiplied by $\boldsymbol{m} \times \partial \boldsymbol{m}$:

$$0 = (\boldsymbol{m} \times \partial \boldsymbol{m}) \cdot \left[\gamma \boldsymbol{m} \times (-2A\partial^2 \boldsymbol{m} + 2D\hat{\boldsymbol{x}} \times \partial \boldsymbol{m} - 2\lambda m_x \hat{\boldsymbol{x}}) - \nu \partial \boldsymbol{m} + \beta \boldsymbol{m} \times \nu \partial \boldsymbol{m} \right].$$

$$(3.30)$$

As in the first case, the calculation is described in the appendix up to equation (D.1) and shown in the following:

$$\partial \left(A(\partial \boldsymbol{m})^2 + \lambda m_x^2 \right) = \frac{\beta \nu}{\gamma} (\partial \boldsymbol{m})^2. \tag{3.31}$$

The non-dissipative time evolution of the system is justifiable for the same reason as the static case treatment. In the vicinity of the critical current, the creation and movement of domain walls are just starting. This means that the movement is slow and can be treated adiabatically or in other words without energy loss or dissipation. In this case, the damping constants α and β are negligible.

$$\partial \left(2A\hat{\boldsymbol{x}} \cdot (\boldsymbol{m} \times \partial \boldsymbol{m}) + D(m_x + \tfrac{\nu}{2D\gamma})^2 \right) = 0 \text{ and } \partial \left(A(\partial \boldsymbol{m})^2 + \lambda m_x^2 \right) = 0$$

In both terms, the derivatives of the quantities inside the bracket are equal to zero. Hence, these quantities have to be constant. This shows that both the linear momentum along the x direction and the total angular momentum along the x direction are conserved. Those constant values are compared for two special cases where the magnetisation is unambiguous. At $x = 0$, the magnetisation points explicitly along the $\boldsymbol{m} = \hat{\boldsymbol{z}}$ direction. At $x \to \infty$, there is no change in the magnetisation $\partial \boldsymbol{m} = 0$ because the magnetisation will point along the anisotropic direction $\boldsymbol{m} = \hat{\boldsymbol{x}}$ as it is the ground state of the system.
On the one hand, combining both equal constant values in the case of the angular momentum leads to:

$$-\partial m_y|_{x=0} = \frac{D}{2A} \pm \frac{\nu}{2A\gamma}. \tag{3.32}$$

This is shown in the appendix in the equation (D.3). On the other hand, the same approach used for the linear momentum equation leads to:

$$(\partial \boldsymbol{m})^2|_{x=0} = \frac{\lambda}{A}. \tag{3.33}$$

This calculation is shown in the equation (D.4).
The partial derivative of the magnetisation at the pinning point is orthogonal to the z-axis $(\partial \boldsymbol{m})^2_{x=0} = (\partial m_x)^2_{x=0} + (\partial m_y)^2_{x=0}$ because of the constant length constraint of the magnetisation. Also, the squared change of the magnetisation has to be greater than zero $0 < (\partial m_x)^2_{x=0}$. The equation for the total angular momentum can be inserted into the linear momentum equation to get a solution of the current independently of the magnetisation.

$$0 < (\partial m_x)^2_{x=0} = \frac{\lambda}{A} - (\partial m_y)^2_{x=0} = \frac{\lambda}{A} - \left(\frac{D}{2A} \pm \frac{\nu}{2A\gamma} \right)^2 \tag{3.34}$$

3. Ferromagnetic domain wall description

This implies that the system stays static as long as $\left(\frac{\nu}{\gamma} \pm D\right)^2 < 4\lambda A$ is fulfilled. The system gets unstable above a critical spin-polarised current density of:

$$\nu_C = \gamma(2\sqrt{\lambda A} \mp D). \tag{3.35}$$

In the case of no DMI, the critical current is independent of the type of the domain wall. With DMI, the current needed is larger for head-to-head domain walls $(+1)$ than in the tail-to-tail case (-1). Hence, the domain walls will start to move at different strengths of the applied spin-polarised current having a different velocity at the same value.

On the one hand, the DMI can lower the requirement needed to create a domain wall in the one-dimensional semi-infinitely long nanowire. Therefore, a crystal with no inversion symmetry, having a DMI contribution, can be utilised to manufacture a racetrack memory system with lower needs in power consumption because of the lower critical current needed. Also, the problem of different speed domain wall types can be overcome with a current strength in between $\gamma(2\sqrt{\lambda A} - D)$ and $\gamma(2\sqrt{\lambda A} + D)$ where the shedding of head-to-head domain walls is possible, while the tail-to-tail domain walls can not be created.

On the other hand, in the case of no current, the stability condition is given by $D^2 < 4\lambda A$. If D^2 has a greater value, the ferromagnetic state is no longer the ground state, and a helical state will be energetically more favourable as a magnetisation orientation. Then, in the spiral state, no domain wall creation is possible at all.

The current depends on both material parameters λ and A from the anisotropy and exchange interaction by a square root. The anisotropy favours an easy axis alignment of the magnetisation. Small currents can not overcome the energy barrier of λ to pull the magnetisation out of the easy axis and create a domain wall. The same holds for the exchange interaction strength. If the current is too weak, then it is energetically favourable to stay parallel to each neighbour for the magnetic moments rather than following the spin current direction. In comparison, very high currents will make the system unstable, as shown in the next section. Therefore, it is justifiable that the current does depend on both parameters.

This analysis of the shedding current can be compared to the ones calculated in the paper of Rodrigues et al. [38] and Sitte et al. [39]. Both of those critical current values share the same dependency on the interaction strength and the anisotropy parameter. This value $\gamma\sqrt{2\lambda A}$ is different from the critical value calculated in this thesis as $2\gamma\sqrt{\lambda A}$ by a factor of $\sqrt{2}$. The difference is located by a different definition of the interaction strength A. In both papers, the interaction strength is defined as $\frac{A}{2}(\partial\boldsymbol{m})^2$, while it is defined as $A(\partial\boldsymbol{m})^2$ here. A straight redefinition to the value $A/2$ shows that both results match. Also, the DMI strength dependency $\pm\gamma D$ is the same when comparing the value in the paper [38] and in this thesis.

The case of $\beta \neq 0$ can not be solved as elegantly as the non-dissipative calculation. Having $\beta \neq 0$ means that the linear and total angular momentum along the x-axis are not conserved anymore. A similar analysis is possible integrating over the total space from 0 to ∞ using the equations with β. Integrating a derivative leads to the

evaluation of the boundary conditions. The β term integrals will be defined as new types of energy as was done in the reference calculation [38]. The angular momentum equation results in:

$$\int_0^\infty dx \partial \left(2A\hat{\boldsymbol{x}} \cdot (\boldsymbol{m} \times \partial \boldsymbol{m}) + D(m_x + \frac{\nu}{2D\gamma})^2 \right) = \int_0^\infty dx \frac{\beta\nu}{\gamma} \hat{\boldsymbol{x}} \cdot (\boldsymbol{m} \times \partial \boldsymbol{m})$$
$$\implies \partial m_y|_{x=0} + \frac{D}{2A} \pm \frac{\nu}{2A\gamma} = \frac{\beta\nu}{2A\gamma} E_{hel}. \tag{3.36}$$

On the left-hand side, the conserved angular momentum term is evaluated both at infinity and zero where the zero term is substracted, as it is the starting value of the integration. On the right-hand side, the integral of $E_hel = \int_0^\infty dx \hat{\boldsymbol{x}} \cdot (\boldsymbol{m} \times \partial \boldsymbol{m})$ is redefined as the helicity energy. That name is chosen because of the term in a DMI form.

The linear momentum calculation is done similarly:

$$\int_0^\infty dx \partial \left(A(\partial \boldsymbol{m})^2 + \lambda m_x^2 \right) = \int_0^\infty dx \frac{\beta\nu}{\gamma} (\partial \boldsymbol{m})^2$$
$$\implies \frac{\lambda}{A} - (\partial \boldsymbol{m})^2|_{x=0} = \frac{\beta\nu}{A\gamma} E_{exch} \tag{3.37}$$

As above, the left side is evaluated at the boundaries of the system and the right side is redefined to the exchange energy $E_{exch} = \int_0^\infty dx (\partial \boldsymbol{m})^2$ because it is an integration of the exchange interaction term over the total system.

These equations can be combined using the same trick as in the $\beta = 0$ case by inserting the $\partial m_y|_{x=0}$ into the second equation. Also, $(\partial \boldsymbol{m})^2$ is used in the same way because of the constant length assumption of the magnetisation vector $\boldsymbol{m}$: $0 < (\partial m_x)^2|_{x=0} = \frac{\lambda}{A} - \frac{\beta\nu}{A\gamma} E_{exch}$. As a result, the following inequality depending on the spin-polarised current ν holds for currents smaller than a critical value and does not hold for currents above it.

$$0 < \frac{\lambda}{A} - (-\frac{D}{2A} \mp \frac{\nu}{2A\gamma} + \frac{\beta\nu}{2A\gamma} E_{hel})^2 - \frac{\beta\nu}{A\gamma} E_{exch} \tag{3.38}$$

Next, the domain wall profile of the one-dimensional semi-infinitely long nanowire system with pinning at the origin is determined below the critical current. In this case, dissipation can be neglected $\beta = 0$ as it is a static configuration. The spatial derivative of the magnetisation is defined in the same way as for the domain wall profile without applied spin current (3.3): $\partial \boldsymbol{m} = \Gamma(x,t)\hat{\boldsymbol{x}} \times \boldsymbol{m} + \Lambda(x,t)\boldsymbol{m} \times (\hat{\boldsymbol{x}} \times \boldsymbol{m})$. This ansatz is inserted into the static case equations:

$$\partial \left(2A\hat{\boldsymbol{x}} \cdot (\boldsymbol{m} \times \partial \boldsymbol{m}) + D(m_x + \frac{\nu}{2D\gamma})^2 \right) = 0 \text{ and } \partial \left(A(\partial \boldsymbol{m})^2 + \lambda m_x^2 \right) = 0$$

The term $(\partial \boldsymbol{m})^2 = (1 - m_x^2)(\Gamma^2 + \Lambda^2)$ is determined in equation (B.1). The term $\hat{\boldsymbol{x}} \cdot (\boldsymbol{m} \times \partial \boldsymbol{m})$ can be determined using the $bac - cab$ rule (A.1) and the cross product properties to analyse the non-vanishing terms: $\hat{\boldsymbol{x}} \cdot (\boldsymbol{m} \times \partial \boldsymbol{m}) = \hat{\boldsymbol{x}} \cdot (\Gamma(\hat{\boldsymbol{x}}\boldsymbol{m}^2 - \boldsymbol{m}(\hat{\boldsymbol{x}} \cdot$

3. Ferromagnetic domain wall description

$\boldsymbol{m}$)) $+ \Lambda \boldsymbol{m} \times (\hat{\boldsymbol{x}}\boldsymbol{m}^2 - \boldsymbol{m}(\hat{\boldsymbol{x}} \cdot \boldsymbol{m}))) = \Gamma(1 - m_x^2)$.

Then, the static state equations are:

$$\partial \left(2A\Gamma(1 - m_x^2) + D(m_x + \frac{\nu}{2D\gamma})^2 \right) = 0 \text{ and } \partial \left(A(1 - m_x^2)(\Gamma^2 + \Lambda^2) + \lambda m_x^2 \right) = 0.$$
(3.39)

Again, the constant values of the conserved quantities will be compared to the exact values at $x \to \infty$. The constant value is different for a system with magnetisation pointing towards the wire direction to an antiparallel one. At first the left equation is considered, using $\left(2A\Gamma(1 - m_x^2) + D(m_x + \frac{\nu}{2D\gamma})^2 \right) |_{x\to\infty} = D \pm \frac{\nu}{\gamma} + (\frac{\nu}{2D\gamma})^2$:

$$2A\Gamma(1 - m_x)(1 + m_x) + Dm_x^2 + \frac{\nu}{\gamma}m_x + (\frac{\nu}{2D\gamma})^2 = D \pm \frac{\nu}{\gamma} + (\frac{\nu}{2D\gamma})^2$$
$$\implies (2A\Gamma + D)(1 + m_x)(1 - m_x) + \frac{\nu}{\gamma}(m_x \mp 1) = 0$$
$$\implies (2A\Gamma + D)(1 \pm m_x) \mp \frac{\nu}{\gamma} = 0$$
$$\implies \Gamma = \pm\frac{\nu}{2A\gamma(1 \pm m_x)} - \frac{D}{2A}.$$
(3.40)

The magnetisation value at $x \to \infty$ can take both values $m_x = \pm 1$ dependent on the domain wall type. Starting from the pinning, the first domain wall created depends on the magnetisation direction along the nanowire. If it is $m_x = -1$, a head-to-head domain wall will start to form, followed by a tail-to-tail domain wall. If $m_x = 1$, the first domain wall created is a tail-to-tail domain wall, followed by a head-to-head one. Hence, the domain wall profile depends on the domain wall type and the top sign indicates a starting magnetisation of $m_x = 1$.

Since all terms have a squared dependency on m_x the right equation does not depend on the magnetisation directly. At $x \to \infty$, a simple λ is the only contribution. A comparison to the equation for any point results in:

$$A(1 - m_x^2)(\Gamma^2 + \Lambda^2) + \lambda m_x^2 = \lambda$$
$$\implies (A(\Gamma^2 + \Lambda^2) - \lambda)m_x^2 = 0$$
$$\implies \Gamma^2 + \Lambda^2 = \frac{\lambda}{A}.$$
(3.41)

As a next step, the Γ of equation (3.40) is inserted into the second equation as well as equation (B.2):

$$\left(\pm\frac{\nu}{2A\gamma(1 \pm m_x)} - \frac{D}{2A} \right)^2 + \left(\frac{\partial m_x}{1 - m_x^2} \right)^2 = \frac{\lambda}{A}.$$
(3.42)

Then, the domain wall profile up to a point $\tilde{x}$ can be determined by an integration from ∞ to $\tilde{x}$ as well as an integration from 0 to $m_{\tilde{x}}$ by a separation of variables of the

term $(\partial m_x)^2$:

$$\tilde{x} = \int_0^{m_{\tilde{x}}} dm_x \frac{1}{(1 - m_x^2)\sqrt{\frac{\lambda}{A} - \left(\pm\frac{\nu}{2A\gamma(1\pm m_x)} - \frac{D}{2A}\right)^2}}. \tag{3.43}$$

This equation can be used to determine the profile of $\boldsymbol{m}$ below the critical current.
As a conclusion of the section, the ferromagnetic LLG equation with an applied spin-polarised current along the nanowire direction was analysed for a semi-infinitely long nanowire with an easy axis anisotropy, an exchange interaction and DMI and pinning orthogonal to the anisotropy at the origin. At first, the effective field of the ferromagnet was calculated to be able to work with the LLG equation analytically. After that, the symmetries of the system given by a rotational invariance around the x-axis and invariance under displacement along the x-axis were used with the Noether theorem to confirm two conserved quantities.
These quantities could be analysed in a static state without dissipation to calculate a critical current value beyond which domain wall shedding is possible at the pinning. Also, the case of dissipation was addressed. Then, the magnetic profile of the system below the critical current could be constructed.

3.5. Ferromagnetic instability

The critical current calculated for a domain wall creation in the last section needs to be scrutinised in terms of the stability of the ferromagnetic state in the total system. A spin-polarised current is a destabilising factor when applied to a perturbation of the ground state. The ferromagnetic state is not stable beyond a critical current value. However, it is questionable if the shedding current is lower or higher than the stability current. That is why the latter condition is examined in this chapter. This analysis is based on the scientific paper of Masell et al. [32].
The LLG equation with applied spin-transfer torque (2.7) with the given functional derivative term (3.25) is used to describe a ferromagnetic nanowire state. The DMI contribution will be neglected in this calculation for simplification. A perturbation of this equation is investigated and a condition beyond which the state itself is not stable will be extracted from the dispersion relation emerging in this formalism. The LLG equation and the effective field are analysed with an abstract current direction $\boldsymbol{\nu}$. The spatial derivatives in the equations are given by gradients of the magnetisation instead. This will not complicate the formalism but generalise the result.
The instability will be determined using the magnetisation in the ground state of the ferromagnetic system $\boldsymbol{m}_0 = \hat{\boldsymbol{x}}$ with a perpendicular perturbation $\boldsymbol{h} = (0, h_y, h_z)^T$. Therefore, the total magnetic state is modelled as $\boldsymbol{m} = (1, h_y, h_z)^T$. This ansatz is inserted into the LLG equation, neglecting all second-order and higher perturbations as they are small in magnitude. Neglecting those terms leads to a linearised LLG equation which is simpler and introduces an analytically solvable problem.

3. Ferromagnetic domain wall description

The linear equation is given by:

$$\boldsymbol{h} - \alpha\hat{\boldsymbol{x}} \times \boldsymbol{h} = -(\boldsymbol{\nu} \cdot \nabla)\boldsymbol{h} + (-2A\gamma\nabla^2 + 2\lambda\gamma + \beta(\boldsymbol{\nu} \cdot \nabla))\hat{\boldsymbol{x}} \times \boldsymbol{h}. \qquad (3.44)$$

The spatial and time derivatives of the x component of the magnetisation vanishes due to the orthogonal perturbation. Hence, the derivative terms must be in the form of $\hat{\boldsymbol{x}} \times \nabla\boldsymbol{h}$ to fulfil the linearity. This leads to the equation shown above.

Next, the magnetisation exposed to the spin-polarised current is modelled as a particular spin wave solution. All possible solutions are given by magnetisation vectors capable of rotating on a sphere around the vector origin. The specific case of a group of spin waves having different angular frequencies ω_i is the plane wave solution with just one frequency ω. This plane wave solution with an amplitude ρ_i for each of the coordinates rotates as $\boldsymbol{h} = \boldsymbol{\rho}\exp\left(i(\omega t - \boldsymbol{q} \cdot \boldsymbol{r})\right)$. The time derivative of a plane wave solution transforms to $\partial_t \exp\left(i(\omega t - \boldsymbol{q} \cdot \boldsymbol{r})\right) = i\omega \exp\left(i(\omega t - \boldsymbol{q} \cdot \boldsymbol{r})\right)$ and the spatial derivative results in $\nabla \exp\left(i(\omega t - \boldsymbol{q} \cdot \boldsymbol{r})\right) = -i\boldsymbol{q}\exp\left(i(\omega t - \boldsymbol{q} \cdot \boldsymbol{r})\right)$. The equation with the ansatz inserted is shown below:

$$i\omega\boldsymbol{h} - i\omega\alpha\hat{\boldsymbol{x}} \times \boldsymbol{h} = i(\boldsymbol{\nu} \cdot \boldsymbol{q})\boldsymbol{h} + (2A\gamma\boldsymbol{q}^2 + 2\lambda\gamma + i\beta(\boldsymbol{\nu} \cdot \boldsymbol{q}))\boldsymbol{h} \times \boldsymbol{h}. \qquad (3.45)$$

The amplitudes ρ_i of the perturbation do not need to be identical in the y and z direction. Therefore, it is convenient to display this formula in a matrix form. The $\hat{\boldsymbol{x}} \times \boldsymbol{h}$ contributions are the off-diagonal elements of the matrix and the $\boldsymbol{h}$ dependent terms build the diagonal elements. Each term will be determined individually.

At first, the effective field term is converted using $\hat{\boldsymbol{x}} \times \boldsymbol{h} = (0, -h_z, h_y)^T$:

$$
\begin{aligned}
(-2A\gamma\nabla^2 &+ 2\lambda\gamma)\hat{\boldsymbol{x}} \times \boldsymbol{h} = 2\gamma(A\boldsymbol{q}^2 + \lambda)\hat{\boldsymbol{x}} \times \boldsymbol{h} \\
&= \begin{pmatrix} 0 & 0 & 0 \\ 0 & 0 & -2\gamma(A\boldsymbol{q}^2 + \lambda) \\ 0 & 2\gamma(A\boldsymbol{q}^2 + \lambda) & 0 \end{pmatrix} \boldsymbol{h} = \begin{pmatrix} 0 & 0 & 0 \\ 0 & 0 & -\Lambda \\ 0 & \Lambda & 0 \end{pmatrix} \boldsymbol{h}.
\end{aligned} \qquad (3.46)
$$

The Gilbert damping term is given by:

$$\alpha\boldsymbol{m} \times \dot{\boldsymbol{m}} = \alpha i\omega\hat{\boldsymbol{x}} \times \boldsymbol{h} = \begin{pmatrix} 0 & 0 & 0 \\ 0 & 0 & -\alpha i\omega \\ 0 & \alpha i\omega & 0 \end{pmatrix} \boldsymbol{h}. \qquad (3.47)$$

The adiabatic spin-transfer torque term is given by:

$$-(\boldsymbol{\nu} \cdot \nabla)\boldsymbol{m} = i(\boldsymbol{\nu} \cdot \boldsymbol{q})\boldsymbol{h} = \begin{pmatrix} i(\boldsymbol{\nu} \cdot \boldsymbol{q}) & 0 & 0 \\ 0 & i(\boldsymbol{\nu} \cdot \boldsymbol{q}) & 0 \\ 0 & 0 & 0 \end{pmatrix} \boldsymbol{h}. \qquad (3.48)$$

The non-adiabatic spin-transfer torque term or β dependent term is given by:

$$\beta\boldsymbol{m} \times (\boldsymbol{\nu} \cdot \nabla)\boldsymbol{m} = -i\beta(\boldsymbol{\nu} \cdot \boldsymbol{q})\hat{\boldsymbol{x}} \times \boldsymbol{h} = \begin{pmatrix} 0 & 0 & 0 \\ 0 & 0 & -i\beta(\boldsymbol{\nu} \cdot \boldsymbol{q}) \\ 0 & i\beta(\boldsymbol{\nu} \cdot \boldsymbol{q}) & 0 \end{pmatrix} \boldsymbol{h}. \qquad (3.49)$$

3. Ferromagnetic domain wall description

Therefore, the total LLG equation assembles to:

$$
\mathbf{0} = \begin{pmatrix} 0 & 0 & 0 \\ 0 & i(\boldsymbol{\nu} \cdot \boldsymbol{q}) - i\omega & -\Lambda - \alpha i\omega + i\beta(\boldsymbol{\nu} \cdot \boldsymbol{q}) \\ 0 & \Lambda + \alpha i\omega - i\beta(\boldsymbol{\nu} \cdot \boldsymbol{q}) & i(\boldsymbol{\nu} \cdot \boldsymbol{q}) - i\omega \end{pmatrix} \boldsymbol{h}. \tag{3.50}
$$

This formalism is based on the three-dimensional magnetisation vector, but the perturbation depends on the y and z coordinates only. The x direction does not contribute to the dynamics of the perturbation and equals zero in both sides of the equation. That is why the three dimensional matrix above can be reduced to a two dimensional one without changing the behaviour.

$$
\mathbf{0} = \begin{pmatrix} i(\boldsymbol{\nu} \cdot \boldsymbol{q}) - i\omega & -\Lambda - \alpha i\omega + i\beta(\boldsymbol{\nu} \cdot \boldsymbol{q}) \\ \Lambda + \alpha i\omega - i\beta(\boldsymbol{\nu} \cdot \boldsymbol{q}) & i(\boldsymbol{\nu} \cdot \boldsymbol{q}) - i\omega \end{pmatrix} \boldsymbol{h} \tag{3.51}
$$

As previously mentioned, the amplitudes of the perturbation ρ_i in the y and z direction do not need to be equal. The two equations from the y and the z components are linearly independent, meaning that the solution does not depend on the perturbation amplitudes if the determinant of the matrix vanishes.

$$
0 = (-i\omega + i(\boldsymbol{\nu} \cdot \boldsymbol{q}))^2 + (\Lambda + \alpha i\omega - i\beta(\boldsymbol{\nu} \cdot \boldsymbol{q}))^2 \tag{3.52}
$$

The two dimensional determinant can be recast in terms of the frequency of the spin wave ω:

$$
0 = (1+\alpha^2)\omega^2 - 2((\boldsymbol{\nu}\cdot\boldsymbol{q}) + i\Lambda\alpha + \alpha\beta(\boldsymbol{\nu}\cdot\boldsymbol{q}))\omega + (1+\beta^2)(\boldsymbol{\nu}\cdot\boldsymbol{q})^2 - \Lambda^2 + 2i\beta(\boldsymbol{\nu}\cdot\boldsymbol{q})\Lambda. \tag{3.53}
$$

This quadratic equation can be solved by the "pq"-formula, which leads to the two solutions:

$$
(1+\alpha^2)\omega_{1/2} = (1+\alpha\beta)(\boldsymbol{\nu} \cdot \boldsymbol{q}) + i\Lambda\alpha \pm i(\alpha - \beta)(\boldsymbol{\nu} \cdot \boldsymbol{q}) + \Lambda). \tag{3.54}
$$

The calculation of this quantity is shown in the appendix up to the equation (E.6). On the one hand, the spin waves proportional to $\exp\left(i(\omega t - \boldsymbol{q} \cdot \boldsymbol{r})\right)$ become unstable if the dispersion relation $\omega_{1/2}$ has a negative imaginary part. This means that the exponential function has a contribution $\exp\left(-i^2|Im(\omega)|t\right) = \exp\left(|Im(\omega)|t\right)$ directly proportional to the magnitude of the imaginary part of the dispersion relation. Hence, the perturbation itself increase exponentially in time. On the other hand, the spin waves are damped exponentially in time for a positive imaginary part of the dispersion relation. A critical value of an applied spin-polarised current can be determined at the boundary between both cases.

$$
Im(\omega_{1/2}) = \frac{\alpha\Lambda \pm (\alpha - \beta)(\boldsymbol{\nu} \cdot \boldsymbol{q})}{(1+\alpha^2)} = \frac{\alpha(\Lambda \pm (\boldsymbol{u} \cdot \boldsymbol{q}))}{(1+\alpha^2)} = \frac{\alpha(2\gamma(A\boldsymbol{q}^2 + \lambda) \pm (\boldsymbol{u} \cdot \boldsymbol{q}))}{(1+\alpha^2)} \tag{3.55}
$$

In the second step, the spin-polarised current is redefined to $\boldsymbol{u} = \frac{\alpha - \beta}{\alpha}$ to get a α and β independent calculation. As already mentioned, the imaginary part should be lower than zero to get an unstable state solution:

$$Im(\omega_{1/2}) = \frac{\alpha(2\gamma(A\boldsymbol{q}^2 + \lambda) \pm (\boldsymbol{u} \cdot \boldsymbol{q}))}{(1 + \alpha^2)} < 0. \tag{3.56}$$

Since α is positive, this factor is not relevant.

$$2A\gamma\boldsymbol{q}^2 + \kappa \pm (\boldsymbol{u} \cdot \boldsymbol{q}) = (2A\gamma\boldsymbol{q} \pm \boldsymbol{u})^2 + 2\gamma\lambda - \frac{\boldsymbol{u}^2}{4A\gamma} < 0 \tag{3.57}$$

The $\boldsymbol{q}^2$ term is combined with the $(\boldsymbol{u} \cdot \boldsymbol{q})$ contribution, using the binomial theorem, to get a squared momentum contribution that can not be lower than zero. This means that the momentum independent solution only depends on $2\gamma\lambda - \frac{\boldsymbol{u}^2}{4A\gamma} < 0$.

$$2\gamma\lambda - \frac{\boldsymbol{u}^2}{4A\gamma} < 0 \iff 2\gamma\lambda < \frac{\boldsymbol{u}^2}{4A\gamma} \iff |\boldsymbol{u}| > 2\gamma\sqrt{2A\lambda} \tag{3.58}$$

The critical current value of the one-dimensional ferromagnetic nanowire system is given by $|\boldsymbol{u}_c| = 2\gamma\sqrt{2A\lambda}$. This marks the boundary above which the ferromagnetic state is not stable anymore. This value can be compared to the critical current (3.35) of domain wall creation in the semi-infinitely long one-dimensional nanowire system with orthogonal pinning to the easy axis at the origin. Besides the pinning point, both systems share the same properties. The ferromagnetic state critical current value determined in this chapter has a crucial impact on the similarly built nanowire's stability for shedding.

Both values can be compared to each other in the case of $\beta = 0$, the non-dissipative case. On that note, $\boldsymbol{u}$ and $\boldsymbol{\nu}$ are equal due to the cancelling α terms. Comparing both values shows that the ferromagnetic instability is greater than the shedding current by a factor of $\sqrt{2}$, neglecting the DMI contribution. This indicates that a domain wall creation in such a nanowire system is possible for ferromagnetic systems.

3.6. Summary of the ferromagnetic calculations

The previous chapter was dedicated to the ferromagnetic description of domain wall systems and a possible application using such systems. At first, the racetrack memory system was introduced as a new method of digital information storage. Then, the profile of domain walls in a one-dimensional ferromagnetic nanowire system had been determined neglecting the spin current contributions. It is shown that the domain wall width is characterised by an interplay between exchange interaction strength and the anisotropic interaction strength.

A rigid body treatment for one-dimensional domain walls was discussed in the following section. The domain wall profile can be treated as a stable structure moving along

the wire using the coordinate of the domain wall centre and the rotation of the domain wall with respect to an axis. The time evolution of these generalised coordinates, also called soft modes, showed that such a description was possible. Furthermore, a generalisation is achievable for antiferromagnetic systems.

The subsequent section did focus on the creation of domain walls in one-dimensional systems. Therefore, pinning of the magnetisation was used with an applied spin-polarised current along the wire direction. In this case, the symmetries of the system could be used for the Noether theorem. The linear momentum and the total angular momentum along the x-axis are conserved. In the non-dissipative case of $\beta = 0$, an analytical solution for the spin current value needed to achieve a domain wall creation or shedding off the pinning point could be determined. This current value is different for the two domain wall types, head-to-head or tail-to-tail, with DMI. The current depends on the exchange interaction strength as well as the anisotropic interaction strength. Also, the domain wall profile was determined in the case of an applied spin-polarised current.

In the last section of the chapter, the stability of the ferromagnetic state itself was tested. A current value beyond which the ferromagnetic state does no longer exist was determined using a perturbative approach for the linearised LLG equation. The calculation explained that this critical current value is higher than the shedding current value. It proves that domain wall creation based on spin-transfer torque at a pinning point is possible for a ferromagnetic system.

In the next chapter, an antiferromagnetic theory is built to determine a critical current value for the domain wall shedding in one-dimensional systems.

4. Antiferromagnetic domain wall description

Up to this point of the thesis, domain wall properties have been derived for one-dimensional ferromagnetic nanowire systems. In this chapter, the ferromagnetic basis is used to develop a theory for synthetic antiferromagnetic systems. A net magnetisation of about zero characterises antiferromagnetic systems. This implies that neighbouring magnetic moments favour an alignment so that this requirement is fulfilled. The most straightforward geometry for such systems is determined by antiparallel neighbouring magnetic moments. In an Ising model type, the exchange interaction term strength A has a negative value instead of a positive one. This penalises the parallel alignment of the adjoining neighbours.

The chapter is structured in three steps. At first, LLG type equations for the antiferromagnetic system are derived based on the ferromagnetic ones. A particular focus is put on the effective field terms. After that, those equations will be used to derive an antiferromagnetic critical current for the shedding of domain walls in the same structure as was done in the ferromagnetic case. In the last section, the determination of the antiferromagnetic instability current is performed and both values are compared.

4.1. The antiferromagnetic LLG equations

The ferromagnetic LLG equation with an applied spin-polarised current (2.7) describes the time evolution of the ferromagnetic state magnetisation. The antiferromagnetic system needs to be treated differently, as it has zero net magnetisation. The system model is one of a synthetic antiferromagnet, a specific case of an antiferromagnet. It is fabricated by two oppositely magnetised ferromagnetic layers, combined by a non-magnetic layer whose thickness is the controlling factor for the interaction between both layers [35]. Those layers will be called sublattices or lattices of the system.

A sketch of a synthetic antiferromagnetic domain wall is shown in figure 4.1, where the lattices are visualised by the colours red and blue. The magnetisation vectors are approximately antiparallel all the time, independently of the domain wall because of the antiferromagnetic coupling strength. Mathematically, both layers are coupled antiferromagnetically by an interlattice exchange interaction. This interaction is the strongest one in the system and leads to both magnetisation vectors aligning antiparallel. The total magnetic energy of a one-dimensional synthetic antiferromagnetic nanowire is modelled as the sum of both lattices total magnetic energy terms and the interaction strength between the lattices.

As previously mentioned, the nearest neighbours of each sublattice, coupled by
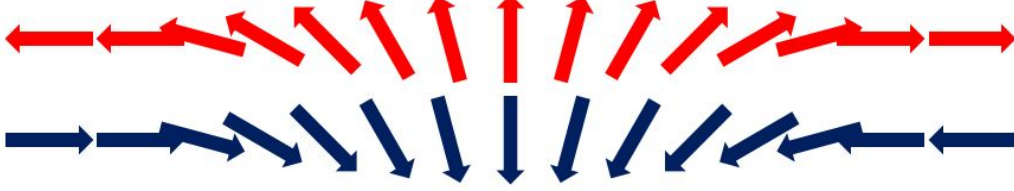
Figure 4.1.: Illustration of an antiferromagnetic domain wall in a one-dimensional synthetic antiferromagnet consisting of two ferromagnetic sublattices - the red and blue marked vectors - which are coupled by an interlattice exchange constant. The magnetisation vector of one of the sublattices is antiparallel to the corresponding adjoining neighbour of the other lattice. Therefore, there is no net magnetisation with or without a domain wall in the antiferromagnetic system. Source: Author's illustration.

an interaction favouring antiparallel alignment, have a combined net magnetisation $|\boldsymbol{m}_1 + \boldsymbol{m}_2| = 0$ in the antiferromagnetic state for the sublattice labels 1 and 2. That quantity applies to all pairs, leading to a vanishing magnetisation of the total sample. Hence, an experimental analysis of the magnetisation is not possible.

Both spin values subtracted can be used as an indicator of the magnetisation change within the sample. However, the choice of the direction of this vector is ambiguous. $(\boldsymbol{m}_1 - \boldsymbol{m}_2)/2$ and $(\boldsymbol{m}_2 - \boldsymbol{m}_1)/2$ both have a magnitude in the order of the magnetisation of the sublattices, but they differ by a minus sign making them point in the opposite directions. The antiferromagnetic theory is usually described in terms of two new variables in the LLG equations [28] [6] [19].

The vector chosen to describe the behaviour of the synthetic antiferromagnet within this thesis is $\boldsymbol{n} = (\boldsymbol{m}_1 - \boldsymbol{m}_2)/2$, a subtraction of the bottom lattice magnetisation vector from the top one. The resulting vector, called Néel vector $\boldsymbol{n}$, points along the direction of the top layer magnetisation and is normalised to the sublattice magnetisation magnitude. Therefore, the red arrows shown in figure 4.1 display what the system would approximately look like in terms of the Néel vector, as the vector origin would be between both sublattice vectors.

A more rigorous defining plot for the two relevant variables of the synthetic antiferromagnet $\boldsymbol{m} = (\boldsymbol{m}_1 + \boldsymbol{m}_2)/2$ and $\boldsymbol{n} = (\boldsymbol{m}_1 - \boldsymbol{m}_2)/2$ is shown in figure 4.2. It displays both values multiplied by a factor of two, so that the vector origin can be recognised. Also, $\boldsymbol{m}_1$ and $\boldsymbol{m}_2$ are pulled towards the same direction to exhibit the direction of the antiferromagnetic magnetisation vector $\boldsymbol{m}$ as well as the small magnitude. $\boldsymbol{m}$ is zero in the case of no kink.

In the following, the total magnetic energy is determined. At first, the sublattice magnetic energies are modelled by the same interactions as in the ferromagnetic system (3.2) with DMI contributions as shown below:

$$E_{1/2} = \int dV (A_{1/2}(\partial \boldsymbol{m}_{1/2})^2 + D_{1/2}\boldsymbol{m}_{1/2} \cdot (\hat{\boldsymbol{x}} \times \partial \boldsymbol{m}_{1/2}) + \lambda_{1/2}(1 - m_{1/2,x}^2)). \quad (4.1)$$
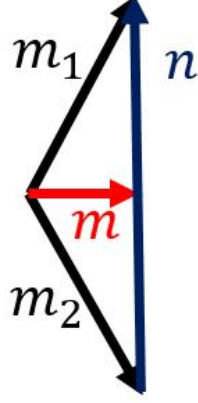
Figure 4.2.: The two relevant variables of the synthetic antiferromagnet $\boldsymbol{m} = (\boldsymbol{m}_1 + \boldsymbol{m}_2)/2$ and $\boldsymbol{n} = (\boldsymbol{m}_1 - \boldsymbol{m}_2)/2$ multiplied by a factor of 2 are displayed to show how they relate to the sublattice magnetisation before the normalisation. The magnetisation vector $\boldsymbol{m}$ is approximately zero throughout the sample. The Néel vector $\boldsymbol{n}$ is used to describe the change of the sublattice magnetisation vectors in the system. Source: Author's illustration.

The interaction between both ferromagnetic parts is modelled as $\epsilon \boldsymbol{m}_1 \cdot \boldsymbol{m}_2$. The interaction strength ϵ is defined positively. Hence, the term is minimised when both sublattice vectors are antiparallel and maximised when they are parallel. This structure realises an antiferromagnetic behaviour of the model.

The combined term is given by:

$$
\begin{aligned}
E_{tot} = \int dV [& A_1(\partial \boldsymbol{m}_1)^2 + D_1 \boldsymbol{m}_1 \cdot (\hat{\boldsymbol{x}} \times \partial \boldsymbol{m}_1) + \lambda_1(1 - m_{1,x}^2) \\
& + A_2(\partial \boldsymbol{m}_2)^2 + D_2 \boldsymbol{m}_2 \cdot (\hat{\boldsymbol{x}} \times \partial \boldsymbol{m}_2) + \lambda_2(1 - m_{2,x}^2) + \epsilon \boldsymbol{m}_1 \cdot \boldsymbol{m}_2].
\end{aligned}
\tag{4.2}
$$

For simplicity reasons, the leading constants given by the exchange interaction strength A, the anisotropic strength λ and the DMI strength D are equal for both lattices. This implies that both parts behave identically since they are similar. In the next step, the definition of the antiferromagnetic vectors $\boldsymbol{m} = (\boldsymbol{m}_1 + \boldsymbol{m}_2)/2$ and $\boldsymbol{n} = (\boldsymbol{m}_1 - \boldsymbol{m}_2)/2$ of the magnetisation and the Néel vector are inserted into the equation (4.2) as $\boldsymbol{m}_1 = \boldsymbol{m} + \boldsymbol{n}$ and $\boldsymbol{m}_2 = \boldsymbol{m} - \boldsymbol{n}$.

$$
\begin{aligned}
E_T = \int dV [& A(\partial(\boldsymbol{m} + \boldsymbol{n}))^2 + D(\boldsymbol{m} + \boldsymbol{n}) \cdot (\hat{\boldsymbol{x}} \times \partial(\boldsymbol{m} + \boldsymbol{n})) + \lambda(1 - (m_x + n_x)^2) \\
& + A(\partial(\boldsymbol{m} - \boldsymbol{n}))^2 + D(\boldsymbol{m} - \boldsymbol{n}) \cdot (\hat{\boldsymbol{x}} \times \partial(\boldsymbol{m} - \boldsymbol{n})) \\
& + \lambda(1 - (m_x - n_x)^2) + \epsilon(\boldsymbol{m} + \boldsymbol{n}) \cdot (\boldsymbol{m} - \boldsymbol{n})].
\end{aligned}
\tag{4.3}
$$

All interaction terms will be analysed separately, starting with the exchange interaction term A. Both square brackets are resolved and added up. The mixed terms

containing $\boldsymbol{m}$ and $\boldsymbol{n}$ cancel out while the pure terms appear twice. As a result, the total exchange term is $2A(\partial\boldsymbol{m})^2 + 2A(\partial\boldsymbol{n})^2$.

The DMI contribution is resolved in the next step: $D(\boldsymbol{m}+\boldsymbol{n})\cdot(\hat{\boldsymbol{x}}\times\partial(\boldsymbol{m}+\boldsymbol{n})) + D(\boldsymbol{m}-\boldsymbol{n})\cdot(\hat{\boldsymbol{x}}\times\partial(\boldsymbol{m}-\boldsymbol{n})) = 2D\boldsymbol{m}\cdot(\hat{\boldsymbol{x}}\times\partial\boldsymbol{m}) + 2D\boldsymbol{n}\cdot(\hat{\boldsymbol{x}}\times\partial\boldsymbol{n})$. Again, the mixing terms vanish because of the minus sign in front of the Néel vector inserted for the bottom magnetisation $\boldsymbol{m}_2$. Both $\boldsymbol{m}_1$ and $\boldsymbol{m}_2$ appear quadratically in the DMI energy density. Therefore, all terms containing a single $\boldsymbol{n}$ emerge twice, once with a minus sign from $\boldsymbol{m}_2$ and once without from the $\boldsymbol{m}_1$ definition. The quadratic terms in $\boldsymbol{n}$ and $\boldsymbol{m}$ appear in both starting terms, leading to the final result.

The anisotropic term gives the last ferromagnetic contribution. Again, this segment has a quadratic dependency on $\boldsymbol{m}_1$ or $\boldsymbol{m}_2$. This indicates that the same symmetry as above can be applied to the anisotropy. The mixed terms cancel while the pure terms and the constant term occur twice: $2\lambda(1 - m_x^2 - n_x^2)$. The antiferromagnetic coupling term $\epsilon(\boldsymbol{m}+\boldsymbol{n})\cdot(\boldsymbol{m}-\boldsymbol{n}) = \epsilon(\boldsymbol{m}^2 - \boldsymbol{n}^2)$ is converted using the binomial rules. Therefore, the total magnetic energy in terms of the new variables of the antiferromagnet is:

$$
\begin{aligned}
E_T(\boldsymbol{m},\boldsymbol{n}) = \int dV (2A(\partial\boldsymbol{m})^2 + 2D\boldsymbol{m}\cdot(\hat{\boldsymbol{x}}\times\partial\boldsymbol{m}) + 2A(\partial\boldsymbol{n})^2 \\
+ 2D\boldsymbol{n}\cdot(\hat{\boldsymbol{x}}\times\partial\boldsymbol{n}) + 2\lambda(1 - m_x^2 - n_x^2) + \epsilon(\boldsymbol{m}^2 - \boldsymbol{n}^2)).
\end{aligned}
\tag{4.4}
$$

This equation is the total magnetic energy of a one-dimensional synthetic antiferromagnetic nanowire modelled by two antiparallel ferromagnetic lattices, coupled antiferromagnetically by a non-magnetic layer in between. It is important to note that other contributions to the total magnetic energy, such as dipolar fields, are neglected, as stated in the effective field section. Those interactions highly depend on the system and its properties needed for future applications. Therefore, materials are manufactured, obtaining the material parameters so that these approximations are justifiable. The exchange interaction constant A of the ferromagnet is renamed as intralattice exchange constant in the antiferromagnetic case. It is still the prefactor giving the interaction strength magnitude to the exchange interaction, but it takes place between neighbours of each of the sublattices independently from each other. The neighbouring magnetic moments of each sublattice behave ferromagnetically, meaning that they tend to align. That is why the constant A is positive, unlike a direct conversion of an Ising model from a ferromagnetic behaviour to an antiferromagnetic one would suggest.

The antiferromagnetic coupling introduces a second coupling of nearest neighbours. It is between neighbours of the two lattices. Hence, the contribution with prefactor ϵ is called the interlattice exchange constant. The interlattice exchange has the highest contribution of interaction strengths to retain the antiferromagnetic state even in a dynamic system.

Having stated that some interaction strengths are greater in magnitude than others and some interaction strengths are even negligibly small, equation (4.4) can be further analysed and some of its terms can be neglected. To do so, ferromagnetic and antiferromagnetic constraints are set. At first, the ferromagnetic sublattices have a saturated magnetisation magnitude normalised to a unit length $|\boldsymbol{m}_{1/2}| = 1$. As for the

ferromagnetic calculations, it is assumed that below the Curie temperature - the temperature beyond which ferromagnetic material gets paramagnetic - there is no change in the magnitude of the magnetisation. This characteristic of the magnetisation shows that the spatial change of $\boldsymbol{m}_{1/2}$ can only be perpendicular to the magnetisation itself $\partial \boldsymbol{m}_{1/2} \cdot \boldsymbol{m}_{1/2} = 0$. A similar structure can be built for the antiferromagnet using this ferromagnetic constraint.

The definition of the antiferromagnetic magnetisation and Néel vector show interesting behaviour based on the constant length constraint. Analogously to the Curie temperature, the length of the Néel vector $|\boldsymbol{n}| = \boldsymbol{n}^2 = ((\boldsymbol{m}_1 - \boldsymbol{m}_2)/2)^2 = ((2\boldsymbol{m}_1)/2)^2 = \boldsymbol{m}_1^2 = 1$ is constant in length below the Néel temperature, a temperature limit above which the antiferromagnetic state is not antiferromagnetic anymore. Accurately, the magnetisation should be precisely zero, and hence the theory independent of it. However, the magnetisation vector in an antiferromagnetic theory is treated as a perturbation. Although the theory is based and calculated on the constant length constraint, this will never hold in the total system evolving in time. That is why the magnetisation vector is used as a perturbative parameter much smaller than the Néel vector $|\boldsymbol{n}| \gg |\boldsymbol{m}|$.

The antiferromagnetic vectors share two traits by definition. The first one is stated by $(\boldsymbol{n}^2 + \boldsymbol{m}^2) = \frac{\boldsymbol{m}_1{}^2 - 2\boldsymbol{m}_1 \cdot \boldsymbol{m}_2 + \boldsymbol{m}_2{}^2}{4} + \frac{\boldsymbol{m}_1{}^2 + 2\boldsymbol{m}_1 \cdot \boldsymbol{m}_2 + \boldsymbol{m}_2{}^2}{4} = \frac{\boldsymbol{m}_1{}^2 + \boldsymbol{m}_2{}^2}{2} = 2/2 = 1$. The magnetisation part is seen as an antiferromagnetic state perturbation and is used to determine the dynamic properties of the state. The second trait is specified by the orthogonality of both vectors by definition $\boldsymbol{n} \cdot \boldsymbol{m} = \frac{(\boldsymbol{m}_1 + \boldsymbol{m}_2)}{2} \cdot \frac{(\boldsymbol{m}_1 - \boldsymbol{m}_2)}{2} = \frac{(\boldsymbol{m}_1{}^2 - \boldsymbol{m}_2{}^2)}{4} = \frac{(\boldsymbol{m}_0{}^2 - \boldsymbol{m}_0{}^2)}{4} = 0$. Often, this will be used to facilitate the equations.

As stated above, the antiferromagnetic constraints are used to estimate the significance of all terms of the total magnetic energy density as shown below:

$$2A(\partial \boldsymbol{m})^2 + 2D\boldsymbol{m} \cdot (\hat{\boldsymbol{x}} \times \partial \boldsymbol{m}) + 2A(\partial \boldsymbol{n})^2 + 2D\boldsymbol{n} \cdot (\hat{\boldsymbol{x}} \times \partial \boldsymbol{n}) + 2\lambda(1 - m_x^2 - n_x^2) + \epsilon(\boldsymbol{m}^2 - \boldsymbol{n}^2).$$
$$(4.5)$$

The magnetisation term of the intralattice exchange interaction $(\partial \boldsymbol{m})^2$ will be tiny as $\boldsymbol{m}$ is nearly zero and it should not change drastically in an antiferromagnet. In comparison, the $(\partial \boldsymbol{n})^2$ term will not be neglected even though it shares the same interaction parameter. The collinear magnetic moments tend to be antiparallel, but the Néel vector can vary and rotate. For example, the usage of a spin-polarised current perpendicular to the spin plane leads to both spins pointing along the current direction due to the torque. The interlattice exchange interaction works as a restoring force, keeping both sublattice moments antiparallel. Hence, the Néel vector will rotate but remains approximately constant in its length. Also, $|\boldsymbol{m}| \approx 0$ still holds as the main factor of the AFM lattice. Therefore, $\boldsymbol{n}$ acts as the antiferromagnetic order parameter, describing the motion of antiferromagnetic structures.

The anisotropic term $\lambda(1 - m_x^2 - n_x^2)$ will be changed by neglecting the m_x^2 term. Since $|\boldsymbol{m}|$ is small, one of its coordinates is even smaller. In comparison, the Néel vector contribution is kept to describe the anisotropic influence on the antiferromagnetic order. Also, the constant factor of λ is kept to reach a vanishing free energy contribution

in the ground state alignment of the sublattice magnetic moments.

The DMI is entirely neglected for a more straightforward calculation. The interaction between both sublattices or interlattice exchange is the strongest of the three remaining interactions. The antiferromagnetic ordering is the leading factor for the system's behaviour, as it would be a ferromagnet without it. This expresses the significance of the interlattice exchange. The $\boldsymbol{n}$ part is neglected, as it remains a constant term in the free energy below the Néel temperature. A constant term can always shift the total magnetic energy term just as the 2λ without changing the time evolution. However, the $\boldsymbol{m}$ part is kept as a perturbative contribution. A strong coupling constant λ shifts the small parameter contribution to a significant value.

The resulting free energy contribution is:

$$E = \int dV (2A(\partial \boldsymbol{n})^2 + 2\lambda(1 - n_x^2) + \epsilon \boldsymbol{m}^2). \tag{4.6}$$

The time evolution of the synthetic antiferromagnet can be described by an adapted version of the LLG equation with applied spin current (2.7) in terms of the sublattices. Since the system is one-dimensional, all derivatives are positioned along the easy axis. Also, the spin-polarised current applied along the wire direction reduces to a scalar value ν. According to the LLG equation for ferromagnetic systems, the sublattice magnetic moments change in time, as they are treated as two coupled ferromagnets coupled antiferromagnetically. Both equations hold at the same time. Therefore, the LLG equations can be redefined in terms of the antiferromagnetic order parameters $\boldsymbol{n}$ and $\boldsymbol{m}$ as was done for the total magnetic energy that is inserted into these new equations. The ferromagnetic starting equations of both lattices are equal:

$$\dot{\boldsymbol{m}}_{1/2} = \gamma \boldsymbol{m}_{1/2} \times \boldsymbol{H}_{\mathrm{eff}_{1/2}} + \alpha \boldsymbol{m}_{1/2} \times \dot{\boldsymbol{m}}_{1/2} - \nu \partial \boldsymbol{m}_{1/2} + \beta \boldsymbol{m}_{1/2} \times \nu \partial \boldsymbol{m}_{1/2}. \tag{4.7}$$

Again, $\boldsymbol{m}_1 = \boldsymbol{m} + \boldsymbol{n}$ and $\boldsymbol{m}_2 = \boldsymbol{m} - \boldsymbol{n}$ are used to determine the equations.

$$
\begin{aligned}
\dot{\boldsymbol{m}}_1 \pm \dot{\boldsymbol{m}}_2 &= \gamma \boldsymbol{m}_1 \times \boldsymbol{H}_{\mathrm{eff}_1} \pm \gamma \boldsymbol{m}_2 \times \boldsymbol{H}_{\mathrm{eff}_2} \\
&+ \alpha \boldsymbol{m}_1 \times \dot{\boldsymbol{m}}_1 \pm \alpha \boldsymbol{m}_2 \times \dot{\boldsymbol{m}}_2 - \nu \partial \boldsymbol{m}_1 \mp \nu \partial \boldsymbol{m}_2 \\
&+ \beta \boldsymbol{m}_1 \times \nu \partial \boldsymbol{m}_1 \pm \beta \boldsymbol{m}_2 \times \nu \partial \boldsymbol{m}_2 \\
&= \gamma (\boldsymbol{m} + \boldsymbol{n}) \times (\frac{\delta E}{\boldsymbol{m}} + \frac{\delta E}{\boldsymbol{n}}) \pm \gamma (\boldsymbol{m} - \boldsymbol{n}) \times (\frac{\delta E}{\boldsymbol{m}} - \frac{\delta E}{\boldsymbol{n}}) \\
&+ \alpha (\boldsymbol{m} + \boldsymbol{n}) \times (\dot{\boldsymbol{m}} + \dot{\boldsymbol{n}}) \pm \alpha (\boldsymbol{m} - \boldsymbol{n}) \times (\dot{\boldsymbol{m}} - \dot{\boldsymbol{n}}) - \nu \partial (\boldsymbol{m} + \boldsymbol{n}) \mp \nu \partial (\boldsymbol{m} - \boldsymbol{n}) \\
&+ \beta (\boldsymbol{m} + \boldsymbol{n}) \times \nu \partial (\boldsymbol{m} + \boldsymbol{n}) \pm \beta (\boldsymbol{m} - \boldsymbol{n}) \times \nu \partial (\boldsymbol{m} - \boldsymbol{n})
\end{aligned}
\tag{4.8}
$$

The $\pm$ differentiates between the two LLG equations with respect to the order parameters $2\boldsymbol{m} = \boldsymbol{m}_1 + \boldsymbol{m}_2$ and $2\boldsymbol{n} = \boldsymbol{m}_1 - \boldsymbol{m}_2$. The $\boldsymbol{m}$ and $\boldsymbol{n}$ only terms do not vanish because of the symmetry of the system in the case of $\dot{\boldsymbol{m}} = \dot{\boldsymbol{m}}_1 + \dot{\boldsymbol{m}}_2$. In the case of $\dot{\boldsymbol{n}} = \dot{\boldsymbol{m}}_1 - \dot{\boldsymbol{m}}_2$, the $\boldsymbol{m}$ and $\boldsymbol{n}$ only terms vanish because of the symmetry of the system. All parts occur twice so that the factors of two cancel out.

$$\dot{\boldsymbol{m}} = \gamma \boldsymbol{m} \times \frac{\delta E}{\delta \boldsymbol{m}} + \gamma \boldsymbol{n} \times \frac{\delta E}{\delta \boldsymbol{n}} + \alpha(\boldsymbol{m} \times \dot{\boldsymbol{m}} + \boldsymbol{n} \times \dot{\boldsymbol{n}}) - \nu \partial \boldsymbol{m} + \beta(\boldsymbol{m} \times \nu \partial \boldsymbol{m} + \boldsymbol{n} \times \nu \partial \boldsymbol{n}) \tag{4.9}$$

$$\dot{\boldsymbol{n}} = \gamma\boldsymbol{m}\times\frac{\delta E}{\delta\boldsymbol{n}}+\gamma\boldsymbol{n}\times\frac{\delta E}{\delta\boldsymbol{m}}+\alpha(\boldsymbol{m}\times\dot{\boldsymbol{n}}+\boldsymbol{n}\times\dot{\boldsymbol{m}})-\nu\partial\boldsymbol{n}+\beta(\boldsymbol{n}\times\nu\partial\boldsymbol{m}+\boldsymbol{m}\times\nu\partial\boldsymbol{n}) \quad (4.10)$$

Those two equations (4.9) and (4.10) describe the time evolution of an antiferromagnetic system if it can be described by two ferromagnetic sublattices, coupled by an interlattice exchange interaction. A generalisation of these equations in a higher dimensional system is achieved by switching $\nu\partial$ to $(\boldsymbol{\nu}\cdot\nabla)$. In this case, the current direction and spatial change can point in any direction.

The LLG equations will be used to determine a critical current value beyond which a domain wall shedding in the synthetic antiferromagnet happens as was done for the ferromagnetic case. Before that, the determination of the effective field terms is done in the next section.

4.2. Variational principle

So far, the equations of motion for the synthetic antiferromagnet (4.9) and (4.10) have been formed using the LLG equations of both sublattices in terms of the new parameters $\boldsymbol{n}$ and $\boldsymbol{m}$. The Néel vector determines the change of order in antiferromagnetic systems over time. The magnetisation serves as a perturbation-like quantity as it is tiny. The LLG equations as time evolution depend on the external spin-polarised current term, including the damping term proportional to β, as well as the damping term with α. Also, the equations are dependent on the change of the total magnetic energy E concerning both parameters $\boldsymbol{n}$ and $\boldsymbol{m}$.

The effective field contributions to the equation are calculated using the antiferromagnetic constraints of $|\boldsymbol{n}| = \boldsymbol{n}^2 = 1$ below the Néel temperature and its implication of $\partial\boldsymbol{n}\cdot\boldsymbol{n} = 0$. This is based on an approach used in the scientific report from Hals et al. [23] and adapted to the formalism used in this thesis.

The total magnetic energy is shown here (4.6):

$$E = \int dV(2A(\partial\boldsymbol{n})^2 + 2\lambda(1 - n_x^2) + \epsilon\boldsymbol{m}^2). \quad (4.11)$$

In the ferromagnetic case, a functional derivative of E with respect to the magnetisation vector $\boldsymbol{m}$ is sufficient to determine the effective field, driving each magnetic moment along its direction. This is shown in the domain wall shedding section of the ferromagnetic domain wall description. However, the correlation between both antiferromagnetic parameters implicates constraints that need to be addressed in the calculation. A functional derivative $\frac{\delta E}{\delta\boldsymbol{m}}$ should depend on both parameters, the $\boldsymbol{n}$ and $\boldsymbol{m}$ state. Mathematically, the right causality is built using a variational approach instead of the functional derivative.

The variational formalism changes the total magnetic energy for one of both parameters. The antiferromagnetic constraints are fulfilled for both. The total magnetic energy is the action of the system and therefore the Hamilton principle can be applied

to it. This principle states that the variation of the energy with respect to a random variation vector $\boldsymbol{\theta}$ vanishes for physical solutions.

Two phase space points with a given position and momentum determine two physical states of a system. A transition from one state to the other is feasible along every possible way between those two points, at least in principle. The physical path taken in the time evolution of the system is given by one of these possibilities. The Hamilton principle states that if the state is varied in terms of a random vector that this variation $\delta_X E = \int dV \boldsymbol{\theta} \cdot (...) = 0$ for any generalised coordinate X vanishes. The equation of motion is the $\boldsymbol{\theta}$ independent part (...). Since the variation of the action is vanishing, this Hamilton principle is also called the principle of least action. The equations of motion are the effective field terms of the LLG equations because they evolve the magnetisation and Néel vector in time, as the effective field should do.

The variation is implemented through the following steps: The order parameter variation are $\boldsymbol{\theta}$ dependent variables $\delta \boldsymbol{n} \sim \boldsymbol{\theta}$ or $\delta \boldsymbol{m} \sim \boldsymbol{\theta}$. Even though, they are chosen so that the variation of the constraint vanishes. In this case, all terms in the form of a constraint are vanishing in the equations of motion. The system will evolve along the directions complying with the constraints.

Hals et al. [23] determined the effective field with respect to the magnetisation $\frac{\delta E}{\delta \boldsymbol{m}}$ by taking "$\boldsymbol{m}$ normal to a fixed $\boldsymbol{n}$" (Hals et al. 2011 [23]). The variation of $\boldsymbol{m}$ as a quantity perpendicular to $\boldsymbol{n}$ can be described by $\delta \boldsymbol{m} = \boldsymbol{\theta} - (\boldsymbol{n} \cdot \boldsymbol{\theta})\boldsymbol{n}$. The second part $(\boldsymbol{n} \cdot \boldsymbol{\theta})\boldsymbol{n}$ is strictly perpendicular to the Néel vector. As stated above, the variation of the $\boldsymbol{n}$ is set to zero in this case $\delta \boldsymbol{n} = 0$. The constant length constraint of $\boldsymbol{n}$ is automatically fulfilled in the case of no change. The orthogonality is tested explicitly: $\delta(\boldsymbol{n} \cdot \boldsymbol{m}) = \boldsymbol{n} \cdot \delta \boldsymbol{m} = \boldsymbol{n} \cdot \boldsymbol{\theta} - (\boldsymbol{n} \cdot \boldsymbol{\theta})\boldsymbol{n} \cdot \boldsymbol{n} = \boldsymbol{n} \cdot \boldsymbol{\theta} - (\boldsymbol{n} \cdot \boldsymbol{\theta}) = 0$. In this calculation, the variation $\delta(\boldsymbol{n} \cdot \boldsymbol{m})$ - which will also be called derivative as it is a change of a mathematical expression - behaves like a derivative and the product rule needs to be deployed. The first term $\delta \boldsymbol{n} \cdot \boldsymbol{m}$ vanishes due to the constant length of $\boldsymbol{n}$. Inserting $\delta \boldsymbol{m}$ into the second term and using $\boldsymbol{n}^2 = 1$ shows that the orthogonality is indeed fulfilled.

The only relevant term in the total magnetic energy (4.6) is given by the interlattice exchange contribution $\epsilon \boldsymbol{m}^2$:

$$\delta(\boldsymbol{m}^2) = 2\boldsymbol{m} \cdot \delta \boldsymbol{m} = 2\boldsymbol{m} \cdot (\boldsymbol{\theta} - (\boldsymbol{n} \cdot \boldsymbol{\theta})\boldsymbol{n}) = 2\boldsymbol{m}\boldsymbol{\theta} - \boldsymbol{m} \cdot \boldsymbol{n}(\boldsymbol{n} \cdot \boldsymbol{\theta}) = 2\boldsymbol{m} \cdot \boldsymbol{\theta}. \quad (4.12)$$

Therefore, the total variation with respect to the magnetisation as follows:

$$\delta_{\boldsymbol{m}} E = \int d\boldsymbol{r} \boldsymbol{\theta} \cdot (2\epsilon \boldsymbol{m}). \quad (4.13)$$

The effective field is given by the $\boldsymbol{\theta}$ independent part $\frac{\delta E}{\delta \boldsymbol{m}} = 2\epsilon \boldsymbol{m}$.

A similar approach can be used for the determination of the effective field in terms of the Néel vector $\frac{\delta E}{\delta \boldsymbol{n}}$. The ansatz chosen is the following: $\delta_{\boldsymbol{n}} E$ is calculated "by parallel transporting $\boldsymbol{m}$ on the sphere that is parametrised by $\boldsymbol{n}$" (Hals et al. 2011 [23]). The constant length constraint of $\boldsymbol{n}$ can be ensured by modelling the change as a rotation perpendicular to the vector direction and proportional to the random

variation direction $\boldsymbol{\theta}$. $\delta\boldsymbol{m} \perp \delta\boldsymbol{n}$ has to hold as the magnetisation $\boldsymbol{m}$ constraint to be orthogonal to $\boldsymbol{n}$. Then, the variation of $\boldsymbol{m}$ should be proportional to $\boldsymbol{\theta}$ as well as perpendicular to $\boldsymbol{m}$ itself. Therefore, $\delta\boldsymbol{m} = \boldsymbol{m} \times (\boldsymbol{\theta} \times \boldsymbol{n})$ is used as the ansatz. The rotation $\delta\boldsymbol{n}$ can be determined by the constraint $\boldsymbol{m} \cdot \boldsymbol{n} = 0$:

$$
\begin{aligned}
\delta(\boldsymbol{m} \cdot \boldsymbol{n}) = \delta\boldsymbol{m} \cdot \boldsymbol{n} + \boldsymbol{m} \cdot \delta\boldsymbol{n} &= \boldsymbol{n} \cdot (\boldsymbol{m} \times (\boldsymbol{\theta} \times \boldsymbol{n})) + \boldsymbol{m} \cdot \delta\boldsymbol{n} \\
&= (\boldsymbol{n} \cdot \boldsymbol{\theta})(\boldsymbol{m} \cdot \boldsymbol{n}) - (\boldsymbol{n} \cdot \boldsymbol{n})(\boldsymbol{\theta} \cdot \boldsymbol{m}) + \boldsymbol{m} \cdot \delta\boldsymbol{n} \\
&= \boldsymbol{m} \cdot (\boldsymbol{n}(\boldsymbol{n} \cdot \boldsymbol{\theta}) - \boldsymbol{\theta}(\boldsymbol{n} \cdot \boldsymbol{n})) + \boldsymbol{m} \cdot \delta\boldsymbol{n} = \boldsymbol{m} \cdot (\boldsymbol{n} \times (\boldsymbol{n} \times \boldsymbol{\theta})) + \boldsymbol{m} \cdot \delta\boldsymbol{n}.
\end{aligned} \tag{4.14}
$$

Consequently, the cross product can be switched for an additional minus sign to get $\delta\boldsymbol{n} = \boldsymbol{n} \times (\boldsymbol{\theta} \times \boldsymbol{n})$. Even though, this vector is explicitly orthogonal to $\boldsymbol{n}$, the constraint $\boldsymbol{n}^2 = 1$ is tested: $\delta(\boldsymbol{n}^2) = 2\boldsymbol{n} \cdot \delta\boldsymbol{n} = 2\boldsymbol{n} \cdot (\boldsymbol{n} \times (\boldsymbol{\theta} \times \boldsymbol{n})) = 2\boldsymbol{n} \cdot (\boldsymbol{\theta}(\boldsymbol{n} \cdot \boldsymbol{n}) - \boldsymbol{n}(\boldsymbol{n} \cdot \boldsymbol{\theta})) = 0$. This ansatz fulfils both constraints. The effective field will be determined in the following steps using the total magnetic energy variation:

$$
\delta_{\boldsymbol{n}} E = \int d\boldsymbol{r} \delta(2A(\partial\boldsymbol{n})^2 + 2\lambda(1 - n_x^2) + \epsilon\boldsymbol{m}^2) \tag{4.15}
$$

The first part of equation (4.15) can be determined using a partial integration:

$$
\begin{aligned}
\delta(2\partial\boldsymbol{n})^2 = 4\partial\boldsymbol{n} \cdot \delta\boldsymbol{n} = -4\partial^2\boldsymbol{n} \cdot (\boldsymbol{n} \times (\boldsymbol{\theta} \times \boldsymbol{n})) &= -4\partial^2\boldsymbol{n} \cdot (\boldsymbol{\theta}(\boldsymbol{n} \cdot \boldsymbol{n}) - \boldsymbol{n}(\boldsymbol{n} \cdot \boldsymbol{\theta})) \\
&= -4\boldsymbol{\theta} \cdot (\partial^2\boldsymbol{n}(\boldsymbol{n} \cdot \boldsymbol{n}) - \boldsymbol{n}(\boldsymbol{n} \cdot \partial^2\boldsymbol{n})) = -4\boldsymbol{\theta} \cdot (\boldsymbol{n} \times (\partial^2\boldsymbol{n} \times \boldsymbol{n})).
\end{aligned} \tag{4.16}
$$

The partial integration has to be used because $\partial\boldsymbol{\theta}$ is ambiguous for a random vector $\boldsymbol{\theta}$. The boundary conditions of the variation vector vanish. Hence, $-4\partial^2\boldsymbol{n} \cdot \delta\boldsymbol{n}$ results in the second step. Afterwards, the ansatz for $\delta\boldsymbol{n}$ is inserted and the $bac - cab$ rule (A.1) is used. Then, the $\boldsymbol{\theta}$ can be pulled out, leaving a different $bac - cab$ rule as the final result.

The anisotropic contribution $\lambda(1 - n_x^2)$ is calculated in a similar way:

$$
\begin{aligned}
\delta(1 - n_x^2) = -2n_x\delta n_x = -2n_x\hat{\boldsymbol{x}} \cdot \delta\boldsymbol{n} &= -2n_x\hat{\boldsymbol{x}} \cdot (\boldsymbol{n} \times (\boldsymbol{\theta} \times \boldsymbol{n})) \\
&= -2n_x\hat{\boldsymbol{x}} \cdot (\boldsymbol{\theta}(\boldsymbol{n} \cdot \boldsymbol{n}) - \boldsymbol{n}(\boldsymbol{n} \cdot \boldsymbol{\theta})) = -2n_x\boldsymbol{\theta} \cdot (\hat{\boldsymbol{x}}(\boldsymbol{n} \cdot \boldsymbol{n}) - \boldsymbol{n}(\boldsymbol{n} \cdot \hat{\boldsymbol{x}})) \\
&= -2n_x\boldsymbol{\theta} \cdot (\boldsymbol{n} \times (\hat{\boldsymbol{x}} \times \boldsymbol{n})).
\end{aligned} \tag{4.17}
$$

The variation of a constant is non-existing. Also, the variation of δn_x can be written as a dot product with the $\boldsymbol{x}$ direction vector as it does not contribute to a product rule in differentiation. The triple product is recast using the $bac - cab$ rule (A.1). Then, the $\boldsymbol{\theta}$ and $\boldsymbol{x}$ are switched and the $bac - cab$ rule is reversed.

The interlattice exchange interaction term will not contribute in this variation because the magnetisation change is supposed to be perpendicular to the magnetisation itself:

$$
\delta\boldsymbol{m}^2 = 2\boldsymbol{m} \cdot \delta\boldsymbol{m} = 2\boldsymbol{m} \cdot (\boldsymbol{m} \times (\boldsymbol{\theta} \times \boldsymbol{n})) = 0. \tag{4.18}
$$

The total variation of the free energy E in terms of the Néel vector can be written as:

$$
\delta_{\boldsymbol{n}} E = \int d\boldsymbol{r} \boldsymbol{\theta} \cdot (-4A\boldsymbol{n} \times (\partial^2\boldsymbol{n} \times \boldsymbol{n}) - 4\lambda n_x(\boldsymbol{n} \times (\hat{\boldsymbol{x}} \times \boldsymbol{n}))). \tag{4.19}
$$

The corresponding effective field is given by $\frac{\delta E}{\delta \boldsymbol{n}} = -4A\boldsymbol{n} \times (\partial^2 \boldsymbol{n} \times \boldsymbol{n}) - 4\lambda n_x \boldsymbol{n} \times (\hat{\boldsymbol{x}} \times \boldsymbol{n})$. Both effective field terms are summarised in the following equation:

$$\frac{\delta E}{\delta \boldsymbol{m}} = 2\epsilon \boldsymbol{m}, \quad \frac{\delta E}{\delta \boldsymbol{n}} = -4A\boldsymbol{n} \times (\partial^2 \boldsymbol{n} \times \boldsymbol{n}) - 4\lambda n_x \boldsymbol{n} \times (\hat{\boldsymbol{x}} \times \boldsymbol{n}). \tag{4.20}$$

Within this section, the foundation for a critical current calculation for domain wall shedding in the one-dimensional synthetic antiferromagnetic nanowire has been completed by the calculation of the effective field terms occurring in the antiferromagnetic LLG equations (4.9) and (4.10). In contrast to the ferromagnetic calculations, the effective field could not be determined using the functional derivative approach as it does not contemplate the antiferromagnetic constraints below the Néel temperature. A variational approach in which the effective field was calculated using the Hamilton principle on the system's action E was chosen instead. The physical path taken from one point in phase space to another one can be calculated using a variation of the collective coordinates while fulfilling the constraint. The resulting equations of motion describe the effective field terms as they point along the direction in which the collective coordinates evolve in time based on the material parameters.

4.3. Antiferromagnetic critical current for shedding

In the previous sections, the LLG equations for a one-dimensional synthetic antiferromagnet with corresponding effective field terms were derived in the equations (4.9), (4.10), (4.20). This system is built with an interlattice exchange interaction, the intralattice exchange interaction and an easy axis anisotropy. Next, a semi-infinitely long nanowire system with the pinning of the Néel vector orthogonal to the easy axis is used to start a domain wall shedding as in the ferromagnetic case. The critical current value is the spin-polarised current strength above which a domain wall starts to detach itself from the pinning point set to the origin. A static case approximation and the use of the Noether theorem will be needed to derive this current value. Although the LLG equations represent the full dynamics of the specified systems, it is necessary to consider simplifications to get an analytical result. A domain wall movement starts at the critical current value and is not present below it. Therefore, the boundary value can be calculated in the stable state below the critical value, which is a static configuration with $\dot{\boldsymbol{m}} = \dot{\boldsymbol{n}} = 0$. Also, a slow detaching and movement of the wall justifies this ansatz. The full LLG equations gets reduced to an α independent quantity. The terms proportional to the dissipative constant β can be neglected because the movement can be treated adiabatically. Any dissipative term is negligible in this approximation. The resulting LLG equations are given by:

$$0 = \gamma \boldsymbol{m} \times \frac{\delta E}{\delta \boldsymbol{m}} + \gamma \boldsymbol{n} \times \frac{\delta E}{\delta \boldsymbol{n}} - \nu \partial \boldsymbol{m}$$
$$0 = \gamma \boldsymbol{m} \times \frac{\delta E}{\delta \boldsymbol{n}} + \gamma \boldsymbol{n} \times \frac{\delta E}{\delta \boldsymbol{m}} - \nu \partial \boldsymbol{n}. \tag{4.21}$$

4. Antiferromagnetic domain wall description

The insertion of the effective field terms (4.20) complete the formalism:

$$0 = \gamma \boldsymbol{m} \times 2\epsilon \boldsymbol{m} + \gamma \boldsymbol{n} \times (-4A\boldsymbol{n} \times (\partial^2 \boldsymbol{n} \times \boldsymbol{n}) - 4\lambda n_x \boldsymbol{n} \times (\hat{\boldsymbol{x}} \times \boldsymbol{n})) - \nu \partial \boldsymbol{m}$$
(4.22)

$$0 = \gamma \boldsymbol{m} \times (-4A\boldsymbol{n} \times (\partial^2 \boldsymbol{n} \times \boldsymbol{n}) - 4\lambda n_x \boldsymbol{n} \times (\hat{\boldsymbol{x}} \times \boldsymbol{n})) + \gamma \boldsymbol{n} \times 2\epsilon \boldsymbol{m} - \nu \partial \boldsymbol{n}.$$

The interlattice exchange term vanishes in the top equation due to a cross product of the same vector. The $bac - cab$ rule is used to rewrite the triple products taking the last cross product as one part:

$$\boldsymbol{m} \times (\boldsymbol{n} \times (\partial^2 \boldsymbol{n} \times \boldsymbol{n})) = \boldsymbol{n}(\boldsymbol{m} \cdot (\partial^2 \boldsymbol{n} \times \boldsymbol{n})) - (\partial^2 \boldsymbol{n} \times \boldsymbol{n})(\boldsymbol{m} \cdot \boldsymbol{n}) = \boldsymbol{n}(\boldsymbol{m} \cdot (\partial^2 \boldsymbol{n} \times \boldsymbol{n}))$$
$$\boldsymbol{m} \times (\boldsymbol{n} \times (n_x\hat{\boldsymbol{x}} \times \boldsymbol{n})) = \boldsymbol{n}(\boldsymbol{m} \cdot (n_x\hat{\boldsymbol{x}} \times \boldsymbol{n})) - (n_x\hat{\boldsymbol{x}} \times \boldsymbol{n})(\boldsymbol{m} \cdot \boldsymbol{n}) = \boldsymbol{n}(\boldsymbol{m} \cdot (n_x\hat{\boldsymbol{x}} \times \boldsymbol{n}))$$

$$\boldsymbol{n} \times (\boldsymbol{n} \times (\partial^2 \boldsymbol{n} \times \boldsymbol{n})) = \boldsymbol{n}(\boldsymbol{n} \cdot (\partial^2 \boldsymbol{n} \times \boldsymbol{n})) - (\partial^2 \boldsymbol{n} \times \boldsymbol{n})(\boldsymbol{n} \cdot \boldsymbol{n}) = -\partial^2 \boldsymbol{n} \times \boldsymbol{n}$$
$$\boldsymbol{n} \times (\boldsymbol{n} \times (n_x\hat{\boldsymbol{x}} \times \boldsymbol{n})) = \boldsymbol{n}(\boldsymbol{n} \cdot (n_x\hat{\boldsymbol{x}} \times \boldsymbol{n})) - (n_x\hat{\boldsymbol{x}} \times \boldsymbol{n})(\boldsymbol{n} \cdot \boldsymbol{n}) = -n_x\hat{\boldsymbol{x}} \times \boldsymbol{n}.$$
(4.23)

The magnetisation vector and the Néel vector are perpendicular to each other by construction. Therefore, the second term of the $\boldsymbol{m}\times$ equations vanish. In the bottom equations, the first part of the $bac - cab$ formula is zero due to the orthogonality between $\boldsymbol{n}$ and its product. The LLG equations are transformed into the following form:

$$0 = 4A\gamma\partial^2 \boldsymbol{n} \times \boldsymbol{n} + 4\lambda n_x \gamma \hat{\boldsymbol{x}} \times \boldsymbol{n} - \nu \partial \boldsymbol{m}$$
(4.24)

$$0 = -4A\gamma\boldsymbol{n}(\boldsymbol{m} \cdot (\partial^2 \boldsymbol{n} \times \boldsymbol{n})) - 4\lambda n_x \gamma \boldsymbol{n}(\boldsymbol{m} \cdot (n_x\hat{\boldsymbol{x}} \times \boldsymbol{n})) + \gamma \boldsymbol{n} \times 2\epsilon \boldsymbol{m} - \nu \partial \boldsymbol{n}. \quad (4.25)$$

Equation (4.25) is multiplied by $\boldsymbol{n}\times$ to cancel out the first two terms. The triple product of the interlattice exchange reforms to an $\boldsymbol{m}$ only term. Then, a solution of the magnetisation vector with respect to the Néel vector is found:

$$2\gamma\epsilon \boldsymbol{m} = -\nu \boldsymbol{n} \times \partial \boldsymbol{n}.$$
(4.26)

The spatial derivative of this equality is determined and inserted into the other LLG equation to get a Néel vector only equation. Therefore, $\partial \boldsymbol{m} = \partial(\boldsymbol{n} \times \partial \boldsymbol{n}) = -\partial^2 \boldsymbol{n} \times \boldsymbol{n}$ needs to be used. The two minus signs occurring lead to a negatively signed result.

$$0 = 4A\gamma\partial^2 \boldsymbol{n} \times \boldsymbol{n} + 4\lambda n_x \gamma \hat{\boldsymbol{x}} \times \boldsymbol{n} - \frac{\nu^2}{2\gamma\epsilon}\partial^2 \boldsymbol{n} \times \boldsymbol{n} = (A - \frac{\nu^2}{8\gamma^2\epsilon})\partial^2 \boldsymbol{n} \times \boldsymbol{n} + \lambda n_x \hat{\boldsymbol{x}} \times \boldsymbol{n} \quad (4.27)$$

As in the ferromagnetic calculations, the one-dimensional semi-infinitely long nanowire system with a pinned origin has two symmetries that can be used to determine the critical current value. The Noether theorem states that "every continuous symmetry

47

of a system entails a conservation law" (Altland and Simons 2010 [3]). As already described in the ferromagnetic domain wall shedding section, the origin of the system is chosen arbitrarily and it can be shifted to a different point. This implies the conservation of the linear magnetic momentum.

Also, the rotation of the system around the x-axis does not change the free energy. Therefore, the rotation invariance leads to a conservation of the total angular momentum around the x-axis. Again, as in the ferromagnetic calculations a multiplication by certain values demonstrate those conservation laws. Those two possible multiplying factors are $\hat{\boldsymbol{x}}$ and $\boldsymbol{n} \times \partial\boldsymbol{n}$. These quantities would not be conserved in the case of dissipation.

The conservation of the angular momentum along the x-axis is shown by the multiplication of equation (4.27) by $\hat{\boldsymbol{x}}$:

$$
\begin{aligned}
0 &= \hat{\boldsymbol{x}} \cdot ((A - \frac{\nu^2}{8\gamma^2\epsilon})\partial^2\boldsymbol{n} \times \boldsymbol{n} + \lambda n_x \hat{\boldsymbol{x}} \times \boldsymbol{n}) \\
0 &= (A - \frac{\nu^2}{8\gamma^2\epsilon})\partial(\hat{\boldsymbol{x}} \cdot (\partial\boldsymbol{n} \times \boldsymbol{n})).
\end{aligned}
\tag{4.28}
$$

The anti-commuting cross product marks $\partial^2\boldsymbol{n} \times \boldsymbol{n} = \partial(\partial\boldsymbol{n} \times \boldsymbol{n})$ and the fact that the anisotropy term equals zero. The equation (4.28) points out that the derivative of the angular momentum along the x-axis is zero. Hence, this quantity is conserved and has a constant value.

The system's boundary conditions at $x = 0$ and $x \to \infty$ can be used to determine the constant value or be compared since they are equal. At $x = 0$, the Néel vector points along the z direction ($\boldsymbol{n} = \hat{\boldsymbol{z}}$) by definition of this pinning. Also, at $x \to \infty$ it points along or against the easy axis of the system $\boldsymbol{n} = \pm\hat{\boldsymbol{x}}$. Those directions can be explained by the fact that the sublattice magnetisation values are the constituents of the Néel vector and the anisotropic axis is the x-axis for both.

Towards infinity, there is no change in the magnetisation direction. Therefore, the spatial derivative of $\boldsymbol{n}$ vanishes: $\partial\boldsymbol{n} = 0$. Then, the constant value of the conserved quantity must be zero as well. At $x = 0$, the Néel vector strictly points along z. The cross product can be determined and both values can be compared:

$$
\partial n_y|_{x=0} = 0.
\tag{4.29}
$$

The material parameters do not contribute to this equality.

The second conservation law of the system is the linear momentum conservation along the x-axis. This can be shown by a multiplication of equation (4.27) by $\boldsymbol{n} \times \partial\boldsymbol{n}$:

$$
0 = (\boldsymbol{n} \times \partial\boldsymbol{n}) \cdot ((A - \frac{\nu^2}{8\gamma^2\epsilon})\partial^2\boldsymbol{n} \times \boldsymbol{n} + \lambda n_x \hat{\boldsymbol{x}} \times \boldsymbol{n}).
\tag{4.30}
$$

The Lagrange identity for vectors (A.2) is used to rewrite the equation. Also, the chain rule of derivation can be applied backwards to get $\partial(\partial\boldsymbol{n})^2 = 2\partial^2\boldsymbol{n} \cdot \partial\boldsymbol{n}$.

$$0 = -2\partial((A - \frac{\nu^2}{8\gamma^2\epsilon})(\partial\boldsymbol{n})^2 + \gamma\lambda n_x^2)$$
$$0 = \partial((A - \frac{\nu^2}{8\gamma^2\epsilon})(\partial\boldsymbol{n})^2 + \gamma\lambda n_x^2). \tag{4.31}$$

The anisotropic part is recast using the same trick $\partial(\partial n_x)^2 = 2n_x\partial^2 n_x$. The constant length constraint $\boldsymbol{n}^2 = 1$ is why the other terms in the Lagrange identity vanish.

The values of both boundary conditions can be checked at $x = 0$ where $\boldsymbol{n} = \hat{\boldsymbol{z}}$ and at $x \to \infty$ where $\boldsymbol{n} = \pm\hat{\boldsymbol{x}}$ and $\partial\boldsymbol{n} = 0$, just as in the angular momentum case. The equation (4.31) for the linear momentum along the x direction at $x \to \infty$ is $\gamma\lambda = $ *constant*. This holds because of $n_x^2 = 1$ at x at infinity. Also, $(A - \frac{\nu^2}{8\gamma^2\epsilon})(\partial\boldsymbol{n}^2)|_{x=0} = $ *constant* is the value of the momentum at $x = 0$. Those equations share the same constant value because of the conservation. Hence, they can be combined to:

$$(A - \frac{\nu^2}{8\gamma^2\epsilon})(\partial\boldsymbol{n}^2)|_{x=0} = \gamma\lambda. \tag{4.32}$$

As in the ferromagnetic computations, the equality can be facilitated using the fact that $(\partial\boldsymbol{n})^2 = (\partial n_x)^2 + (\partial n_y)^2 + (\partial n_z)^2$. Also used are $(\partial n_z)^2 = 0$ at $x = 0$ from the constant length constraint and $(\partial n_y)^2 = 0$ at $x = 0$ because of the angular momentum conservation formula (4.29).

$$(\partial n_x^2)|_{x=0} = \frac{\gamma\lambda}{A - \frac{\nu^2}{8\gamma^2\epsilon}} \tag{4.33}$$

The squared change of n_x must be greater or equal to zero mathematically. The boundary term at which the equation does not hold anymore is given at the point of $(\partial n_x^2)|_{x=0} = 0$. Anything below zero is an instability of the system. If the state is not stable anymore, a domain wall will start to detach itself and move along the wire in the electron current direction. The condition of instability is tested below:

$$0 < \frac{\gamma\lambda}{A - \frac{\nu^2}{8\gamma^2\epsilon}}. \tag{4.34}$$

Both γ and λ are positive constants. Hence, the condition for the squared current strength is $\nu^2 < 8\gamma^2\epsilon A$ to match the inequality. This is equivalent to a critical value of:

$$\nu_c = 2\gamma\sqrt{2A\epsilon}. \tag{4.35}$$

All currents greater than the one in equation (4.35) fulfil the same condition and lead to an unstable state with domain wall creation and movement along the nanowire direction. A comparison of the ferromagnetic case $\nu_C = 2\gamma\sqrt{\lambda A}$ without DMI to

the antiferromagnetic one (4.35) shows that both depend on the square root of the intralattice exchange interaction $\sqrt{A}$ and the gyromagnetic ratio γ.

The intralattice exchange interaction or exchange interaction in a ferromagnetic system favours parallel alignment of the same lattice magnetic moments. No interaction strength leads to a system where all magnetic moments point along the easy axis of the anisotropy and both sublattice magnetisation vectors are antiparallel. An application of a spin-polarised current along the wire at an orthogonal pinning point would lead to an easy domain wall creation since the neighbouring spins have no force to keep them parallel. At interaction strengths much greater than the other interactions, this force is dominant. Domain wall shedding is only possible for huge currents because all magnetic moments want to be parallel to each sublattice neighbour, but the domain wall is determined by a constant rotation of the magnetisation vector within. The fact that the current strength needed grows in a non-linear way can not be illuminated by such an argument. However, those two cases show that the square root dependency of the critical current for shedding in terms of the intralattice exchange interaction is justifiable.

The critical current does also depend on the interlattice exchange interaction with a square root proportionality. This can be explained by the boundary cases as well. The sublattice magnetic moments are modelled antiparallel at the beginning, with or without interlattice exchange. At first, the case of no interlattice exchange is discussed. The adjoining neighbour spins of the same lattice align due to the intralattice exchange. Also, both sublattices will either align with the anisotropic direction or antiparallel to it. Hence, towards large x, both sublattice magnetisations will be parallel or antiparallel.

As the total magnetic energy was built, other interactions such as the dipole-dipole interaction were neglected because they were much smaller in their strength compared to the interlattice exchange. Keeping this approximation, small currents applied along the wire direction force both magnetisation values at the pinning point to rotate along the wire direction independently of each other. Then, some kind of ferromagnetic domain wall structures will move in each of the sublattices like in a ferromagnetic nanowire system. Also, no DMI in the system indicates that both types of a domain wall will move at the same velocity [38].

However, this approximation is not very realistic. Other interactions like the demagnetisation field, produced by the ferromagnetic state, will change this consideration. Adjacent spins between the sublattices are forced to align to the other magnetic moments due to this field. Since both sublattices are ferromagnetic, the system should behave like a ferromagnetic system in total. This means that the critical current will be comparable to a ferromagnetic value when a first domain wall is created. The bottom layer, which has a magnetisation value towards the negative x-axis, will rotate towards the positive axis.

On the one hand, minimal interlattice exchange values result in lower energy required to get a kink between antiferromagnetic coupled magnetic moments as shown in figure 4.2. Then, domain walls can be efficiently built because currents will push both sublattices spins towards the x direction at a lower energy requirement and adjoining

neighbour magnetic moments of the same lattice tend to align due to the intralattice exchange. This leads to a domain wall building. On the other hand, high exchange values lead to high energy levels needed to get a kink in between the magnetisation vectors. In this case, large spin-polarised currents are needed to change both magnetisation values towards the easy axis direction to build up domain walls. Therefore, after neglecting the limit of no interlattice exchange in the system, a square root dependency of the critical current with respect to the interlattice exchange strength ϵ is justifiable.

The ferromagnetic current depends on the anisotropic strength λ, while the antiferromagnetic one does not in this approximation. This is surprising since the easy axis anisotropy is the main factor for the system's structure along the wire. It is assumable that different strengths of this anisotropy would change the current. For example, no anisotropy would mean that all magnetic moments align with the pinning direction due to the intralattice exchange, and a domain wall creation with a current along the nanowire direction is not possible. Also, an anisotropy $\lambda \to \infty$ blocks any type of domain wall creation since all magnetisation values unequal to the x direction are not in the energetic minimum. Therefore, an anisotropic dependency of the critical current is justifiable but cannot observed.

An expansion to this formalism is done by adding more terms to the total magnetic energy. For example, in the ferromagnetic case, the DMI changed the current value needed and showed that different domain wall types behave differently. Also, different kinds of anisotropies create different behaviour. The 180° domain walls built in this formalism are not uniquely defined because the Néel vector could also be pointing in the negative direction without changing the formalism. The ground states of a system with such an anisotropy can not be distinguished in an experiment because of the vanishing magnetisation of antiferromagnetic systems. However, 90° domain walls built by a different anisotropy have two ground states, which can be measured together.

Such a geometry of a one-dimensional synthetic antiferromagnetic nanowire system with a pinning point can be tested for a domain wall shedding with different materials to verify this calculation. The pinning could be used in the future as a write head for a synthetic antiferromagnetic racetrack memory system which Parkin and Yang [35] proposed.

The critical current value for shedding and its square root dependency on both the interlattice exchange and the intralattice exchange will be tested in a simulation in the next chapter. Also, the critical current value for shedding needs to be compared to the critical current to break the antiferromagnetic ground state along the anisotropic direction. If this value were lower than the shedding current one, no application of the formalism would be possible because the system would not be stable anymore in the region of possible shedding. Within the next section, this stability calculation will be performed.

4.4. Antiferromagnetic instability

So far, a theory for a one-dimensional synthetic antiferromagnetic nanowire system has been built using two ferromagnetic sublattices with an interlattice exchange interaction. Also, an intralattice exchange interaction and easy axis anisotropy has been used for the model. Now, the antiferromagnetic instability critical current value will be determined.

A spin-polarised current can perturb the antiferromagnetic state and if it is large enough, it can destabilise the state. It is necessary to know if such a critical current value is greater or lower than the shedding current because if it is lower, the antiferromagnetic state would not exist at a current where shedding could happen and a racetrack application would not be possible. Therefore, an ansatz for determining such a destabilising or instability current is established in this section.

The one-dimensional synthetic antiferromagnetic nanowire system with an easy axis anisotropy and interlattice as well as intralattice exchange interaction with a total magnetic energy of equation (4.6) is taken without pinning. This system has the ground state value of $\boldsymbol{n} = \pm\hat{\boldsymbol{x}}$. A perturbation is subjected to this system perpendicular to the ground state value to get a destabilisation condition. Both, the magnetisation $\boldsymbol{m}$ and the Néel vector $\boldsymbol{n}$ are taken for this perturbation $\boldsymbol{n} = \hat{\boldsymbol{x}} + (0, n_y, n_z)^T = \hat{\boldsymbol{x}} + \boldsymbol{h}$ and $\boldsymbol{m} = (m_x, m_y, m_z)^T$. The constraint $\boldsymbol{n}^2 = 1$ is built in by the ground state direction and justifies the orthogonal perturbation to it $\boldsymbol{h}$. Mathematically, the x component has to vanish because of this constraint $|\boldsymbol{n}|^2 = 1 = (1+n_x)^2 + n_y^2 + n_z^2 = 1 + 2n_x + (n_x^2 + n_y^2 + n_z^2) \to n_x = 0$. The magnetisation is set to be a perturbation like in the other calculations because of $\boldsymbol{n} \gg \boldsymbol{m}$.

The perturbation ansatz is inserted into the antiferromagnetic LLG equations (4.9) and (4.10). The method used for the calculation is called linearisation of the system because a higher order than linear expressions are magnitudes smaller than the rest and will be neglected to facilitate the formalism. Without such a simplification, finding an analytical result is much more complicated or even impossible.

The Néel vector contains the ground state $\hat{\boldsymbol{x}}$ and a perpendicular perturbation vector $\boldsymbol{h}$. A spatial or time derivative of this quantity is given by $\dot{\boldsymbol{n}} = \dot{\hat{\boldsymbol{x}}} + \dot{\boldsymbol{h}} = \dot{\boldsymbol{h}}$ and $\partial\boldsymbol{n} = \partial\hat{\boldsymbol{x}} + \partial\boldsymbol{h} = \partial\boldsymbol{h}$. Both the time and spatial derivative of the ground state direction vanish as it is a constant value, but the change is non-vanishing for the perturbation. Also, the perturbation change of the magnetisation is non-vanishing. The results from the variational principle 4.20 are inserted since they fulfil the antiferromagnetic

4. Antiferromagnetic domain wall description

restrictions of $\boldsymbol{n}^2 = 1$ and $\boldsymbol{n} \cdot \boldsymbol{m} = 0$:

$$
\begin{aligned}
\boldsymbol{m} \times \frac{\delta E}{\delta \boldsymbol{m}} &= 0 \\
\boldsymbol{m} \times \frac{\delta E}{\delta \boldsymbol{n}} &= -4A\boldsymbol{m} \times (\boldsymbol{n} \times (\partial^2 \boldsymbol{n} \times \boldsymbol{n})) - 4\lambda n_x \boldsymbol{m} \times (\boldsymbol{n} \times (\hat{\boldsymbol{x}} \times \boldsymbol{n})) \\
&= -4A\boldsymbol{n}(\boldsymbol{m} \cdot (\partial^2 \boldsymbol{n} \times \boldsymbol{n})) - 4\lambda n_x \boldsymbol{n}(\boldsymbol{m} \cdot (\hat{\boldsymbol{x}} \times \boldsymbol{n})) \\
\boldsymbol{n} \times \frac{\delta E}{\delta \boldsymbol{m}} &= 2\epsilon \boldsymbol{n} \times \boldsymbol{m} \\
\boldsymbol{n} \times \frac{\delta E}{\delta \boldsymbol{n}} &= -4A\boldsymbol{n} \times (\partial^2 \boldsymbol{n}(\boldsymbol{n}^2) - \boldsymbol{n}(\partial^2 \boldsymbol{n} \cdot \boldsymbol{n})) - 4\lambda n_x \boldsymbol{n} \times (\hat{\boldsymbol{x}}(\boldsymbol{n}^2) - \boldsymbol{n}(\hat{\boldsymbol{x}} \cdot \boldsymbol{n})) \\
&= -4A\boldsymbol{n} \times \partial^2 \boldsymbol{n} - 4\lambda n_x \boldsymbol{n} \times \hat{\boldsymbol{x}}.
\end{aligned}
\tag{4.36}
$$

The four possible combinations of the LLG equations are shown above. The full equations with the ansatz inserted are given by:

$$
\begin{aligned}
\dot{\boldsymbol{m}} &= -4A\gamma(\hat{\boldsymbol{x}} + \boldsymbol{h}) \times \partial^2(\hat{\boldsymbol{x}} + \boldsymbol{h}) - 4\lambda\gamma((\hat{\boldsymbol{x}} + \boldsymbol{h}))_x(\hat{\boldsymbol{x}} + \boldsymbol{h}) \times \hat{\boldsymbol{x}} \\
&\quad + \alpha(\boldsymbol{m} \times \dot{\boldsymbol{m}} + (\hat{\boldsymbol{x}} + \boldsymbol{h}) \times (\dot{\hat{\boldsymbol{x}}} + \dot{\boldsymbol{h}})) - \nu\partial\boldsymbol{m} + \beta\nu(\boldsymbol{m} \times \partial\boldsymbol{m}) + \beta\nu(\hat{\boldsymbol{x}} + \boldsymbol{h}) \times (\dot{\hat{\boldsymbol{x}}} + \dot{\boldsymbol{h}}) \\
&= -4A\gamma\hat{\boldsymbol{x}} \times \partial^2\boldsymbol{h} + 4\lambda\gamma\hat{\boldsymbol{x}} \times \boldsymbol{h} + \alpha\hat{\boldsymbol{x}} \times \dot{\boldsymbol{h}} - \nu\partial\boldsymbol{m} + \beta\nu(\hat{\boldsymbol{x}} \times \partial\boldsymbol{h})
\end{aligned}
\tag{4.37}
$$

$$
\begin{aligned}
\dot{\boldsymbol{h}} = \dot{\hat{\boldsymbol{x}}} + \dot{\boldsymbol{h}} &= -4A\gamma\boldsymbol{m} \times ((\hat{\boldsymbol{x}} + \boldsymbol{h}) \times (\partial^2(\hat{\boldsymbol{x}} + \boldsymbol{h}) \times (\hat{\boldsymbol{x}} + \boldsymbol{h}))) \\
&\quad - 4\lambda\gamma(\hat{\boldsymbol{x}} + \boldsymbol{h})_x\boldsymbol{m} \times ((\hat{\boldsymbol{x}} + \boldsymbol{h}) \times (\hat{\boldsymbol{x}} \times (\hat{\boldsymbol{x}} + \boldsymbol{h}))) + 2\epsilon\gamma(\hat{\boldsymbol{x}} + \boldsymbol{h}) \times \boldsymbol{m} \\
&\quad + \alpha(\boldsymbol{m} \times (\dot{\hat{\boldsymbol{x}}} + \dot{\boldsymbol{h}}) + (\hat{\boldsymbol{x}} + \boldsymbol{h}) \times \dot{\boldsymbol{m}}) - \nu\partial\boldsymbol{n} + \beta((\hat{\boldsymbol{x}} + \boldsymbol{h}) \times \nu\partial\boldsymbol{m} + \boldsymbol{m} \times \nu\partial(\hat{\boldsymbol{x}} + \boldsymbol{h})) \\
&= 2\epsilon\gamma\hat{\boldsymbol{x}} \times \boldsymbol{m} + \alpha\hat{\boldsymbol{x}} \times \dot{\boldsymbol{m}} - \nu\partial\boldsymbol{h} + \beta\nu(\hat{\boldsymbol{x}} \times \partial\boldsymbol{m}).
\end{aligned}
\tag{4.38}
$$

In both equations, all derivative terms need to be according to $\boldsymbol{h}$ to be non-vanishing. If such a term is also dependent on magnetisation, it will get neglected since it can not be linear in the perturbation. In the $\dot{\boldsymbol{n}}$ equation, the intralattice exchange and anisotropic exchange term are of a higher order than the linear one. The interlattice exchange term is only dependent on the magnetisation. Both equations up to first order in perturbations are displayed below as equation (4.39):

$$
\begin{aligned}
\dot{\boldsymbol{m}} &= -4A\gamma\hat{\boldsymbol{x}} \times \partial^2\boldsymbol{h} + 4\lambda\gamma\hat{\boldsymbol{x}} \times \boldsymbol{h} + \alpha\hat{\boldsymbol{x}} \times \dot{\boldsymbol{h}} - \nu\partial\boldsymbol{m} + \beta\nu(\hat{\boldsymbol{x}} \times \partial\boldsymbol{h}) \\
\dot{\boldsymbol{h}} &= 2\epsilon\gamma\hat{\boldsymbol{x}} \times \boldsymbol{m} + \alpha\hat{\boldsymbol{x}} \times \dot{\boldsymbol{m}} - \nu\partial\boldsymbol{h} + \beta\nu(\hat{\boldsymbol{x}} \times \partial\boldsymbol{m}).
\end{aligned}
\tag{4.39}
$$

The x component of the three-dimensional vectors - the magnetisation and perturbation of the Néel vector - are zero. For example, the x component of the magnetisation has to vanish to fulfil the antiferromagnetic constraints because the ground state direction along x enforces that $m_x = 0$ by $\boldsymbol{n} \cdot \boldsymbol{m} = 1m_x + h_y m_y + h_z m_z = 0$. Then, the

two equations can be written in the following two-dimensional form:

$$(\partial_t + \nu\partial)\begin{pmatrix} m_y \\ m_z \end{pmatrix} = (-4A\gamma\partial^2 + 4\lambda\gamma + \alpha\partial_t + \beta\nu\partial)\begin{pmatrix} h_z \\ -h_y \end{pmatrix}$$

$$(2\epsilon\gamma + \alpha\partial_t + \beta\nu\partial)\begin{pmatrix} m_y \\ m_z \end{pmatrix} = (\partial_t + \nu\partial)\begin{pmatrix} h_z \\ -h_y \end{pmatrix}.$$

$$(4.40)$$

Those four equations are separated with respect to m_y and h_z as well as m_z and h_y. A Fourier transformation of both vectors $\boldsymbol{m}$ and $\boldsymbol{h}$ in time and space can be used to reduce the total number of equations to two. The Fourier transformation is defined by:

$$\begin{pmatrix} m_y \\ m_z \end{pmatrix} = \int d\omega'' d\boldsymbol{q}'' \begin{pmatrix} k(\omega'', \boldsymbol{q}'') \\ l(\omega'', \boldsymbol{q}'') \end{pmatrix} e^{i\omega''t - i\boldsymbol{q}''\cdot\boldsymbol{r}} \quad \begin{pmatrix} h_y \\ h_z \end{pmatrix} = \int d\omega' d\boldsymbol{q}' \begin{pmatrix} f(\omega', \boldsymbol{q}') \\ g(\omega', \boldsymbol{q}') \end{pmatrix} e^{i\omega't - i\boldsymbol{q}'\cdot\boldsymbol{r}}.$$

$$(4.41)$$

This translates the system into frequency and momentum space $(\boldsymbol{r}, t) \mapsto (\boldsymbol{q}, \omega)$. The Fourier transformation is a transformation into a complete set of basis vectors given by the exponential functions which are orthonormal. Each basis vector contributes to this transformation by an amplitude $X(\omega, \boldsymbol{q})$. The amplitudes f, g, k, l used for the perturbation components do not have be equal for the given perturbation directions. However, before this transformation is used, it is crucial to note that an amplitude $X(\omega')$ can be determined for a given ω by a multiplication of the corresponding orthonormal functions. Within this example, the momentum $\boldsymbol{q}'$ is neglected for simplicity reasons. The calculation for the momentum is analogue.

$$X(\omega') = \int dt e^{-i\omega't} X(t) = \int dt e^{-i\omega't} \int d\omega X(\omega) e^{i\omega t}$$

$$X(\omega') = \int dt \int d\omega e^{-i(\omega'-\omega)t} X(\omega) = \int d\omega \delta(\omega' - \omega) X(\omega) = X(\omega')$$

$$(4.42)$$

Hence, multiplying the transformed equations (4.40) by the orthonormal basis vectors (4.41) depending on ω will lead to a projection onto this frequency. For each possible frequency, the equations need to be fulfilled. The derivatives occurring in the equations act on the exponential term, yielding $i\omega$ or $-iq_x \equiv -iq$ terms. The x components of the magnetisation and Néel vector momentum remain after a ∂_x derivative. The integration cancels out due to the delta distribution $\delta(\omega' - \omega)$ leading to a derivative-free theory only depending on ω and q and the amplitudes of the perturbations. The resulting equations are:

$$(i\omega - i\nu q)\begin{pmatrix} k \\ l \end{pmatrix} = (4A\gamma q^2 + 4\lambda\gamma + i\alpha\omega - \beta\nu q)\begin{pmatrix} g \\ -f \end{pmatrix} \tag{4.43}$$

$$(2\epsilon\gamma + i\alpha\omega - \beta\nu q)\begin{pmatrix} k \\ l \end{pmatrix} = (i\omega - i\nu q)\begin{pmatrix} -g \\ f \end{pmatrix}. \tag{4.44}$$

4. Antiferromagnetic domain wall description

4. Antiferromagnetic domain wall description

The Néel vector dependent terms are separated from the magnetisation ones on both sides. The prefactors in front of the vectors can be joined into one constant M. Those four equations can be connected into two equations determined by the Néel vector perturbation amplitudes and M:

$$\frac{4A\gamma q^2 + 4\lambda\gamma + i\alpha\omega - i\beta\nu q}{i\omega - i\nu q}\begin{pmatrix} g \\ -f \end{pmatrix} = \frac{i\omega - i\nu q}{2\epsilon\gamma + i\alpha\omega - i\beta\nu q}\begin{pmatrix} -g \\ f \end{pmatrix}. \tag{4.45}$$

The equality can be written into a matrix form using that the off-diagonal contribution is zero. This leads to the system of equations:

$$\begin{pmatrix} M & 0 \\ 0 & M \end{pmatrix}\begin{pmatrix} f \\ g \end{pmatrix} = 0. \tag{4.46}$$

The determinant has to vanish to get two linearly independent amplitudes of the Néel vector perturbation as in the ferromagnetic case (3.51). Then, the calculation reduces to $M = 0$ only since both off-diagonal terms of the matrix are zero.

$$M^2 = [(4A\gamma q^2 + 4\lambda\gamma + i\alpha\omega - i\beta\nu q)(2\epsilon\gamma + i\alpha\omega - i\beta\nu q) + (i\omega - i\nu q)^2]^2 = 0 = M \tag{4.47}$$

The equality can be used to determine the dispersion relation of ω with respect to q, which is analysed to get t instability condition:

$$
\begin{aligned}
0 &= (4A\gamma q^2 + 4\lambda\gamma + i\alpha\omega - i\beta\nu q)(2\epsilon\gamma + i\alpha\omega - i\beta\nu q) + (i\omega - i\nu q)^2 \\
0 &= -(1+\alpha^2)\omega^2 + [2(1+\alpha\beta)\nu q + i\alpha(4A\gamma q^2 + 4\lambda\gamma + 2\epsilon\gamma)]\omega \\
&\quad + 8(A\gamma q^2 + \lambda\gamma)\epsilon\gamma - (1+\beta^2)(\nu q)^2 - i\beta\nu q(4A\gamma q^2 + 4\lambda\gamma + 2\epsilon\gamma) \\
\omega_{1/2} &= \frac{2(1+\alpha\beta)\nu q + i\alpha(4A\gamma q^2 + 4\lambda\gamma + 2\epsilon\gamma)}{2(1+\alpha^2)}\pm \\
&\quad \left[\left(\frac{2(1+\alpha\beta)\nu q + i\alpha(4A\gamma q^2 + 4\lambda\gamma + 2\epsilon\gamma)}{2(1+\alpha^2)}\right)^2 \right. \\
&\quad \left. + \frac{8(A\gamma q^2 + \lambda\gamma)\epsilon\gamma - (1+\beta^2)(\nu q)^2 - i\beta\nu q(4A\gamma q^2 + 4\lambda\gamma + 2\epsilon\gamma)}{1+\alpha^2}\right]^{1/2}.
\end{aligned}
\tag{4.48}
$$

The parenthesis is facilitated at first. Then, the equality is arranged regarding the power of the frequency. The "pq"-formula is applied to get the dispersion relation. This can be written as:

$$
\begin{aligned}
2(1+\alpha^2)\omega_{1/2} &= 2(1+\alpha\beta)\nu q + i\alpha(4A\gamma q^2 + 4\lambda\gamma + 2\epsilon\gamma)\pm \\
&\quad \left[\left(2(1+\alpha\beta)\nu q + i\alpha(4A\gamma q^2 + 4\lambda\gamma + 2\epsilon\gamma)\right)^2 \right. \\
&\quad \left. + 4(1+\alpha^2)[8(A\gamma q^2 + \lambda\gamma)\epsilon\gamma - (1+\beta^2)(\nu q)^2] - i\beta\nu q(4A\gamma q^2 + 4\lambda\gamma + 2\epsilon\gamma)\right]^{1/2}.
\end{aligned}
\tag{4.49}
$$

If ω has an imaginary part lower than zero, the system will become unstable as shown in the ferromagnetic calculations. In this case, the exponential term $e^{-i\omega t}$ will be real

55

and positive. It means that the amplitude in front of this factor increases exponentially in time. No spin wave system can be stable under such a condition.

It is essential to analyse the value of the square root in terms of its real and imaginary part. The most general solution can be calculated by rewriting the imaginary square root $\sqrt{z}$ as a form $\sqrt{x+iy} = \pm\sqrt{\frac{|z|+x}{2}} \pm i\,\text{sgn}(y)\sqrt{\frac{|z|-x}{2}}$ [2]. This general equation is too complex to get an analytical result most of the times and is not favoured for this reason. However, for numerical calculations, it could be used. The imaginary part of the square root is analysed together with the imaginary part in front of the square root to see when it becomes negative. Apart from this direct rewriting, the usage of the polar form of the imaginary unit yields a result.

The following formalism is based on the considerations of Davi R. Rodrigues. Any imaginary number $z = a + ib$ can be cast into a form depending on the length of the quantity $R = \sqrt{a^2 + b^2}$ and a phase factor φ. The polar representation of the imaginary number is $z = Re^{i\varphi} = R(\cos\varphi + i\sin\varphi)$. Hence, the square root of a complex number can be calculated as follows: $\sqrt{a+ib} = (Re^{i\varphi})^{1/2} = \sqrt{R}e^{i\varphi/2} = \sqrt{R}(\cos\left(\frac{\varphi}{2}\right) + i\sin\left(\frac{\varphi}{2}\right))$. The imaginary part is $\text{Im}(z) = \sqrt{R}\sin\left(\frac{\varphi}{2}\right)$. The phase factor φ is calculated using a comparison of the polar and non-polar representation of z: $\text{Im}(z) = b = R\sin(\varphi)$. Consequently, the phase is $\varphi = \arcsin\left(\frac{b}{R}\right)$.

At first, the complex number inside the square root of equation (4.49) needs to be divided into a real and an imaginary part:

$$a = -4(\alpha+\beta)^2(\nu q)^2 - \alpha^2(4A\gamma q^2 + 4\lambda\gamma + 2\epsilon\gamma)^2 + 32(1+\alpha^2)(A\gamma q^2 + \lambda\gamma)\epsilon\gamma$$
$$b = 4\alpha(1+\alpha\beta)\nu q(4A\gamma q^2 + 4\lambda\gamma + 2\epsilon\gamma) - 4(1+\alpha^2)\beta\nu q(4A\gamma q^2 + 4\lambda\gamma + 2\epsilon\gamma) \quad (4.50)$$
$$= 4(\alpha-\beta)\nu q(4A\gamma q^2 + 4\lambda\gamma + 2\epsilon\gamma).$$

Next, the imaginary part of $\sqrt{a+ib}$ is changed:

$$\text{Im}(\sqrt{z}) = \sqrt{R}\sin\left(\frac{\varphi}{2}\right) = \sqrt{R}\sin\left(\frac{\arcsin\left(\frac{b}{R}\right)}{2}\right) = \frac{b}{\sqrt{2R}\sqrt{\sqrt{\frac{R^2-b^2}{R^2}}+1}}$$
$$= \frac{b}{\sqrt{2R}\sqrt{\sqrt{\frac{a^2}{R^2}}+1}} = \frac{b}{\sqrt{2}\sqrt{\sqrt{a^2}+R}} = \frac{b}{\sqrt{2(a+R)}}. \quad (4.51)$$

The sine function is simplified to the first equality of the second line using Mathematica 12 [52]. The squared length of a complex number R^2 is the same as the square of the real and imaginary part. A $1/R$ factor is pulled out of the root. Then, the denominator reduces to $\sqrt{2(a+R)} = \sqrt{2(a+\sqrt{a^2+b^2})}$.

All critical current derivations in this thesis use the fact that dissipation is very small around the critical value. The constants α and β are negligible in the second-order $\alpha^2 \approx \beta^2 \approx 0$. Every term of the real and imaginary part with a squared or higher damping are disregarded for the following calculation. The real part reduces to $a \approx 32(A\gamma q^2 + \lambda\gamma)\epsilon\gamma + \mathcal{O}(\alpha^2, \beta^2, \alpha\beta)$ and the imaginary part is the same as before. The

squared imaginary part vanishes $b^2 = \mathcal{O}(\alpha^2, \beta^2, \alpha\beta) \approx 0$. This shows the length R is approximately the same as the real part $a + R \approx 2a$. Hence, the linear imaginary part in terms of damping is:

$$\text{Im}(\sqrt{z}) \approx \frac{b}{2\sqrt{a}} + \mathcal{O}(\alpha^2, \beta^2, \alpha\beta) = \frac{(\alpha-\beta)\nu q(4A\gamma q^2 + 4\lambda\gamma + 2\epsilon\gamma)}{\sqrt{8(A\gamma q^2 + \lambda\gamma)\epsilon\gamma}} + \mathcal{O}(\alpha^2, \beta^2, \alpha\beta). \tag{4.52}$$

Consequently, the imaginary part of the dispersion relation (4.49) takes the following form:

$$\text{Im}(\omega_{1/2}) = \frac{1}{2(1+\alpha^2)}\left[\alpha(4A\gamma q^2 + 4\lambda\gamma + 2\epsilon\gamma) \pm \frac{(\alpha-\beta)\nu q(4A\gamma q^2 + 4\lambda\gamma + 2\epsilon\gamma)}{\sqrt{8(A\gamma q^2 + \lambda\gamma)\epsilon\gamma}}\right]$$
$$= \frac{\alpha(4A\gamma q^2 + 4\lambda\gamma + 2\epsilon\gamma)}{2(1+\alpha^2)\sqrt{8(A\gamma q^2 + \lambda\gamma)\epsilon\gamma}}\left[\sqrt{8(A\gamma q^2 + \lambda\gamma)\epsilon\gamma} \pm \frac{(\alpha-\beta)}{\alpha}\nu q\right]. \tag{4.53}$$

All pieces in front of the bracket are positive, as all constants are defined as positive. The sign of the equality is decided by the sign of the $\sqrt{8(A\gamma q^2 + \lambda\gamma)\epsilon\gamma} \pm \frac{(\alpha-\beta)}{\alpha}\nu q$ factor. The system becomes unstable if it is negative and remains in the ground state for a positive sign. The critical current value is extracted from the transition point of both states.

$$0 = \sqrt{8(A\gamma q^2 + \lambda\gamma)\epsilon\gamma} \pm \frac{(\alpha-\beta)}{\alpha}\nu q$$
$$0 = \left(8\gamma^2 A\epsilon - \frac{(\alpha-\beta)^2}{\alpha^2}\nu^2\right)q^2 + 8\gamma^2\lambda\epsilon \tag{4.54}$$

The $\pm$ dependent piece is subtracted and both sides of the upper equality are squared. Then, the structure is rearranged to the bottom form. As a result, $8\gamma^2 A\epsilon = \frac{(\alpha-\beta)^2}{\alpha^2}\nu^2$ is needed to fulfil the requirement. This shows that the critical current value for the stability of a synthetic antiferromagnetic system in one dimension is:

$$\nu_{ci} = \gamma\sqrt{8A\epsilon}\frac{\alpha}{\alpha-\beta}. \tag{4.55}$$

The stability of the system is decided by the same structure $\gamma\sqrt{8A\epsilon}$ as for the shedding case (4.35). The difference of both depends on the damping factor β. However, a direct comparison with $\beta \neq 0$ is impossible. The domain wall creation current was established using $\beta = 0$ and it would change without this assumption. For example, in the ferromagnetic calculations $\beta \neq 0$ meant that the linear and angular momentum were not conserved variables. The same is predicted for the antiferromagnet. Therefore, the current values change drastically.

The stability and shedding current are the same when $\beta = 0$. In this case, the α

cancels out and the shedding derivation is valid for comparison. Ideally, the instability current is larger than the creation current, as it shows that a domain wall driven system is possible before it breaks down. Nevertheless, this picture is not ruined. Every calculation performed was done using certain assumptions, for example: $\boldsymbol{m} \ll 1$ or $\alpha \ll 1$. An alteration of these assumptions does have consequences for the calculations. A larger magnetisation changes the total magnetic energy of the system because all second-order terms were neglected. Also, the small damping assumption has been used to get the result. A recalculation of ν_{ci} with different presumptions will enlighten if both structures differ. However, it is questionable if an analytical solution is possible if one of those hypotheses is changed.

Also, the ferromagnetic calculation proved that DMI could lower the critical current requirement. An analysis of both currents with DMI could show different values. Otherwise, another method, geometry of the sample or material parameters, have to lower the domain wall creation requirements. Nevertheless, a confirmation that the shedding current is well below the stability current can be made using simulations of the pinned nanowire system for different material parameter sets. If only spin waves and chaotic states, but no shedding are observed, the stability current is lower than the creation current. In the following chapter, the theoretical shedding current (4.35) is tested for a set of parameters to see if the square root dependency of the current on the material parameters hold. Within this test, shedding is observed well below the instability of the sample.

4.5. Summary of the antiferromagnetic calculations

In this chapter, the antiferromagnetic description of a one-dimensional nanowire system was established. This antiferromagnetic system consists of two ferromagnetic sublattices on top of each other, coupled between adjoining neighbours of each sublattice. Such a system is called synthetic antiferromagnet as it is fabricated. Each subsystem also has an exchange interaction within and an easy axis anisotropy.

Mathematically, the antiferromagnetic system is modelled as the total magnetic energy of each sublattice system added up with the linking exchange interaction. This total magnetic energy is adapted into new coordinates called antiferromagnetic magnetisation and Néel vector. Such a collinear system, having adjacent magnetic moments pointing antiparallel, leads to a magnetisation of about zero and Néel vector in the order of the sublattice moments. Therefore, the magnetisation vector acts as a perturbation of the system, while the subtraction of the sublattice vectors is used to describe the system's dynamics.

The LLG equations have been adapted using the new generalised coordinates as well. Also, the effective fields in these equations needed to be calculated differently from the ferromagnetic case because of antiferromagnetic constraints to the order parameters. The formalism of the variational principle was used to determine the effective field terms, including the antiferromagnetic constraints. After that, the domain wall shedding current could be calculated the same way as in the ferromagnetic case using the

steady-state approach and neglecting the dissipative contributions. The symmetries of the system could be analysed to discover the conserved quantities according to the Noether theorem. Comparing the constant value at different positions in the system resulted in a critical current value beyond which domain walls will form and move along the synthetic antiferromagnetic nanowire.

At last, the determination of a general instability current for one-dimensional synthetic antiferromagnetic nanowires was performed. A linearisation of the system and a Fourier transformation into frequency-momentum space achieved a simplification of both antiferromagnetic LLG equations without any derivatives. Also, the dissipative current terms were neglected to facilitate the equations. A quadratic dispersion relation for the frequency was discovered using the result of the linearisation. This quantity was analysed further to see when it develops negative and imaginary. The total magnetic system becomes unstable since the spin wave description of the Fourier transformation will diverge. Both critical values were compared in the $\beta = 0$ case.

In the next chapter, simulations of the system are analysed to investigate if the critical current for shedding is reasonable. It also examines if the instability current is higher than the domain wall creation current.

5. Simulation of synthetic antiferromagnetic domain walls

The critical current for the domain wall shedding of a synthetic antiferromagnet (4.35) needs to be tested to check its plausibility. In addition, it is crucial to know that the instability current is above the creation current. Both can be tested using numerical micromagnetic simulations. The software package used for the simulations is Mumax3.10 from the DyNaMat group in Gent [50] [17]. It is an open source application to the python 3 programming language.

Mumax3 simulations are run from the command line. The code is saved in text files (*.txt) or mumax files (*.mx3), while the simulation outputs are saved in a table and log file (*.txt) with all physical quantities of interest. The magnetisation state is also saved in *.ovf format or NumPy files for further analysis. The time evolution of magnetic systems is realised by calculating the LLG equations with adjustable time steps. Therefore, it is a numerical method and not an analytical model.

Mumax3 uses a two-dimensional or three-dimensional grid as the simulation box. Each cell of the grid is orthorhombic. The simplest case is a primitive rectangular cell with identical side lengths. The first step of the simulation initialisation is the specification of the geometry of the system. The synthetic antiferromagnet is modelled as a 256x1x2 grid. Choosing all grid parameters in powers of 2 is beneficial for the computation time needed [50].

The first coordinate is the length of the nanowire. The second one is the width, while the third coordinate describes the height of the system. A synthetic antiferromagnet is built from two ferromagnets on top of each other, separated by a non-magnetic layer. This layer can be specified, but it is not essential because alternative modelling neglects this zone while being computationally efficient.

In the next step, the cell properties have to be specified. Each cell has the dimensions of 1x1x1 nanometre in length. Mumax3 features material region with different characteristics. That enables the definition of the top layer and bottom layer as two ferromagnetic regions. Both share the same material properties as in the analytical calculations. However, the behaviour of both can be coupled by an extra function called $ext\_InterExchange$(Region 1, Region 2, Coupling strength). As stated above, this method is more efficient than building a custom interaction with a non-magnetic layer while giving approximately the same result. A detailed explanation of both models is found in a mumax3 workshop [31] by J. Leliaert and J. Mulkers.

Another material region is needed to design the pinning. A third region is defined along the nanowire direction ranging from $-\infty$ including the first cell of the wire. The range stops at $-127nm$ as Mumax3 positions the simulation box centre at the

origin. The box has a total length of $256nm$ in the x direction. The command $frozenspins.setregion$(Region, Strength) freezes all spins of the region for a strength of 1. Hence, the two spins in the region 3 are set explicitly to a Néel vector of $\boldsymbol{n} = (0,0,1)^T$ by $m.setCell(0,0,1,vector(0,0,1))$ and $m.setCell(0,0,0,vector(0,0,-1))$. Both sublattice regions 1 and 2 share the x-axis by $uniform(\pm 1, 0.1, 0)$ with a canting in the y direction. All vectors of the system, one for each cell, are multiplied by the saturation magnetisation value after they are normalised. Therefore, the canting term does not change the behaviour. This canting is used to get a physical minimisation of the energy before the simulation starts.

A relaxation of the grid should always be the first step before the time evolution and data recording starts. The initial state needs to be adjusted to the effective field interactions by relaxation. Those interactions are enabled by setting values to predefined constants. $Ku1$ determines an anisotropy along a vector axis. The vector is specified by $AnisU = vector(1,0,0)$ as the easy axis. Aex enforces the intralattice exchange interaction. It is set to be the same for both sublattices, but it can be regulated for each region.

Other interactions that are not specified explicitly are not activated. One exception is the demagnetisation field of the ferromagnet. It is the static magnetic field produced by the magnetic moments. The theoretical model assumes just the interlattice exchange between the layers. Hence, the demagnetisation field should alter the result. That is why it is turned off for the simulations even though the result would be more realistic enabling it.

The theoretical predictions assume no dissipation $\alpha = \beta = 0$, whereas the simulation needs at least one of the two factors to stabilise the time evolution. It is not needed for the current identification as this value is determined at the boundary where the movement starts. At this point, the change of the system is adiabatic. The β equivalent used in Mumax3 is set to zero and the α factor is set to 0.1 for all simulations.

The spin-transfer torque pieces of the LLG equation (2.7) can be modelled in two different ways in Mumax3. One possibility is the "Slonczewski spin-transfer torque" [30] which is defined differently in this thesis. The Slonczewski expression is used to model spin-transfer torques between fixed magnetisation layers and free layers. One example of this is the MRAM.

The second possibility is the "Zhang-Li spin-transfer torque" [30] used in Mumax3. The magnetisation dependency is the same as for the spin-transfer components in this thesis. However, the prefactors are different. It contains α and ξ compared to a β used in this formalism. Nevertheless, the prefactors used in a simulation can take a broad range depending on the material. It is not extraordinary when two simulations take a different set of material parameters. Physical systems with antiferromagnetic properties exist for a range of parameters, not single values only. Therefore, all damping terms are governed by the one prefactor α, which is chosen as in many other simulations [31] and analysis [10].

The material parameters of the interlattice exchange interaction, intralattice exchange interaction, and anisotropy also have a broad range of possible strengths. Today, the samples can be manufactured in nanometre sizes, sharing similar characteristics with

various constants. One example of such a small size pattern is the molecular beam epitaxy method [49]. The material parameters suggested in the Mumax3 workshop [31] for synthetic antiferromagnets are $Ku1 = 800kJm^{-3}$, $Aex = 15pJm^{-1}$ and the interlayer exchange $Interex = -0.5pJm^{-3}$ demonstrate typical value. Even though these parameter values are realistic, a critical current analysis of simulation based on the parameters leads to strengths in the order $10^{13}Am^{-2}$. Such an electron stream is strong enough to fuse any nanowire. Hence, a different set of parameters needs to be used for the analysis.

The evaluation of the critical current strength is done utilising the bisection method [27]. It takes two values, one above the boundary and one below. The mean value of both is used to begin a simulation. This numerical time evolution is started with the *runwhile*(*Condition*) command. The condition used to control the end of the run is set to a domain wall passing linked with an or condition to an end time. If one of both states is reached, the simulation stops. The magnetisation of the top layer cell at the origin is compared to the easy axis magnetisation value. If $|\boldsymbol{m}_{middle} - \boldsymbol{m}_{easy}|$ is smaller than 1.8, the simulation continues. If it is larger, the simulation interrupts and the current is recorded, as a domain wall has passed the middle of the nanowire. In this case, the magnetisation of the selected cell is nearly orthogonal to the easy axis.

Two cases are distinguished. First, when no domain wall has passed within the time set, the current value is set as the lower boundary of the bisection method. Second, when a wall has passed, the current value is set as the upper boundary of the bisection method. Then, the new mean value is calculated and the next run is started using the current. This leads to a reliable result. The accuracy of the method can be calculated using $\frac{b-a}{2^{n+1}} < \epsilon$ for the top value b, the bottom value a, the accuracy ϵ and the number of steps n [27]. The gap between the boundaries is reduced by a factor of two each step. 16 steps are needed using a start of $b = 10^{13}$ and $a = 10^{10}$ to get a precision of $\epsilon = 10^8$. Here, it is the lowest boundary of steps used for each simulation and the broadest range of the limits.

The spin-polarised current strength of the Zhang-Li spin-transfer torque is specified by a simple $j = vector(x, y, z)$ in Mumax3. The current direction is based on the positive current flow. Therefore, a minus sign in $-x_{val}$ states that the electrons of the current moves along the nanowire direction. As stated above, the electron current needs to be lower than $10^{13}Am^{-2}$ to be applicable. This current needs to be converted to the spin current velocity $\boldsymbol{\nu}$ of the LLG equations (2.8). The critical current needed for shedding in a synthetic antiferromagnetic system with easy axis anisotropy and two types of exchange interaction is $\nu = \gamma\sqrt{8A\epsilon}$ (4.35) for a normalised magnetisation. Any simulation done in this thesis runs with a saturation magnetisation of $M_s = 580e3Am^{-1}$. This factor is the same one as used in the Mumax3 workshop simulation examples.

The theoretical spin velocity calculated needs to be adjusted with an M_s factor for comparison. The spin current used in a simulation is j while the theoretical value is

ν_c.

$$j = \frac{2eM_s}{P\mu_B}\nu_c = \frac{2eM_s\gamma}{P\mu_B}\sqrt{8A\epsilon} \tag{5.1}$$

The connection of both is still missing an additional M_s from the theoretical determination. Inserting all values shows that the simulation and analytics are approximately the same for $\nu_c \approx \gamma\sqrt{8M_sA\epsilon}$. The current does depend on the root of the saturation magnetisation $\sqrt{M_s}$ to be comparable to numerical calculations. In the following, the analytical value will be determined as:

$$j_T = \frac{2eM_s\gamma}{P\mu_B}\sqrt{8M_sA\epsilon}. \tag{5.2}$$

The standard set of parameters used for the simulations are $Ku1 = 8kJm^{-3}$, $Aex = 80fJm^{-1}$ and $Interex = -0.5fJm^{-3}$. All of them are reduced by at least two magnitudes compared to the Mumax3 workshop values [31]. The critical current value is at approximately $3.49 \cdot 10^{11} Am^{-2}$. The domain wall creation of the proposed constants can be verified visually using the *autosave(m, time)* command for every time step *time*. The generated *.ovf files can be animated using the Mumax3-view web browser page [11]. If one parameter is tuned to a tiny or immense value while the others are kept constant, strange domain wall structures can be observed directly. Therefore, the standard set is validated and a broad range around those conditions with physical domain walls is identified. A summary of the lower and upper limits is displayed in the table below.

The interlattice exchange and intralattice exchange are tested to see if the current

Parameter	Standard value	Lower boundary	Upper boundary
$Ku1$	$8kJm^{-3}$	$80Jm^{-3}$	$220kJm^{-3}$
Aex	$80fJm^{-1}$	$0.8fJm^{-1}$	$8pJm^{-1}$
$Interex$	$-0.5fJm^{-3}$	$-4aJm^{-3}$	$-0.5pJm^{-3}$

Table 5.1.: The standard values used for the anisotropy strength $Ku1$, the intralattice exchange constant Aex and the interlattice exchange constant $Interex$ are presented together with lower and upper limits used in this analysis. Source: Author's illustration.

depends on both by a square root. The anisotropy is investigated as well since some dependency is expected. At first, the interlattice exchange is analysed. The figure 5.1 displays the simulation data in the range from $-4aJm^{-3}$ to $-0.5pJm^{-3}$ by blue dots. The data are fitted by a square root function in the form of $a\sqrt{bx-c}+d$, taking four open parameters a, b, c and d. The SciPy *curve_fit* function [43] is used for the fit. It requires the data points and the fit function to estimate the optimal parameters by a least squared method. The analytics curve is determined by j_T of equation (5.2) and multiplied by an extra factor to match the data.

The highest current is at the strongest coupling as expected. It is well below the
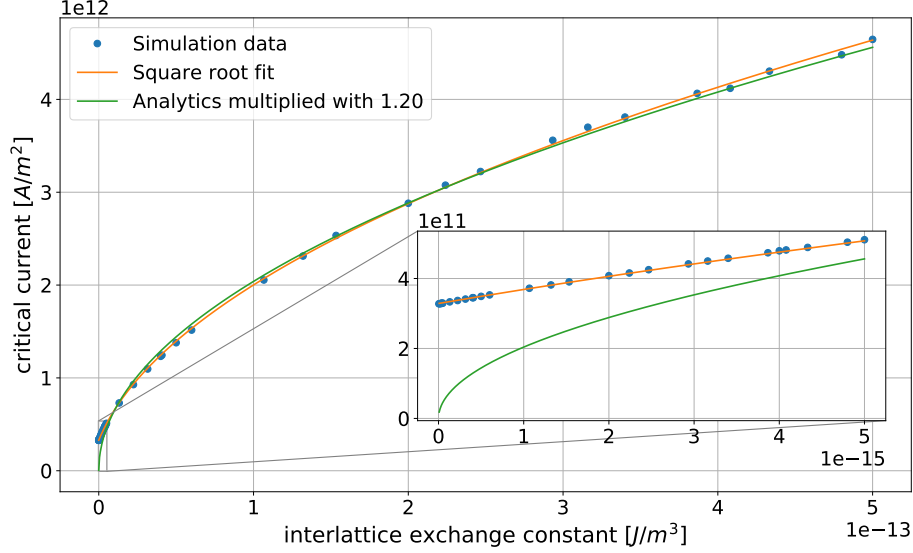
Figure 5.1.: The figure displays the simulation data of the critical electron current for domain wall shedding for different interlattice exchange constant strengths. The data are fitted by a square root function and compared to the analytical solution (5.2) for confirmation. Also, the lowest parameter region is highlighted in the smaller window. Source: Author's illustration.

$10^{13} Am^{-2}$ mark of wire fusing. The square root fit shows that the correlation of the exchange strength and the electrical current is as expected. The theoretical curve displays a similar square root dependency, but it diverges at the smallest range of parameters. The model does not account for an offset value of current needed to get a domain wall creation for a missing interlattice exchange. In this case, the nanowire is a simple ferromagnet and the ferromagnetic critical current (3.35) depends on the exchange interaction and the anisotropy. Both of them are unchanged and unequal to zero. That is why the limit of no interlattice coupling results in ferromagnetic behaviour instead of the theoretical zero of the green curve. The ferromagnetic critical current for the standard parameters is $2.72 \cdot 10^{11} Am^{-11}$. This is in good agreement with the data points with the lowest coupling strength. At high coupling strengths, the system is governed by antiferromagnetic coupling. Therefore, the critical currents match.

The theoretical value has to be multiplied by a factor of 1.2 to match. This is not surprising as the theoretical prediction used no β damping and neglected all interactions apart from the three ones specified. The electron current definition has a $1/(1 + \beta^2)$ part (2.8) which is set to 1 in this analysis. Also, no temperature dependency was expected. All of those simplifications change the outcome. The simulation was done using the approximation of no demagnetisation field. The β equivalent was neglected, but the damping pieces of the equation are α dependent in Mumax3. Then, the time evolution accuracy is coupled to the time step interval used for the simulation. A

smaller time step enhances the accuracy but takes longer to simulate in total. Therefore, a difference lower than one magnitude between both values is explainable. The theoretical prediction is plausible for the interlattice exchange.

A similar analysis is done for the intralattice exchange constant. A square root dependency is forecast by the theory. Figure 5.2 displays the simulation data of the critical electric current for a set of intralattice constants. The fit to the data unveils that it
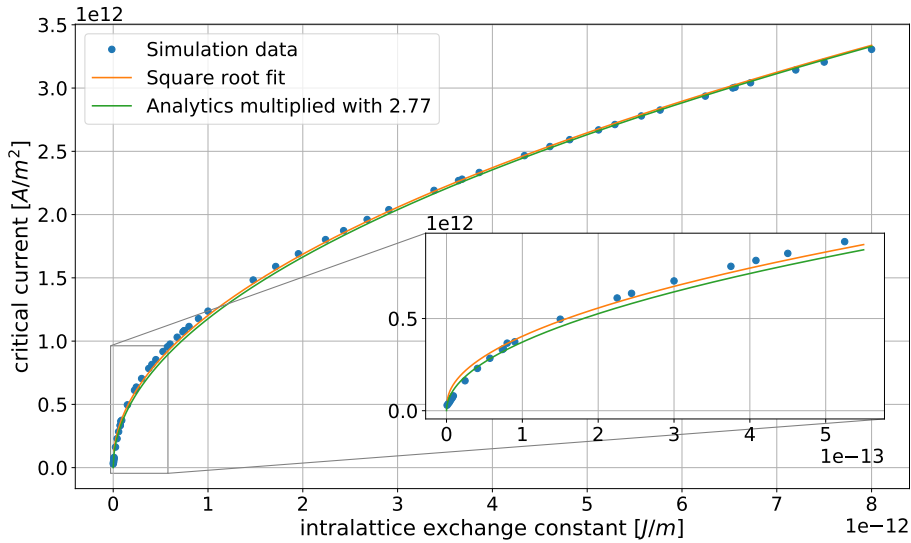
Figure 5.2.: The figure displays the simulation data of the critical electron current for domain wall shedding for different intralattice exchange constant strengths. The data are fitted by a square root function and compared to the analytical solution (5.2) for confirmation. Also, the lowest parameter region is highlighted in the smaller window. Source: Author's illustration.

matches the square root dependency. The theoretical curve needs to be multiplied by a factor of 2.77 to overlap with the fit and the data points. The multiplication factor needed to match the data is low enough to validate the calculation for the same reason as for the interlattice exchange.

It is expected that a correction factor is needed to combine both simplified models. However, the difference of this coefficient to the other exchange is surprising. The interlattice constant is set to a value where the system behaves antiferromagnetic. Nevertheless, the neglected interactions may have a greater impact on the material parameter intralattice exchange than the manufactured interlattice exchange.

The theoretical curve and the data is comparable at the lowest parameters used. No ferromagnetic behaviour is expected in contrast to the interlattice case. Still, both magnetic states - the ferromagnetic and antiferromagnetic one - approach a zero current needed for a domain wall creation when the intralattice exchange vanishes. Next neighbours along the nanowire will not be constricted to be parallel and magnetic moments will rotate with the spin current unhindered.

5. Simulation of synthetic antiferromagnetic domain walls

The two exchange constants change the critical current needed for shedding as expected. However, the theory does not involve anisotropy strength. Hence, the current needed should stay approximately constant. This parameter adjusts the force keeping the magnetic moments parallel or antiparallel to the easy axis. The domain wall width is determined by the anisotropy (3.9). The ferromagnetic theory predicts that the critical current changes with the anisotropy. Therefore, an anisotropic dependency of the synthetic antiferromagnet critical current is reasonable.

Figure 5.3 demonstrates the critical current change with respect to the anisotropy. The data points do not remain constant and do not change in a square root behaviour as for the ferromagnet. Instead, the 4th root describes the slope agreeable. From the theoretical point, including β and other interactions could show another term in the critical current with $\sqrt[4]{\lambda}$. Besides that, the data cannot be analysed further.

The instability current was checked as well. The calculations showed that both criti-
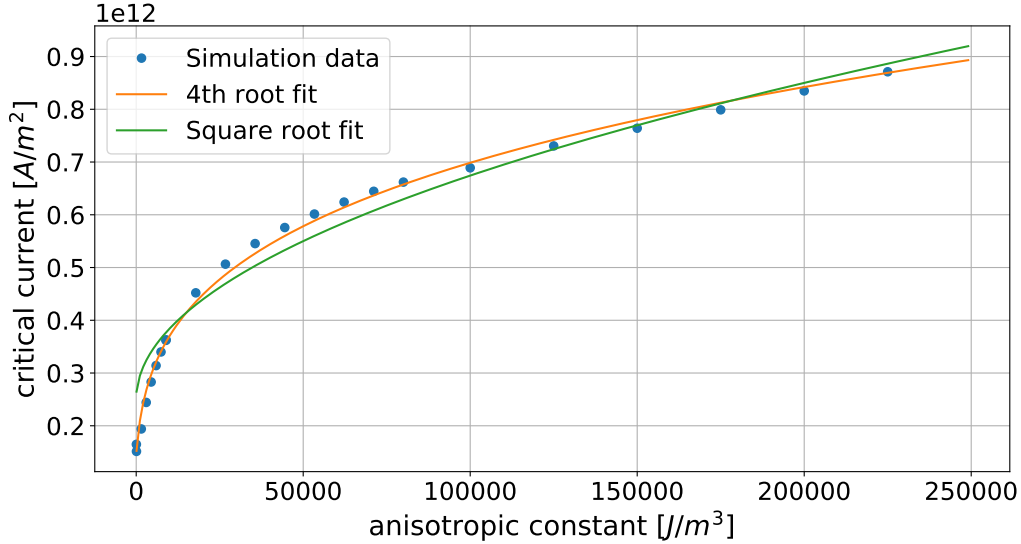
Figure 5.3.: The figure displays the simulation data of the critical electron current for domain wall shedding for different anisotropy constant strengths. The data are fitted by a square root function and 4th root function for confirmation of the dependency. Source: Author's illustration.

cal currents have the same value but the instability current should be higher than the shedding current. The data explains that the theoretical prediction for the shedding is valid within the assumptions. Also, single domain walls are created and moved at currents higher than the critical value. Therefore, the instability condition needs to be higher than the current values tested. A new approach to instability can lead to an accurate result. Nevertheless, a racetrack memory system of a synthetic antiferromagnetic nanowire is possible based on the theory and simulations.

The analysis of the synthetic antiferromagnetic instability (4.55) did leave the question if the $|\boldsymbol{m}| \approx 0$ constraint was justifiable. The magnetisation vector time evolution in

the centre of the nanowire is checked by a 20 cycle simulation between $10^{10}-10^{12}Am^{-2}$ with standard parameters. Each run is cut off after $20ns$ if no domain wall did pass. The magnetisation vector is saved every $0.1ns$. Figure 5.5 displays the time evolution of $|\boldsymbol{m}|$ in 9 parts as 9 of the 20 runs showed a domain wall. The highest current is used at the top left and the critical current value is shown at the bottom right. The x-axis is ongoing in the number of total time steps simulated. All subplots aligned yield the total simulation. However, the last $0.5ns$ are cut out at each part.

The rising edges at the right of each plot indicate a domain wall approaching the centre. The magnetisation value climbs to values higher than 1.8 and fall to zero at a new cycle. This does not include new information, but it reduces the visibility of tiny magnetisation changes. That is why the highest magnitude displayed is at about 0.2. Figure 5.4 shows a domain wall displayed using Mumax3-view. The large magnetisation values of 1.8 appear as both sublattices rotate towards the y-axis. This breaks down the antiferromagnetic order in the domain wall while it is kept outside of it.

The top left flank in the figure 5.5 is approached with a large noise due to a current

Figure 5.4.: The figure displays the centre of the nanowire simulated in Mumax3 illustrated by Mumax3-view. A synthetic antiferromagnetic domain wall is shown at the centre. The vectors of both lattices point along the y direction of the system. Source: Author's illustration in Mumax3-view [11].

much larger than the critical one. The other domain walls do not show such a large noise factor. The magnetisation vibrates at the start of each new cycle. The subplot in the middle left demonstrates that 4 runs were done below the critical current and the last one above it. Hence, a total of 20 noise blocks are visible throughout the graph. The initial magnetisation reacts to the spin current added and rotates slightly until it achieves a stable state or a domain wall is created.

The $|\boldsymbol{m}| \approx 0$ constraint holds when no domain wall passes, but it does not within a domain wall structure. The magnetisation rotation towards the y-axis for both sublattices is also predicted for an instability of the system. The instability is characterised by spin waves throughout the nanowire. Those can rotate like domain walls. Therefore, $|\boldsymbol{m}| \approx 0$ is no preset for the instability. The shedding current calculation is not affected by this interpretation as it describes the creation of a domain wall at

the pinning point instead of the change of the total system.

The simulations for the synthetic antiferromagnet showed that the theoretical pre-
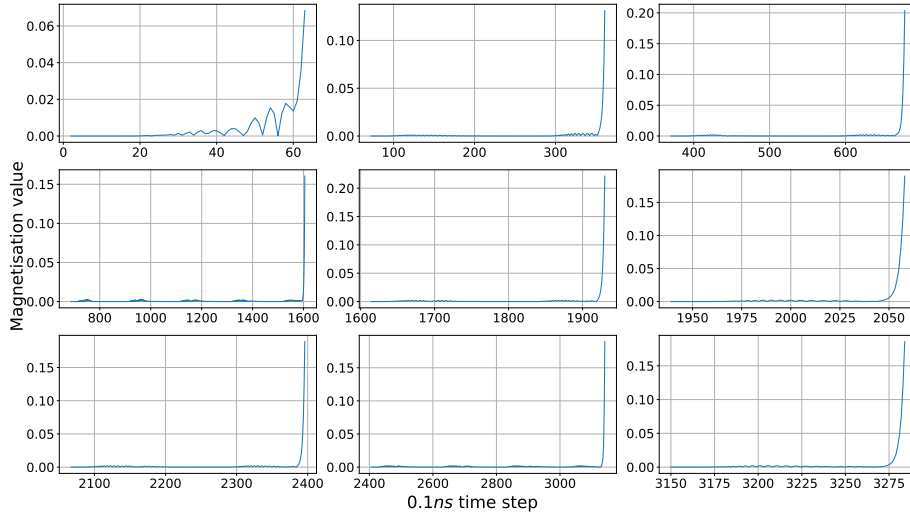
Figure 5.5.: The figure displays the magnetisation evolution in time at the centre of the nanowire in a simulation. It is an ongoing graph split into parts from the top left to the bottom right. The x-axis is divided into $0.1ns$ time steps. A total of 20 runs were taken. A domain wall passes at each rising edge. The curves are cut off at the highest magnitude of 0.2 to highlight the preceding change of the magnetisation value. Source: Author's illustration.

dictions for the shedding current are justifiable but that an anisotropy dependency is expected. The analysis of the magnetisation vector magnitude $|\boldsymbol{m}|$ demonstrates that the small size approximation does hold outside of spin wave and domain wall structures. Therefore, the instability current should be recalculated without the constraint.

6. Conclusion and outlook

Building up a formalism to describe the shedding of domain walls in one-dimensional synthetic antiferromagnetic nanowires was the primary goal of this thesis. Simulations should confirm these calculations. A racetrack memory system of synthetic antiferromagnetic nanowires is the main focus for a future application.

At first, it was crucial to describe the different possible domain wall types. Also, the micromagnetic LLG equation and the total magnetic energy needed to be discussed as the main equations of the thesis [16]. The ferromagnetic theory of the main domain wall characteristics was necessary to use it for the antiferromagnetic formalism. The domain wall profile and width were calculated to see that both are material parameter dependent [38] [46]. The contour can be treated as a rigid body at low energies. An external spin-polarised current moves domain wall structures by spin-transfer torque. Therefore, the domain wall motion is facilitated by a Thiele approach [45]. The corresponding Hamiltonian equations were derived with two generalised coordinates, the domain wall centre position and angle [36] [37].

The domain wall statics and dynamics were needed to see that racetrack memory systems can be realised [34] [35]. A semi-infinitely long nanowire system was used to derive a critical current strength for a spin-polarised current needed to shed domain walls off a pinning point [38] [39]. The Noether theorem determined the two conserved quantities of the system [3]. Those were needed to calculate the critical current. The ferromagnetic shedding was compared to an instability current of ferromagnetic systems. A perturbation orthogonal to the easy axis was used to determine a dispersion relation dependent on the spin current strength. Above the critical value, the spin wave perturbation in the system will grow exponentially in time. The calculation showed that this current is higher than the shedding current and a racetrack application is possible in the ferromagnetic case [32].

Antiferromagnetic systems have the benefit that the total magnetisation in the system is about zero. Synthetic antiferromagnets are manufactured by two oppositely magnetised ferromagnetic layers on top of each other. The interlayer thickness determines the antiferromagnetic coupling strength between both [35]. Therefore, a nanowire system is possible similar to the ferromagnetic one and domain wall properties of the antiferromagnet can be examined the same way.

At first, the LLG equations of the antiferromagnetic system were built using new coordinates, the magnetisation and the Néel vector [19] [28]. Then, the effective field was calculated using a variational approach that regards the antiferromagnetic constraints [23]. The Thiele approach showed that antiferromagnetic domain walls could be described and moved the same way and racetrack systems are theoretically possible if a domain wall can be created [36] [37]. Therefore, a critical current of domain wall

shedding was derived using the Noether theorem as in the ferromagnetic case [38]. This current validates that racetracks are possible in synthetic antiferromagnets and it shows a bottom limit for the electrical current strength needed to realise it.

The determination of an instability current should confirm that shedding was possible at a stable state. However, the result is the same as the shedding current. Hence, either it is not possible, or the assumptions used for the calculation are wrong. A simulation of the domain wall shedding was used to confirm the theory. Mumax3 was chosen to simulate a pinned synthetic antiferromagnetic nanowire [17] [50]. A range of parameters was tested. This proved the theoretical predictions of the interlattice and intralattice exchange constants. Also, an unexpected anisotropic dependency was seen. Adding more interaction to the system and neglecting fewer terms in the calculations could show this behaviour.

The simulations demonstrate a range of current strengths at which shedding was possible while the system remained stable. Therefore, it is confirmed that the instability current needs to be corrected. The magnetisation vector magnitude was analysed to see if the small magnetisation approximation for the antiferromagnet applies to instability calculation. It showed that the magnetisation remains constant when no domain wall passes. However, both sublattice magnetisation vectors point along the same direction in the domain wall centre. Hence, the approximation is not acceptable and the instability current needs to be recalculated without vanishing small magnetisation.

The computation done in this thesis demonstrates the static and dynamic properties of domain walls in ferromagnetic and antiferromagnetic systems. All calculations show that the racetrack memory system can be built. Experiments need to be used to verify the theoretical foundation for the currents. Then, systems with different material parameters could lower the required current. Ferromagnetics showed that systems with DMI have a lower energy requirement for shedding. The same needs to be checked for synthetic antiferromagnets.

Also, the Néel vector was chosen arbitrarily in the calculations and it can not be measured in experiments for the given anisotropy. A different anisotropy with 90° domain walls, instead of the 180° ones, leads to measurable Néel vectors. Hence, a theory of shedding using this anisotropy is helpful to understand the domain wall creation and is needed to explicitly measure the Néel vector time evolution. Then, noncollinear antiferromagnetic systems can be tested as well. After these calculations and experiments, higher dimensional synthetic antiferromagnets can be analysed.

Bibliography

1. Abert, C. W.
   Discrete Mathematical Concepts in Micromagnetic Computations
   PhD thesis (Universität Hamburg, Hamburg, 2013).

2. Abramowitz, M. & Stegun, I. A.
   Handbook of Mathematical Functions with Formulas, Graphs, and Mathematical Tables ninth Dover printing, tenth GPO printing
   (Dover, New York, 1964).

3. Altland, A. & Simons, B.
   Condensed matter field theory 2nd ed.
   (Cambrigde University Press, Cambridge, 2010).

4. ATP Electronics,Inc.
   3D NAND Stacking Memory Cells
   last access: 20.05.2021.
   `https://www.atpinc.com/blog/3d-nand-ssd-sd-flash-memory-storage-what-is`.

5. Baibich, M. N., Broto, J. M., Fert, A., Van Dau, F. N., Petroff, F., Etienne, P., Creuzet, G., Friederich, A. & Chazelas, J.
   Giant Magnetoresistance of (001)Fe/(001)Cr Magnetic Superlattices.
   Phys. Rev. Lett. **61,** 2472–2475
   (21 Nov. 1988).

6. Bar'yakhtar, V. G., Ivanov, B. A. & Chetkin, M. V.
   Dynamics of domain walls in weak ferromagnets.
   Soviet Physics Uspekhi **28,** 563–588
   (July 1985).

7. Berger, L.
   Emission of spin waves by a magnetic multilayer traversed by a current.
   Phys. Rev. B **54,** 9353–9358
   (13 Oct. 1996).

8. Binasch, G., Grünberg, P., Saurenbach, F. & Zinn, W.
   Enhanced magnetoresistance in layered magnetic structures with antiferromagnetic interlayer exchange.
   Phys. Rev. B **39,** 4828–4830
   (7 Mar. 1989).

9. Clarke, D. J., Tretiakov, O. A., Chern, G.-W., Bazaliy, Y. B. & Tchernyshyov, O.

Dynamics of a vortex domain wall in a magnetic nanostrip: Application of the collective-coordinate approach.
Phys. Rev. B **78,** 134412
(13 Oct. 2008).

10. Coey, J.
Magnetism and Magnetic Materials First
(Cambrigde University Press, New York, 2010).

11. DyNaMat Group Gent.
Mumax-view
last access: 02.05.2021.
`https://mumax.ugent.be/mumax-view/`.

12. Dzyaloshinsky, I.
A thermodynamic theory of "weak" ferromagnetism of antiferromagnetics.
Journal of Physics and Chemistry of Solids **4,** 241–255. ISSN: 0022-3697.
`https://www.sciencedirect.com/science/article/pii/0022369758900763`
(1958).

13. Eggert, S.
One-dimensional quantum wires: A pedestrian approach to bosonization
2009.
eprint: `0708.0003`.

14. Evans, D. M., Garcia, V., Meier, D. & Bibes, M.
Domains and domain walls in multiferroics.
Physical Sciences Reviews **5.**
`https://doi.org/10.1515/psr-2019-0067`
(2020).

15. Everschor, K., Garst, M., Binz, B., Jonietz, F., Muehlbauer, S., Pfleiderer, C. & Rosch, A.
Rotating skyrmion lattices by spin torques and field or temperature gradients.
Phys. Rev. B **86,** 054432
(5 Aug. 2012).

16. Everschor-Sitte, K.
Current-Induced Dynamics of Chiral Magnetic Structures
PhD thesis (Universität zu Köln, Köln, 2012).

17. Exl, L., Bance, S., Reichel, F., Schrefl, T., Peter Stimming, H. & Mauser, N. J.
LaBonte's method revisited: An effective steepest descent method for micromagnetic energy minimization.
Journal of Applied Physics **115,** 17D118
(2014).

18. Gilbert, T.
Classics in Magnetics A Phenomenological Theory of Damping in Ferromagnetic Materials.

Magnetics, IEEE Transactions on **40,** 3443–3449
(Dec. 2004).

19. Gomonay, H. V. & Loktev, V. M.
Spin transfer and current-induced switching in antiferromagnets.
Phys. Rev. B **81,** 144427
(14 Apr. 2010).

20. Guimarães, F., Suckert, J., Chico, J., Juba, B., Dos Santos Dias, M. & Lounis, S.
Comparative study of methodologies to compute the intrinsic Gilbert damping:
interrelations, validity and physical consequences.
Journal of Physics: Condensed Matter **31**
(Mar. 2019).

21. Hals, K. M. D. & Brataas, A.
Spin-orbit torques and anisotropic magnetization damping in skyrmion crystals.
Phys. Rev. B **89,** 064426
(6 Feb. 2014).

22. Hals, K. M. D. & Everschor-Sitte, K.
New Boundary-Driven Twist States in Systems with Broken Spatial Inversion
Symmetry.
Phys. Rev. Lett. **119,** 127203.
`https://link.aps.org/doi/10.1103/PhysRevLett.119.127203`
(2017).

23. Hals, K. M. D., Tserkovnyak, Y. & Brataas, A.
Phenomenology of Current-Induced Dynamics in Antiferromagnets.
Phys. Rev. Lett. **106,** 107206.
`https://link.aps.org/doi/10.1103/PhysRevLett.106.107206`
(10 Mar. 2011).

24. Huang, K.
Statistical Mechanics 2nd ed.
(John Wiley & Sons, Hoboken, 1987).

25. Jin, H. & Miyazaki, T.
Magnetic Anisotropy
(Springer-Verlag, Berlin, 2021).

26. Jungwirth, T., Marti, X., Wadley, P. & Wunderlich, J.
Antiferromagnetic spintronics.
Nature Nanotechnology **11,** 231–241.
`https://link.aps.org/doi/10.1103/PhysRev.120.91`
(3 Mar. 2016).

27. Keesling, J.
Bisection Method
last access: 02.05.2021.
`https://people.clas.ufl.edu/kees/files/Bisection.pdf`.

Bibliography

28. Kosevich, A., Ivanov, B. & Kovalev, A.
Magnetic Solitons.
Physics Reports **194,** 117–238. ISSN: 0370-1573
(1990).

29. Landau, L. & Lifshitz, E.
On the theory of the dispersion of magnetic permeability in ferromagnetic bodies.
Phys. Z. Sowjet. **8,** 153–169
(1935).

30. Leliaert, J. & Mulkers, J.
Mumax3-workshop session 1
last access: 02.05.2021.
`https://mumax.ugent.be/mumax3-workshop/tutorial1.pdf`.

31. Leliaert, J. & Mulkers, J.
Mumax3-workshop session 4
last access: 02.05.2021.
`https://mumax.ugent.be/mumax3-workshop/tutorial4.pdf`.

32. Masell, J., Rodrigues, D. R., McKeever, B. F. & Everschor-Sitte, K.
Spin-transfer torque driven motion, deformation, and instabilities of magnetic skyrmions at high currents.
Phys. Rev. B **101,** 214428.
`https://link.aps.org/doi/10.1103/PhysRevB.101.214428`
(21 June 2020).

33. Moriya, T.
Anisotropic Superexchange Interaction and Weak Ferromagnetism.
Phys. Rev. **120,** 91–98.
`https://link.aps.org/doi/10.1103/PhysRev.120.91`
(1 Oct. 1960).

34. Parkin, S. S. P., Hayashi, M. & Thomas, L.
Magnetic Domain-Wall Racetrack Memory.
Science **320,** 190–194
(2008).

35. Parkin, S. S. P. & Yang, S.
Memory on the racetrack.
Nature Nanotechnology **10,** 195–198
(3 Mar. 2015).

36. Rodrigues, D.
Towards a new generation of nonvolatile memory devices: creation and manipulation of topological magnetic structures by electric current
PhD thesis (Texas A&M University, College Station, 2018).

37. Rodrigues, D. R., Everschor-Sitte, K., Tretiakov, O. A., Sinova, J. & Abanov, A.
Spin texture motion in antiferromagnetic and ferromagnetic nanowires.

Phys. Rev. B **95,** 174408
(17 May 2017).

38. Rodrigues, D. R., Sommer, N. & Everschor-Sitte, K.
Facilitating domain wall injection in magnetic nanowires by electrical means.
Physical Review B **101.** ISSN: 2469-9969.
`http://dx.doi.org/10.1103/PhysRevB.101.224410`
(June 2020).

39. Sitte, M., Everschor-Sitte, K., Valet, T., Rodrigues, D. R., Sinova, J. & Abanov, A.
Current-driven periodic domain wall creation in ferromagnetic nanowires.
Phys. Rev. B **94,** 064422.
`https://link.aps.org/doi/10.1103/PhysRevB.94.064422`
(6 Aug. 2016).

40. Slonczewski, J.
Current-driven excitation of magnetic multilayers.
Journal of Magnetism and Magnetic Materials **159,** L1–L7
(1996).

41. Spiceworks Inc.
Data Storage Trends in 2020 and Beyond
last access: 20.05.2021.
`https://www.spiceworks.com/marketing/reports/storage-trends-in-2020-and-beyond/`.

42. Stiles, M. D. & Zangwill, A.
Anatomy of spin-transfer torque.
Phys. Rev. B **66,** 014407
(1 June 2002).

43. The SciPy community.
scipy.optimize.curve_fit
last access: 02.05.2021.
`https://docs.scipy.org/doc/scipy/reference/generated/scipy.optimize.curve_fit.html`.

44. Thiaville, A., Nakatani, Y., Miltat, J. & Suzuki, Y.
Micromagnetic understanding of current-driven domain wall motion in patterned nanowires.
Europhysics Letters (EPL) **69,** 990–996
(Mar. 2005).

45. Thiele, A. A.
Steady-State Motion of Magnetic Domains.
Phys. Rev. Lett. **30,** 230–233
(6 Feb. 1973).

46. Tretiakov, O. A. & Abanov, A.

Current Driven Magnetization Dynamics in Ferromagnetic Nanowires with a Dzyaloshinskii-Moriya Interaction.
Phys. Rev. Lett. **105,** 157201
(15 Oct. 2010).

47. Tretiakov, O. A., Clarke, D., Chern, G.-W., Bazaliy, Y. B. & Tchernyshyov, O.
Dynamics of Domain Walls in Magnetic Nanostrips.
Phys. Rev. Lett. **100,** 127204
(12 Mar. 2008).

48. Tveten, E. G., Qaiumzadeh, A., Tretiakov, O. A. & Brataas, A.
Staggered Dynamics in Antiferromagnets by Collective Coordinates.
Phys. Rev. Lett. **110,** 127208
(12 Mar. 2013).

49. Ueda, K., Hamaya, K., Yamamoto, K., Ando, Y., Sadoh, T., Maeda, Y. & Miyao, M.
Low-temperature molecular beam epitaxy of a ferromagnetic full-Heusler alloy Fe2MnSi on Ge(111).
Applied Physics Letters **93,** 112108
(2008).

50. Vansteenkiste, A., Leliaert, J., Dvornik, M., Helsen, M., Garcia-Sanchez, F. & Van Waeyenberge, B.
The design and verification of MuMax3.
AIP Advances **4,** 107133
(2014).

51. White, R. M.
Quantum theory of magnetism
(Springer-Verlag, Berlin, 2007).

52. Wolfram Research, Inc.
Mathematica, Version 12.2
Champaign, IL, 2020.
`https://www.wolfram.com/mathematica`.

A. Vector identities

$bac - cab$ rule:

$$\boldsymbol{a} \times (\boldsymbol{b} \times \boldsymbol{c}) = \boldsymbol{b}(\boldsymbol{a} \cdot \boldsymbol{c}) - \boldsymbol{c}(\boldsymbol{a} \cdot \boldsymbol{b}) \tag{A.1}$$

Lagrange identity:

$$(\boldsymbol{a} \times \boldsymbol{b}) \cdot (\boldsymbol{c} \times \boldsymbol{d}) = (\boldsymbol{a} \cdot \boldsymbol{c})(\boldsymbol{b} \cdot \boldsymbol{d}) - (\boldsymbol{a} \cdot \boldsymbol{d})(\boldsymbol{b} \cdot \boldsymbol{c}) \tag{A.2}$$

Spatial product:

$$\boldsymbol{a} \cdot (\boldsymbol{b} \times \boldsymbol{c}) = \boldsymbol{c} \cdot (\boldsymbol{a} \times \boldsymbol{b}) = \boldsymbol{b} \cdot (\boldsymbol{c} \times \boldsymbol{a}) = -\boldsymbol{a} \cdot (\boldsymbol{c} \times \boldsymbol{b}) = -\boldsymbol{c} \cdot (\boldsymbol{b} \times \boldsymbol{a}) = -\boldsymbol{b} \cdot (\boldsymbol{a} \times \boldsymbol{c}) \tag{A.3}$$

B. Domain wall profile

This chapter of the appendix illuminates essential steps of the ferromagnetic domain wall profile calculation. In the first step, $(\partial \boldsymbol{m})^2$ is analysed.

$$
\begin{aligned}
(\partial \boldsymbol{m})^2 &= (\Gamma(x,t)\hat{\boldsymbol{x}} \times \boldsymbol{m} + \Lambda(x,t)\boldsymbol{m} \times (\hat{\boldsymbol{x}} \times \boldsymbol{m}))^2 \\
&= \Gamma^2(\hat{\boldsymbol{x}} \times \boldsymbol{m})^2 + \Lambda^2(\boldsymbol{m} \times (\hat{\boldsymbol{x}} \times \boldsymbol{m}))^2 + \Gamma\Lambda(\hat{\boldsymbol{x}} \times \boldsymbol{m}) \cdot (\boldsymbol{m} \times (\hat{\boldsymbol{x}} \times \boldsymbol{m})) \quad \text{(B.1)} \\
&= (1 - m_x^2)(\Gamma^2 + \Lambda^2)
\end{aligned}
$$

The Lagrange identity (A.2) is used to facilitate the Γ^2 term: $(\hat{\boldsymbol{x}} \times \boldsymbol{m})^2 = \hat{\boldsymbol{x}}^2\boldsymbol{m}^2 - (\hat{\boldsymbol{x}} \cdot \boldsymbol{m})^2 = 1 - m_x^2$ and to compute the absolute value of a cross product for the Λ^2 term: $(\boldsymbol{m} \times (\hat{\boldsymbol{x}} \times \boldsymbol{m}))^2 = \boldsymbol{m}^2(\hat{\boldsymbol{x}} \times \boldsymbol{m})^2 - ((\hat{\boldsymbol{x}} \times \boldsymbol{m}) \cdot \boldsymbol{m})^2 = (\hat{\boldsymbol{x}} \times \boldsymbol{m})^2 = \hat{\boldsymbol{x}}^2\boldsymbol{m}^2 - (\hat{\boldsymbol{x}} \cdot \boldsymbol{m})^2 = 1 - m_x^2$. Both $\hat{\boldsymbol{x}}$ and $\boldsymbol{m}$ are normalised vectors. The cross term $\Gamma\Lambda(\hat{\boldsymbol{x}} \times \boldsymbol{m}) \cdot (\boldsymbol{m} \times (\hat{\boldsymbol{x}} \times \boldsymbol{m})) = 0$ is vanishing as Λ and Γ term are orthogonal by construction.

The DMI strength of the total magnetic energy can be rearranged using the vector properties: $\Gamma\boldsymbol{m} \cdot (\hat{\boldsymbol{x}} \times (\hat{\boldsymbol{x}} \times \boldsymbol{m})) = \Gamma\boldsymbol{m} \cdot (\hat{\boldsymbol{x}}m_x - \boldsymbol{m}\hat{\boldsymbol{x}}^2) = \Gamma(m_x^2 - 1)$ and $\Lambda\boldsymbol{m} \cdot (\hat{\boldsymbol{x}} \times (\boldsymbol{m} \times (\hat{\boldsymbol{x}} \times \boldsymbol{m}))) = \Lambda\boldsymbol{m} \cdot (\hat{\boldsymbol{x}} \times (\hat{\boldsymbol{x}} - m_x\boldsymbol{m})) = -\Lambda m_x\boldsymbol{m} \cdot (\hat{\boldsymbol{x}} \times \boldsymbol{m}) = -\Lambda m_x\hat{\boldsymbol{x}} \cdot (\boldsymbol{m} \times \boldsymbol{m}) = 0$. Hence, the total DMI strength is given by $-D\Gamma(1 - m_x^2)$.

The spatial derivative of the magnetisations x component is $\partial m_x = \Lambda(1 - m_x^2)$. Therefore, the parametrization of $m_x = \tanh{(f(x))}$ can be used to recast the Λ concerning $f(x)$:

$$
\begin{aligned}
\Lambda &= \frac{\partial m_x}{1 - m_x^2} = \frac{\partial(\tanh{(f(x))})}{1 - \tanh{(f(x))}^2} \\
\Lambda^2 &= \frac{(\partial(\tanh{(f(x))}))^2}{(1/\cosh{(f(x))^2})^2} = (\partial f(x))^2.
\end{aligned}
\qquad \text{(B.2)}
$$

$1 - \tanh{(f(x))}^2 = 1/\cosh{(f(x))}^2$ is used as $\cosh{(f(x))}^2 - \sinh{(f(x))}^2 = 1$ holds by definition. The derivative of the hyperbolic tangent function will resolve in the following chain rule: $\partial(\tanh{(f(x))}) = \frac{1}{\cosh{(f(x))^2}}\partial f(x)$. Then, the $\cosh f(x)$ parts will cancel.

$g(f(x))$ can be analysed using ∂m_y of the ansatz $\frac{\cos{(g)}}{\cosh{(f)}}$ compared to the derivative of another ansatz $\partial \boldsymbol{m} = \Gamma\hat{\boldsymbol{x}} \times \boldsymbol{m} + \Lambda\boldsymbol{m}(\hat{\boldsymbol{x}} \times \boldsymbol{m})$ in the y component. The first derivative resolves to $\partial m_y = \partial(\frac{\cos{(g)}}{\cosh{(f)}}) = -\frac{\tanh{(f)}}{\cosh{(f)}}\partial f \cos{(g)} - \frac{1}{\cosh{(f)}}\sin{(g)}\partial g$. The second one reduces to $\partial m_y = -\Gamma m_z - \Lambda\tanh{(f)}m_y = -\Gamma\frac{\sin{(g)}}{\cosh{(f)}} - \partial f\frac{\tanh{(f)}}{\cosh{(f)}}\cos{(g)}$. $\Lambda = \frac{1}{\Xi}$ and the values $m_y = \frac{\cos{(g)}}{\cosh{(f)}}$ and $m_z = \frac{\sin{(g)}}{\cosh{(f)}}$ have been inserted. Then, both possible solutions need to match. Each expression is compared and differences lead to

constraints.

$$-\Gamma\frac{\sin(g)}{\cosh(f)} - \partial f\frac{\tanh(f)}{\cosh(f)}\cos(g) = -\frac{\tanh(f)}{\cosh(f)}\partial f\cos(g) - \frac{1}{\cosh(f)}\sin(g)\partial g \quad \text{(B.3)}$$

The discrepancy in the equality is solved if $\Gamma = \partial g$. The fixed Γ value of the one-dimensional nanowire system indicates that $g(f(x)) = x\Gamma = \frac{xD}{2A}$ after integrating by x.

C. Rigid body treatment of a domain wall

The time derivative of the total magnetic energy E depends on the change of the Hamiltonian. Since the Hamiltonian has no direct time dependency, the derivative can be separated into a $\dot{\boldsymbol{m}}$ term as well as the effective field $\boldsymbol{H}_{\text{eff}}$. That dissociation is an application of the chain rule of differentiation.

$$
\begin{aligned}
\dot{E} = \int dV \dot{H} &= \int dV \frac{\delta H}{\delta \boldsymbol{m}} \cdot \dot{\boldsymbol{m}} = \int dV \boldsymbol{H}_{\text{eff}} \cdot \dot{\boldsymbol{m}} \\
&= \int dV \boldsymbol{H}_{\text{eff}} \cdot (\gamma \boldsymbol{m} \times \boldsymbol{H}_{\text{eff}} + \alpha \boldsymbol{m} \times \dot{\boldsymbol{m}} - (\boldsymbol{\nu} \cdot \nabla)\boldsymbol{m} + \beta \boldsymbol{m} \times (\boldsymbol{\nu} \cdot \nabla)\boldsymbol{m}) \\
&= \int dV [\boldsymbol{m} \cdot (\gamma \boldsymbol{H}_{\text{eff}} \times \boldsymbol{H}_{\text{eff}}) + \alpha \dot{\boldsymbol{m}} \cdot (\boldsymbol{H}_{\text{eff}} \times \boldsymbol{m}) \\
&\quad + \beta(\boldsymbol{\nu} \cdot \nabla)\boldsymbol{m} \cdot (\boldsymbol{H}_{\text{eff}} \times \boldsymbol{m}) - \boldsymbol{H}_{\text{eff}} \cdot (\boldsymbol{\nu} \cdot \nabla)\boldsymbol{m})] \\
&= (\boldsymbol{\nu} \cdot \nabla_X)E - \frac{1}{\gamma} \int dV (\alpha \dot{\boldsymbol{m}} + \beta(\boldsymbol{\nu} \cdot \nabla)\boldsymbol{m})(\dot{\boldsymbol{m}} + (\boldsymbol{\nu} \cdot \nabla)\boldsymbol{m})
\end{aligned}
\tag{C.1}
$$

The LLG equation with a spin-transfer torque contribution (2.7) is inserted for the change of the magnetisation $\dot{\boldsymbol{m}}$ in the second line. After that, the spatial products are revised by equation (A.3). The cross product of two parallel vectors is vanishing and the $(\boldsymbol{H}_{\text{eff}} \times \boldsymbol{m})$ term is substituted by the LLG equation without damping to get to the final line of the equation.

The equation is linear in dissipation for simplicity as both constants α and β are much smaller than one and negligible in higher orders. $\int dV \boldsymbol{H}_{\text{eff}} \cdot (\boldsymbol{\nu} \cdot \nabla)\boldsymbol{m}) = -(\boldsymbol{\nu} \cdot \nabla_X)E$ can be substituted because of the ansatz (3.17) where the spatial derivative of E with respect to X is the same as a $\partial \boldsymbol{m}$ term. In this case, ∇ is just a partial derivative along the x-axis in the one-dimensional system where the current is applied along the wire $\boldsymbol{\nu} = \nu \hat{\boldsymbol{x}}$. The ∇ is displayed to analyse the problem as general as possible.

The corresponding Hamiltonian equation in terms of the collective coordinates or soft modes position X and tilting angle Φ is $\dot{E} = \{E, H_m\} = \nu \partial_X E$. The Poisson bracket $\{E, H_m\}$ should fulfil both $\dot{E} = \nu \partial_X E$ with an current applied and $\dot{E} = 0$ without an current. The ansatz $H_m = E \pm \nu \Phi$ is chosen and tested in the following calculation:

$$
\begin{aligned}
\dot{E} = \{E, H_m\} &= \{E, E \pm \nu \Phi\} = \{E, E\} \pm \{E, \nu \Phi\} \\
&= \pm(\pm(\partial_X E \partial_\Phi \nu \Phi - \partial_\Phi E \partial_X \nu \Phi)) = \nu \partial_X E \partial_\Phi \Phi = \nu \partial_X E
\end{aligned}
\tag{C.2}
$$

At first, H_m is inserted. Then, the Poisson brackets linearity is used to separate the two terms, with the first one being zero because of the commutative derivatives inside

the bracket. The magnetic energy depends on both X and Φ. Therefore, the second term $\{E, \Phi\}$ evaluates to $\pm$ the derivatives because of $\{X, \Phi\} = \pm 1$. Both $\pm$ cancel and the derivative of the angle Φ concerning the position X is zero. In the end, the only term remaining depends on the derivative of Φ for Φ that is one. Hence, the calculation shows that the ansatz fulfils the requirements needed.

D. Domain wall shedding

The static case LLG equation for ferromagnetic systems (2.7) with the effective field (3.25) is stated below:

$$0 = \gamma \boldsymbol{m} \times (-2A\partial^2 \boldsymbol{m} + 2D\hat{\boldsymbol{x}} \times \partial \boldsymbol{m} - 2\lambda m_x \hat{\boldsymbol{x}}) - \nu\partial \boldsymbol{m} + \beta \boldsymbol{m} \times \nu\partial \boldsymbol{m}.$$

This equation is multiplied by either $\hat{\boldsymbol{x}}$ or $\boldsymbol{m} \times \partial \boldsymbol{m}$ to obtain a formula for both conserved quantities, the linear momentum conservation and the total angular conservation along the x-axis.

At first, the linear momentum conservation equation will be computed by the multiplication with $\boldsymbol{m} \times \partial \boldsymbol{m}$:

$$0 = (\boldsymbol{m} \times \partial \boldsymbol{m}) \cdot \left[\gamma \boldsymbol{m} \times (-2A\partial^2 \boldsymbol{m} + 2D\hat{\boldsymbol{x}} \times \partial \boldsymbol{m} - 2\lambda m_x \hat{\boldsymbol{x}}) - \nu\partial \boldsymbol{m} + \beta \boldsymbol{m} \times \nu\partial \boldsymbol{m}\right]$$

$$0 = -2A\gamma \left[(\boldsymbol{m} \cdot \boldsymbol{m})(\partial^2 \boldsymbol{m} \cdot \partial \boldsymbol{m}) - (\boldsymbol{m} \cdot \partial^2 \boldsymbol{m})(\partial \boldsymbol{m} \cdot \boldsymbol{m})\right]$$
$$+ 2D(\boldsymbol{m} \times \partial \boldsymbol{m}) \cdot (\boldsymbol{x}(\boldsymbol{m} \cdot \partial \boldsymbol{m}) - \partial \boldsymbol{m} m_x)$$
$$- 2\lambda m_x \left[(\boldsymbol{m} \cdot \boldsymbol{m})(\partial \boldsymbol{m} \cdot \hat{\boldsymbol{x}}) - (\boldsymbol{m} \cdot \hat{\boldsymbol{x}})(\partial \boldsymbol{m} \cdot \boldsymbol{m})\right]$$
$$- \nu(\partial \boldsymbol{m} \times \partial \boldsymbol{m}) \cdot \boldsymbol{m} + \beta \left[(\partial \boldsymbol{m} \cdot \partial \boldsymbol{m})(\boldsymbol{m} \cdot \boldsymbol{m}) - (\partial \boldsymbol{m} \cdot \boldsymbol{m})(\partial \boldsymbol{m} \cdot \boldsymbol{m})\right]$$

$$0 = -2A\partial^2 \boldsymbol{m} \cdot \partial \boldsymbol{m} - 2\lambda m_x \partial \boldsymbol{m} \cdot \hat{\boldsymbol{x}} + \frac{\beta}{\gamma}(\partial \boldsymbol{m})^2$$

$$0 = -A\partial(\partial \boldsymbol{m})^2 - \lambda\partial m_x^2 + \frac{\beta}{\gamma}(\partial \boldsymbol{m})^2$$

$$\implies \partial\left(A(\partial \boldsymbol{m})^2 + \lambda m_x^2\right) = \frac{\beta}{\gamma}(\partial \boldsymbol{m})^2.$$

(D.1)

The double cross products from the exchange term, the anisotropy strength and the dissipative β expression are recast using the Lagrange identity (A.2). The constant length constraint of the magnetisation vector $\boldsymbol{m}^2 = \boldsymbol{m} \cdot \boldsymbol{m} = 1$ and its inheritance of $\boldsymbol{m} \cdot \partial \boldsymbol{m} = 0$ are inserted. The spin-transfer torques spatial product can be rotated using the equation (A.3) to prove that the expression does not contribute. The DMI term is converted by the $bac - cab$ rule for triple products (A.1). Both parts vanish because of $\boldsymbol{m} \cdot \partial \boldsymbol{m} = 0$.

The remaining items of the equation are shown in the third line. This calculation should result in the conservation of the linear momentum in the nanowire system. Hence, there should be some dependency on the linear momentum derivative equal to zero $\partial(\partial \boldsymbol{m} + \Theta) = 0$. If the derivative of something is zero, the derivated part is constant. In this case, if $\partial(\partial \boldsymbol{m} + \Theta) = 0$ for some $\Theta \neq -\partial \boldsymbol{m}$, then the linear momentum $\partial \boldsymbol{m}$ is conserved.

D. Domain wall shedding

The chain rule for derivation can be applied backwards to rewrite the exchange interaction term with $\partial(\partial\boldsymbol{m})^2 = 2\partial^2\boldsymbol{m}\cdot\partial\boldsymbol{m}$ and $\partial m_x^2 = 2m_x\partial m_x$. Combining both structures and adding them to the left side leads to the last equation. In the case of a vanishing dissipation, as expected in the regime of the critical current, the linear momentum is a conserved quantity.

An equation for the conservation of the total angular momentum along the x direction in the nanowire can be built similarly. The static case LLG equation shown above is multiplied by the unit vector along the x direction $\hat{\boldsymbol{x}}$:

$$0 = \hat{\boldsymbol{x}}\cdot\left[\gamma\boldsymbol{m}\times(-2A\partial^2\boldsymbol{m} + 2D\hat{\boldsymbol{x}}\times\partial\boldsymbol{m} - 2\lambda m_x\hat{\boldsymbol{x}}) - \nu\partial\boldsymbol{m} + \beta\boldsymbol{m}\times\nu\partial\boldsymbol{m}\right]$$

$$0 = -2A\gamma\hat{\boldsymbol{x}}\cdot(\boldsymbol{m}\times\partial^2\boldsymbol{m}) + 2D\gamma\hat{\boldsymbol{x}}\cdot(\hat{\boldsymbol{x}}(\boldsymbol{m}\cdot\partial\boldsymbol{m}) - \partial\boldsymbol{m}(\hat{\boldsymbol{x}}\cdot\boldsymbol{m}))$$
$$\quad - 2\lambda\gamma m_x\hat{\boldsymbol{x}}\cdot(\boldsymbol{m}\times\hat{\boldsymbol{x}}) - \nu\hat{\boldsymbol{x}}\cdot\partial\boldsymbol{m} + \beta\hat{\boldsymbol{x}}\cdot(\boldsymbol{m}\times\partial\boldsymbol{m})$$

$$0 = -2A\gamma\partial\left[\hat{\boldsymbol{x}}\cdot(\boldsymbol{m}\times\partial\boldsymbol{m})\right] + 2D\gamma m_x\partial m_x - \nu\partial m_x + \beta\hat{\boldsymbol{x}}\cdot(\boldsymbol{m}\times\partial\boldsymbol{m}) \qquad\text{(D.2)}$$

$$\implies 2A\partial\left[\hat{\boldsymbol{x}}\cdot(\boldsymbol{m}\times\partial\boldsymbol{m})\right] + D\partial m_x^2 + \frac{\nu}{\gamma}\partial m_x = \frac{\beta}{\gamma}\hat{\boldsymbol{x}}\cdot(\boldsymbol{m}\times\partial\boldsymbol{m})$$

$$\implies \partial\left(2A\left[\hat{\boldsymbol{x}}\cdot(\boldsymbol{m}\times\partial\boldsymbol{m})\right] + D(m_x + \frac{\nu}{2D\gamma})^2\right) = \frac{\beta}{\gamma}\hat{\boldsymbol{x}}\cdot(\boldsymbol{m}\times\partial\boldsymbol{m}).$$

As in the calculation for the linear momentum, the DMI term is converted using the $bac - cab$ rule for triple products (A.1). One part is zero because of $(\boldsymbol{m}\cdot\partial\boldsymbol{m})$. In the fourth line, a partial derivative is pulled in front to get a conserved quantity structure. For the exchange interaction, the reverse chain rule is given by:

$$\hat{\boldsymbol{x}}\cdot(\boldsymbol{m}\times\partial^2\boldsymbol{m}) = \hat{\boldsymbol{x}}\cdot(\partial\boldsymbol{m}\times\partial\boldsymbol{m}) + \hat{\boldsymbol{x}}\cdot(\boldsymbol{m}\times\partial^2\boldsymbol{m}) = \partial\left[\hat{\boldsymbol{x}}\cdot(\boldsymbol{m}\times\partial\boldsymbol{m})\right].$$

The DMI term $2m_x\partial m_x = \partial m_x^2$ is also adjusted by the chain rule of derivation. $D\partial m_x^2 + \frac{\nu}{\gamma}\partial m_x = \partial(m_x^2 + \frac{\nu}{\gamma}m_x)$ is the same as $\partial D(m_x + \frac{\nu}{2D\gamma})^2$ since the derivative of a constant $\partial D(\frac{\nu}{2D\gamma})^2 = 0$ is zero. In the end, a formula for total angular momentum conservation is found in the case of vanishing dissipation.

The two conserved quantities are constants in space so that they can be compared for different coordinates. In both cases, the magnetisation is explicitly pointing along the $\boldsymbol{m} = \hat{\boldsymbol{z}}$ direction at $x = 0$. There is no change in the magnetisation at infinity because it will point along the anisotropic direction as it is the system's ground state.

The angular momentum evaluation is done in the following:

$$\left(2A\hat{\boldsymbol{x}}\cdot(\boldsymbol{m}\times\partial\boldsymbol{m}) + D(m_x + \frac{\nu}{2D\gamma})^2\right)_{x=0} = 2A(m_y\partial m_z - m_z\partial m_y)_{x=0} + D\left(\frac{\nu}{2D\gamma}\right)^2$$

$$= -2A\partial m_y|_{x=0} + D\left(\frac{\nu}{2D\gamma}\right)^2$$

and

$$\left(2A\hat{\boldsymbol{x}}\cdot(\boldsymbol{m}\times\partial\boldsymbol{m}) + D(m_x + \frac{\nu}{2D\gamma})^2\right)_{x\to\infty} = D(m_x + \frac{\nu}{2D\gamma})^2_{x\to\infty} = D \pm \frac{\nu}{\gamma} + D\left(\frac{\nu}{2D\gamma}\right)^2$$

$$\implies -\partial m_y|_{x=0} = \frac{D}{2A} \pm \frac{\nu}{2A\gamma}.$$

D. Domain wall shedding

$$(D.3)$$

The spatial product of the exchange interaction term has no m_y contribution at $x = 0$. The spatial derivative is bound to be perpendicular to $\hat{\boldsymbol{z}}$ because it is the magnetisation direction. That is why the partial derivative of m_y is non-vanishing. Also, a constant $D\left(\frac{\nu}{2D\gamma}\right)^2$ is independent of the spatial coordinate. At $x \to \infty$, the exchange term is vanishing as the magnetisation static. However, the anisotropy is equal for the magnetisation pointing along the nanowire direction or antiparallel to it, which is why the m_x value can be either positive or negative ± 1 depending on the type of the domain wall. A head-to-head domain wall resolves to -1 and the tail-to-tail case to $+1$ based on the geometry of the pinned nanowire.

The combination of both values, as they are equal, results in $-\partial m_y|_{x=0} = \frac{D}{2A} \pm \frac{\nu}{2A\gamma}$. The $\boldsymbol{m}$ independent constant $D\left(\frac{\nu}{2D\gamma}\right)^2$ contributes in both cases. That is why both terms cancel in the last equation.

The same approach is used for the linear momentum case:

$$\left(A(\partial\boldsymbol{m})^2 + \lambda m_x^2\right)_{x=0} = A(\partial\boldsymbol{m})^2_{x=0} \text{ and } \left(A(\partial\boldsymbol{m})^2 + \lambda m_x^2\right)_{x\to\infty} = (\lambda m_x^2)_{x\to\infty} = \lambda$$

$$\implies (\partial\boldsymbol{m})^2_{x=0} = \frac{\lambda}{A}.$$

$$(D.4)$$

For $x = 0$, the x component of $\boldsymbol{m}$ is zero and the partial derivative is $(\partial\boldsymbol{m})^2_{x=0} = (\partial m_x)^2_{x=0} + (\partial m_y)^2_{x=0}$. In the case of $x \to \infty$, the x component depends on the domain wall type $m_x = \pm 1$. Also, there is no spatial change of $\boldsymbol{m}$. Hence, the squared term is independent of the domain wall type.

E. Ferromagnetic instability

The ferromagnetic instability condition for a one-dimensional nanowire system is determined by linearising the LLG equation with spin-transfer torque terms. The perturbation is set to be orthogonal to the ground state with a plane wave ansatz for each of the perturbation components. The determinant of the two-dimensional matrix can be used to get a condition of the spin current up to which the system is stable. The determinant has a quadratic dependency on the frequency ω.

$$0 = (1+\alpha^2)\omega^2 - 2((\boldsymbol{\nu}\cdot\boldsymbol{q}) + i\Lambda\alpha + \alpha\beta(\boldsymbol{\nu}\cdot\boldsymbol{q}))\omega + (1+\beta^2)(\boldsymbol{\nu}\cdot\boldsymbol{q})^2 - \Lambda^2 + 2i\beta(\boldsymbol{\nu}\cdot\boldsymbol{q})\Lambda. \quad \text{(E.1)}$$

At first, the "pq"-formula is applied to get the general dispersion relation:

$$(1 + \alpha^2)\omega_{1/2} = ((1 + \alpha\beta)(\boldsymbol{\nu} \cdot \boldsymbol{q}) + i\Lambda\alpha)\pm$$
$$\sqrt{((1 + \alpha\beta)(\boldsymbol{\nu} \cdot \boldsymbol{q}) + i\Lambda\alpha)^2 - (1 + \alpha^2)\left[(1 + \beta^2)(\boldsymbol{\nu} \cdot \boldsymbol{q})^2 - \Lambda^2 + 2i\beta(\boldsymbol{\nu} \cdot \boldsymbol{q})\Lambda\right]}. \quad \text{(E.2)}$$

A factor of $\frac{1}{1+\alpha^2}$ was pulled out of the square root, leaving a $(1 + \alpha^2)$ factor at the last part.

$$(1 + \alpha^2)\omega_{1/2} = ((1 + \alpha\beta)(\boldsymbol{\nu} \cdot \boldsymbol{q}) + i\Lambda\alpha)\pm$$
$$\sqrt{-(\alpha^2 + \beta^2)(\boldsymbol{\nu} \cdot \boldsymbol{q})^2 + 2\alpha\beta(\boldsymbol{\nu} \cdot \boldsymbol{q})^2 + 2i\Lambda(\alpha - \beta)(\boldsymbol{\nu} \cdot \boldsymbol{q}) + \Lambda^2} \quad \text{(E.3)}$$

Then, the binomial theorem $(a + b)^2 = a^2 + 2ab + b^2$ is used to to rewrite the $(\boldsymbol{\nu} \cdot \boldsymbol{q})^2$ dependent term.

$$(1+\alpha^2)\omega_{1/2} = (1+\alpha\beta)(\boldsymbol{\nu}\cdot\boldsymbol{q}) + i\Lambda\alpha \pm \sqrt{-(\alpha - \beta)^2(\boldsymbol{\nu} \cdot \boldsymbol{q})^2 + 2i\Lambda(\alpha - \beta)(\boldsymbol{\nu} \cdot \boldsymbol{q}) + \Lambda^2}$$
$$\text{(E.4)}$$

After that, the remaining square root terms are merged using the binomial theorem again. Also, the minus in front of the first term in the square root is adapted to the imaginary number $-1 = i^2$.

$$(1 + \alpha^2)\omega_{1/2} = (1 + \alpha\beta)(\boldsymbol{\nu} \cdot \boldsymbol{q}) + i\Lambda\alpha \pm \sqrt{(i(\alpha - \beta)(\boldsymbol{\nu} \cdot \boldsymbol{q}) + \Lambda)^2} \quad \text{(E.5)}$$

The combined squared expression cancels the square root, leading to the final version:

$$(1 + \alpha^2)\omega_{1/2} = (1 + \alpha\beta)(\boldsymbol{\nu} \cdot \boldsymbol{q}) + i\Lambda\alpha \pm (i(\alpha - \beta)(\boldsymbol{\nu} \cdot \boldsymbol{q}) + \Lambda) \quad \text{(E.6)}$$

F. Eigenständigkeitserklärung

Hiermit erkläre ich, dass ich die eingereichte Arbeit selbstständig verfasst und keine anderen als die angegebenen Quellen oder Hilfsmittel (einschließlich elektronischer Medien und Online-Quellen) benutzt habe. Mir ist bewusst, dass ein Täuschungsversuch oder ein Ordnungsverstoß vorliegt, wenn sich diese Erklärung als unwahr erweist.

Mainz, den 20.05.2021

Raphael Kromin